Erasmus University Rotterdam
Erasmus School of Economics

MSc. Econometrics and Management Science - Quantitative Finance
February 29, 2024

Spillovers in sovereign debt markets in the Eurozone

Author:
Arthur van Roest (505615)

Supervisor:
Prof. dr. D.J.C. van Dijk

Second Assessor:
T. van der Zwan

Abstract

In this study, we investigate spillover dynamics in the sovereign debt market in the Eurozone using 10-year yield spreads from ten early adopters of the common currency. We introduce a novel multiple shock spillover measure enabling us to measure spillovers from a block of countries simultaneously, allowing us to analyse spillovers from the core to the periphery, and the other way around. Additionally, we perform a comparison of time-varying multiple shock and bilateral spillover measurements from rolling-window, repeated weighted least squares, and TVP-VAR model estimates. Our novel multiple shock spillover index shows that during the sovereign debt crisis, spillovers from a simultaneous shock to the core and periphery were low, whereas bilateral spillovers reached peak levels. This reveals that during the sovereign debt crisis, a larger than normal share of spillover occurred within the core and periphery, rather than between the core and periphery. In the bilateral spillover analysis, we find substantial temporal variation in spillovers, with Belgium, France, Italy, and Spain playing a prominent role in the transmission of spillovers. Throughout the sample period, most countries are neither net recipients nor net transmitters of spillovers but rather switch back and forth between being net recipients and net transmitters. Furthermore, we do not find evidence for consistent spillovers from the periphery to the core, or the other way around. The TVP-VAR model appears most suitable for the timely detection of spillovers as it produces relatively smooth spillover measures that respond to new information quickly. In contrast, the rolling-window estimates exhibit episodes of increased spillovers that last as long as an observation that pertains to a shock is included in the rolling window, and the repeated weighted least squares produce smooth, but less time-variant spillover measurements.

Acknowledgements

I would like to express my gratitude to my supervisor, Prof. Dr. Dick van Dijk, for his invaluable guidance, support, and encouragement throughout the duration of my thesis. His expertise, insightful feedback, and unwavering commitment have been instrumental in shaping this work and guiding me through the research process.

I would also like to extend my appreciation to Terri van der Zwan, my second assessor, for generously dedicating time and effort to evaluate this thesis.

Contents

1 Introduction

Ever since the inception of the *European Coal and Steel Community (ECSC)*, the earliest predecessor of the *European Union (EU)*, in the 1950s, European countries have sought ways to collaborate in order to promote peace and prosperity on the European continent. The establishment of a common market that allowed the free movement of products, services, and labour was at the time regarded as one of the major steps in advancing economic integration within the EU. In 1991, economic cooperation was further intensified with the Maastricht Treaty and the establishment of the *Economic and Monetary Union (EMU)*. After years of careful preparation, twelve member states of the EU took a major step forward in economic integration in 1999, by adopting a common currency, the euro. This group of countries, together with later adopters of the euro, is commonly referred to as the *Eurozone (EZ)* or *Euro Area (EA)*. The new currency was first introduced in a non-physical form, until notes and coins began to circulate in 2002, rapidly replacing old currencies. The adoption of this new common currency was one of many policies intended to advance economic and financial integration, which in hindsight was empirically proved successful, as Eurozone countries have experienced substantial economic and financial convergence (Ehrmann et al., 2011; Gunnella et al., 2021).

However, the negative consequences of economic and financial integration gained much prominence during the sovereign debt crisis, which unfolded in the aftermath of the 2008 global financial meltdown. Some of the so-called periphery countries, Spain, Greece, Ireland, Italy, and Portugal, had accumulated unsustainable fiscal deficits and government debt. The situation was worsened by the fact that these countries could not devalue their currency due to their use of a common currency. Financial distress in Greece led to a loss of investors' confidence in sovereign bonds in Greece, prompting investors to start questioning whether the financial distress in Greece could spill over to other countries. As a consequence, international markets required greater sovereign risk premia, setting off a sequence of fiscal bailouts, further trouble in the banking system, the downgrading of all EMU countries but Germany, and IMF intervention in several EU countries. The sovereign debt crisis revealed the strong intertwining of European financial markets and the risk of spillovers.

In this paper, we investigate to what extent sovereign yield spreads have been subject to spillovers from other Eurozone countries since the adoption of the common currency. More specifically, we research whether spillovers depict temporal variation throughout the sample period. As an accurate and timely assessment of spillovers is paramount, we evaluate several measurement methods for time-varying spillovers and assess their strengths and weaknesses. Additionally, we propose a novel multiple shock spillover measure that enables us to assess the spillover from shocks in multiple countries simultaneously. We apply this novel measure to evaluate spillovers from the Eurozone core to yield spreads in periphery countries, and the other way around.

For the purpose of our analysis, we use 10-year sovereign bond yield spreads for Austria, Belgium, Finland, France, Greece, Ireland, Italy, the Netherlands, Portugal, and Spain. The sample ranges the full existence period of the Eurozone, from 04/01/1999 to 01/08/2023. To measure the bilateral linkages of sovereign debt markets, we use spillover measures based on the generalised forecast error variance decomposition of a VAR model, as in Diebold and Yilmaz (2009, 2012). Since the adoption of the common currency, the Eurozone has been faced with numerous events, such as the great financial crisis, the Eurozone debt crisis, the COVID-19 pandemic, and the Russian invasion of Ukraine. It is not inconceivable that spillovers are not constant throughout the sample period, hence we measure temporal variation of spillovers in the sovereign debt markets. To evaluate the temporal variation of spillovers, Diebold and Yilmaz (2009, 2012) propose to use rolling-window estimation. However, this approach often exhibits large jumps up and down after a shock occurs or when an observation that pertains to a shock exits the rolling window. Moreover, the rolling-window approach requires the choice of a window size, which is more often than not chosen arbitrarily. To overcome these issues, we can estimate the time-varying dynamics of spillover with the repeated weighted least squares approach over the full sample, in the spirit of Bataa et al. (2013), or we can estimate a time-varying parameter VAR (TVP-VAR) model using forgetting factors, such as described by Antonakakis et al. (2020). To determine the most accurate and timely measurement method of spillovers in the sovereign debt market, we perform a comparison of the three different estimation methods: the rolling-window approach, the repeated weighted least squares, and the TVP-VAR approach.

In light of the sovereign debt crisis, where unsustainable fiscal deficits and public debt in periphery countries had triggered a loss of investors' confidence across the Eurozone, we would to answer the question of whether developments in either the core or the periphery of the Eurozone spill over into countries in the other block. Previously, Claeys and Vašíček (2014) have attempted to analyse EU-wide developments by augmenting the VAR framework of Diebold and Yilmaz (2009, 2012) with common factors, where one of the factors can be interpreted as the difference between the core and periphery. Rather than using a factor-augmented VAR approach, we propose a novel multiple shock spillover measure that enables us to measure spillovers from a group of countries to the remainder of countries. This novel spillover measure is based on the multiple shock forecast error variance decomposition (van der Zwan, 2023). In contrast to the ordinary spillover measures of Diebold and Yilmaz (2009, 2012) which only measure bilateral spillovers, our novel measure allows us to analyse spillovers between blocks of countries. To answer our question of whether shocks in either the core or periphery could spill over into countries in the other block, we implement our novel multiple shock spillover index to assess the spillover effect from a simultaneous shock to the core and periphery.

The introduction of the multiple shock spillover index enables us to measure the spillovers from the core and periphery. The ordinary and multiple shock spillover differ in the fact that the multiple shock spillover index does not measure spillovers within the core and periphery, result-

ing in a much lower spillover measure compared to the ordinary spillover index. This indicates that, although a substantial amount of spillovers is transmitted between the core and periphery, the lion's share of spillover occurs within the core and periphery. Spillovers from simultaneous shocks to the core and periphery were particularly influential during the introduction of the euro to the general public, the financial crisis, and the COVID-19 pandemic. However, throughout the sovereign debt crisis, the multiple shock spillover index experienced a negative trend, which stands in contrast to the ordinary spillover index. This shows that spillovers from the core *(periphery)* only influence sovereign yield spreads in periphery *(core)* countries to a limited extent, hence studying the within-effect and bilateral relations is crucial to understanding the full extent of spillover dynamics of sovereign debt markets in the Eurozone. Our bilateral spillover analysis shows that Belgium, France, Italy, and Spain are key players in the transmission of spillovers. The prominent role of these countries in spillover dynamics in the Eurozone can be attributed to the large size of their economies (except Belgium) and the high level of public debt. Throughout the full sample period, these four countries are the only net transmitters of spillovers, with all other countries being net recipients. However, spillovers depict a high degree of temporal variation, and we find that most countries are not consistently net recipients nor net transmitters, but they rather switch back and forth between being a net recipient and net transmitter throughout the sample period. In general, we note that countries tend to switch between being net recipients and transmitters in periods of crisis. For example, during the sovereign debt crisis, Austria went from being a net recipient to being a net transmitter. In many cases, these switches are temporary, but in some cases, the switch persists after the underlying crisis has ended. In the comparison of estimation methods, we find all three methods produce very similar-looking time-varying spillover patterns, however, whereas the rolling-window approach exhibits large jumps up and down after a shock occurs or when an observation that pertains to a shock exits the rolling window, the repeated weighted least squares and TVP-VAR approaches produce smoother time-varying parameter estimates. Overall, parameter estimates from the TVP-VAR model tend to adjust to newer information quicker, while the repeated weighted least squares method produces smoother, but less time-variant, parameter estimates.

Understanding spillover dynamics in sovereign debt markets in the Eurozone is essential for policy-makers, including central bankers, to anticipate and possibly prevent a future sovereign debt crisis. The extent to which, for example, distress in sovereign debt markets is emanating from a single country as opposed to a group of countries can influence the policy response to be undertaken. A timely response is paramount when it comes to detecting and managing crises, hence quick and accurate detection of changes in spillovers is a favourable attribute of a spillover measurement methodology. Moreover, a thorough analysis of spillovers in sovereign debt markets improves investors' understanding of the risk and diversification benefits of investing in the sovereign debt market in the Eurozone. In addition, dynamic spillover analysis allows policy-makers and banks to anticipate consequences of foreign yield shocks to the financial sector, as sovereign bond yield increases feed into the financial sector by affecting the balance sheets of fi-

nancial institutions, reducing domestic banks' ratings and pushing up their funding costs (Bank for International Settlements, 2011).

Our study contributes to the academic literature on spillovers in sovereign debt markets in the Eurozone in two important ways. First, we analyse dynamic spillovers in the sovereign debt market in the Eurozone using rolling-window, repeated weighted least squares, and TVP-VAR approach and we compare the estimates, finding that for the purpose of timely detection of spillovers, the TVP-VAR is most suitable. Secondly, we propose a novel multiple shock spillover measure, which enables us to analyse spillovers from a group of countries, in our case the Eurozone core and periphery.

This paper is structured as follows, first, we discuss relevant previous research in Section 2. Next, in Section 3 we discuss the sovereign yield data and the transformations that we use to conduct our analysis. In Section 4, we discuss the estimation methods and spillover measures, including our novel multiple shock spillover measures, that we use to analyse spillover dynamics in the Eurozone. We present the results of our analysis in Section 5. Finally, we draw the conclusion to our study in Section 6.

2 Literature

The adoption of the common currency and the transition to the EMU has led to a rapid integration in financial markets, including the sovereign bond market, as pointed out by Ehrmann et al. (2011). In the early stage of the EMU, several studies have analysed co-movement among euro-denominated sovereign yield spreads, finding that integration of the government bond markets is stronger for EMU countries in contrast to non-EMU members (Christiansen, 2007; Caporale and Girardi, 2011). Likewise, in the examination of sovereign yield spreads responses to bad news, Cappiello et al. (2006) document significant evidence of a structural break in correlation after the introduction of the euro. The strong integration of yield spreads continued throughout the financial crisis, as is found by Sosvilla-Rivero and Morales-Zumaquero (2012) who document evidence of unidirectional causality in bond yields of 11 EMU countries during the period 2001–2010. The determinants of the yield spread for EMU countries are different than for non-EMU countries, as Balli (2009) finds that unlike in other bond markets, risk factors and other macroeconomic and fiscal indicators are not able to explain the sovereign bond yields after the beginning of the monetary union, which can be seen as a sign for perfect financial integration. However, the relation between macroeconomic and expected fiscal fundamentals is not constant, as Afonso et al. (2015) show that the menu of macro and fiscal risks priced by markets has been significantly enriched since March 2009, including international financial risk and liquidity risk. According to Favero et al. (2010) differences in liquidity, the availability of derivatives markets for sovereign bonds, and a different response of national markets to global factors are the main sources of differences in sovereign debt yields in the Eurozone.

The purpose of our research is to provide insight into the occurrence of spillovers in the sovereign debt market in the Eurozone since the introduction of the euro. Spillovers in the sovereign debt market in the Eurozone have attracted much attention after the Great Financial Crisis and the Eurozone crisis. In this period, financial distress in Greece led to a sharp decline in investors' confidence in sovereign bonds in Greece, prompting investors to start questioning whether the financial distress in Greece could spill over to other countries. According to Bølstad and Elhardt (2018), investors in Eurozone sovereign debt began to question the willingness of European institutions to rescue specific economies from October 2009 onwards. This activated a self-fulfilling crisis, as the fear of default led investors to demand higher risk premiums, increasing the risk of default (De Grauwe and Ji, 2013). Furthermore, Attinasi et al. (2009) suggest that the rescue packages for the banking sector and the economic fallout of the crisis cast doubt on the debt sustainability of sovereign debt in several Eurozone countries, leading to so-called wake-up calls (Bekaert et al., 2014; De Santis, 2012; Giordano et al., 2013; Ludwig, 2014). A multitude of studies find empirical evidence of the existence of spillovers amongst Eurozone countries with periphery countries being the primary exporters of sovereign risk (De Santis, 2012; Metiu, 2012; Galariotis et al., 2016; González-Sánchez, 2018). Although the prevalent view is that shocks originating from the periphery countries are the main sources of sovereign risk, there are also recent studies indicating that core countries are the main transmitters of spillovers in the Eurozone. (BenSaïda, 2018; Chatziantoniou and Gabauer, 2021)

In view of the fact that timely and accurate detection of changes in spillovers is a favourable attribute of a spillover measurement methodology, we perform a comparison of estimation methods that can be used to compute time-varying spillover dynamics using the VAR-based framework of Diebold and Yilmaz (2009, 2012). The first method, the rolling-window estimation, has been proposed in the original paper by Diebold and Yilmaz (2009) as a method to analyse temporal variation of spillovers in global equity markets. Since then, several studies have utilised the spillover framework of Diebold and Yilmaz (2009, 2012) and their rolling-window approach to study spillovers in the sovereign debt markets in the EMU. Fernández-Rodríguez et al. (2015) analyse spillovers in sovereign debt markets since the inception of the Eurozone, finding that periphery countries become dominant transmitters of spillovers during the European debt crisis. Antonakakis and Vergos (2013) zoom in specifically on the period of the financial and sovereign debt crisis, finding that periphery countries operate in a more destabilising manner than the core countries, supplying spillover to both core and periphery countries. The repeated weighted least squares approach has, as far as we know, not been used to measure spillover dynamics. Similar approaches have been used in the past for many other applications, e.g. Bataa et al. (2013). To complete the comparison, we follow Antonakakis et al. (2020) and estimate a time-varying parameter VAR (TVP-VAR) model using forgetting factors in the spirit of Koop and Korobilis (2013, 2014). This methodology has been applied to sovereign debt markets in the EMU by Chatziantoniou and Gabauer (2021), finding episodes of fragmentation between the connectedness of the yields of various states after the 2008 crisis, with core countries being the main

transmitters of shocks. To gain insight into which method produces superior measurements of spillover dynamics, we perform a comparative analysis.

The sovereign debt market in the Eurozone does not operate as a system independent of international financial markets. Previous studies, such as Codogno et al. (2003) and Bernoth et al. (2012), substantiate that a major part of the bond yield spreads in the EU is determined by a global surge in risk aversion and other external factors. This is affirmed by Afonso et al. (2015), who find that international financial risk is priced in by the markets since the financial crisis. To account for international and EU-wide developments, Claeys and Vašíček (2014) augment the spillover framework of Diebold and Yilmaz (2009, 2012) with common factors that account for EU-wide developments, finding that spillover effects dominate the domestic fundamental factors for Eurozone countries. Their analysis gives prominence to Italy and Spain as key transmitters of spillovers during the sovereign debt crisis, while periphery countries are shown to be more vulnerable to spillovers than countries that belong to the Eurozone core. In our study, instead of using common factors, we introduce a novel multiple shock spillover index based on the work of van der Zwan (2023), enabling us to analyse spillovers from a number of countries simultaneously. We apply this novel spillover measure to investigate spillover dynamics from the core countries to the periphery countries, and the other way around.

3 Data

The dataset considered for this study contains daily observations of the 10-year government benchmark yield for eleven Eurozone countries retrieved from *Datastream*[1]. The government benchmark yield is based on the most representative bond available for the given maturity band at each point in time. Generally, that is the latest issue within the given maturity band, where consideration is also given to yield, issue size, and coupon (FTSE Russel Group, 2023). To construct the benchmark yield, the yield to redemption - the interest rate where the current value of the bond (calculated on the basis of the rates and the accumulated interest) is equal to the cash value of all future yields (interest payments and redemptions) - is calculated for this benchmark bond. Because we would like to assess spillovers throughout the full existence period of the Eurozone, our sample contains 4216 observations ranging from 04/01/1999 to 01/08/2023. The countries in consideration are Austria, Belgium, Finland, France, Germany, Greece, Ireland, Italy, the Netherlands, Portugal, and Spain. The remaining nine Eurozone countries are not considered in this study because they adopted the euro only recently, or due to the limited availability of the 10-year sovereign bond yield.

[1]The *Datastream* codes for the 10-year government benchmark yields used in our analysis can be found in Appendix A.

Figure 1: 10-year sovereign bond yield spreads in the period from 1999 to 2023.

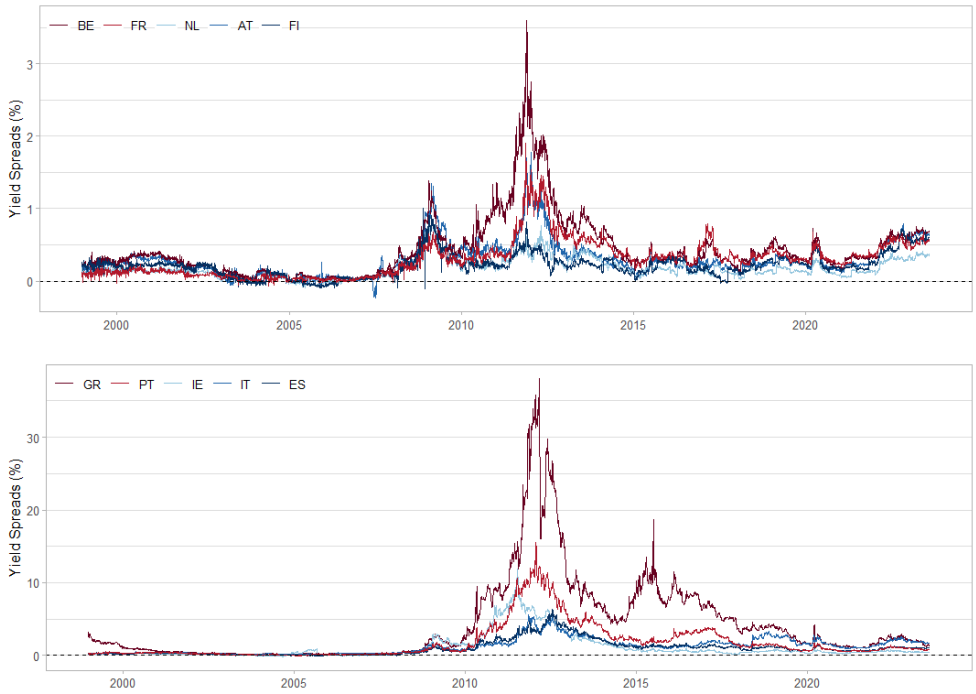

Note: the 10-year sovereign yield spreads for countries in the Eurozone core are displayed in the upper graph, while the yield spreads for periphery countries are depicted in the lower graph. Abbreviations: AT, Austria; BE, Belgium; ES, Spain; FI, Finland; FR, France; GR, Greece; IE, Ireland; IT, Italy; NL, the Netherlands; PT, Portugal.

In this study, we measure sovereign credit risk using the 10-year bond yield spread, which is the difference between the 10-year bond yield of the country in question and the German 10-year yield. In literature, the 10-year bond yield spread is often regarded as an important measure of sovereign credit risk, as it measures the premium required by investors to lend money to a government compared to investing in a risk-free investment, such as the German government bond. To measure sovereign risk, longer maturities are preferred as they better reflect a government's ability to repay its debt in the long term. One disadvantage of using yield spreads is the need to exclude the reference yield, in our case the 10-year German bond yield, from the analysis. Although CDS spreads are arguably a better measure of sovereign credit risk, we aim to measure spillover during the whole period of existence of the Eurozone. Prior to the financial crisis, CDS markets were not quite as developed and hence illiquid, which makes sovereign debt spreads a preferred measure of sovereign risk.

The Eurozone can roughly be categorised into two parts: the core, and the periphery. The former consists of Austria, Belgium, Finland, France, and the Netherlands, whereas the latter includes countries such as Greece, Italy, Ireland, Portugal, and Spain. Countries in the periphery are typically characterised by higher public debt and a lack of fiscal discipline. In

these countries, high debt and fiscal deficits are often accompanied by a high interest rate on sovereign debt, as can be seen in Figure 1. The upper graph exhibits the 10-year sovereign yield spread for the countries that compose the core, and the lower graph displays yield spreads in the periphery countries. In these figures, we can observe a large discrepancy between yield spreads in the core and periphery countries, with periphery countries frequently facing yield spreads of magnitude greater than 5%, whereas the highest yield spread for core countries occurred in Belgium during the sovereign debt crisis reaching a level of just above 3.5%. Looking at the whole sample period, we observe that in the upper graph yield spreads declined in the period between 1999 and 2007, showing the convergence of sovereign debt markets that followed the economic and financial integration that occurred after the adoption of the common currency. Convergence was abruptly interrupted, first by the financial crisis, and later by the sovereign debt crisis. Financial and economic turmoil in periphery countries was accompanied by unprecedented increases in sovereign yield spreads, particularly for Greece and to a lesser extent Ireland and Portugal. The sovereign debt crisis also had an effect on core countries, driving the yield spreads to elevated levels, albeit remaining very low compared to the yield spreads in the periphery. In the post-crisis period, from 2014 onward, we observe a decreasing trend with the exception of Greece whose yield spread remains very high until 2018. Although the yield spread data of Greece contains potentially relevant information, the yield spread reaches exceptional levels for a prolonged period of time. To assess whether the yield spread of Greece has a disproportionate influence on the results, we perform all analysis excluding Greece in Appendix C and compare the results with the results including Greece, finding that Greece's influence is very limited. In the more recent period, small hikes can be observed around the pandemic period and during the energy crisis caused by the Russian invasion of Ukraine. Throughout the sample period, including times of crisis, we observe very strong co-movement of sovereign yield spreads. This indicates the possibility that countries affect each other or that there are possibly common drivers determining the yield spread levels across sovereign debt markets in the Eurozone.

Table 1 displays the mean, standard deviation, skewness, kurtosis, minimum, maximum, and augmented Dickey-Fuller test statistics for the level and first difference of sovereign yield spreads. The descriptive statistics illustrate that core and periphery countries are different in several ways. First, the mean yield spread of periphery countries is substantially higher than for core countries. Secondly, the yield spreads of periphery countries, and their first difference, exhibit higher standard deviation. Finally, the skewness of the first difference in periphery countries is negative (except in Italy), whereas skewness is positive for core countries. These descriptive statistics underline the difference between core and periphery in the Eurozone. For all countries, we notice that all first differences are skewed and fat-tailed (excess kurtosis). Sovereign yield spreads are dependent on macroeconomic and (expected) fiscal fundamentals (Afonso et al., 2015), hence trends and seasonality in yield spreads are expected to occur coinciding with business and credit cycles. Due to the prominent role of fundamentals as determinants of sovereign yield spreads, we expect yield spreads to be non-stationary. To test whether this holds true in an empirical

Table 1: Descriptive statistics of 10-year government bond yield spreads

	AT	BE	ES	FI	FR	GR	IE	IT	NL	PT
Yield spreads										
Mean	0.295	0.441	0.976	0.213	0.303	4.186	1.074	1.233	0.177	1.737
Std.	0.245	0.424	1.074	0.157	0.253	5.839	1.707	1.050	0.137	2.412
Skewness	1.741	2.608	1.850	0.931	1.592	2.617	2.635	1.159	1.294	2.362
Kurtosis	7.569	12.086	6.659	4.640	7.161	11.118	9.925	4.297	5.636	8.671
Min	-0.236	-0.020	-0.088	-0.109	-0.071	0.060	-0.178	0.071	-0.092	-0.090
Max	1.832	3.603	6.341	1.009	1.902	38.062	11.896	5.579	0.897	15.557
ADF	-3.017	-2.289	-1.668	-2.928	-2.877	-1.948	-1.591	-2.367	-3.190	-1.187
First differences										
Mean	0.000	0.000	0.000	0.000	0.000	0.000	0.000	0.000	0.000	0.000
Std	0.028	0.032	0.058	0.033	0.027	0.370	0.069	0.062	0.021	0.104
Skewness	0.258	0.367	-1.009	-0.345	0.088	-24.748	-1.641	0.291	0.484	1.325
Kurtosis	15.274	26.227	33.307	85.271	15.531	1290.810	61.308	22.574	15.232	111.605
Min	-0.280	-0.355	-0.968	-0.668	-0.227	-19.641	-1.312	-0.723	-0.166	-1.925
Max	0.280	0.371	0.546	0.621	0.294	4.218	0.898	0.670	0.184	2.137
ADF	-21.111**	-20.891**	-20.226**	-21.317**	-21.692**	-20.391**	-20.523**	-20.462**	-21.875**	-24.864**

Note: the table shows descriptive statistics of the yield spreads and their first differences. ADF denotes the augmented Dickey-Fuller test (Dickey and Fuller, 1979) with 5%(1%) critical values of -2.86(-3.44); The 5% and 1% significance levels are denoted by * and ** respectively. Abbreviations: AT, Austria; BE, Belgium; ES, Spain; FI, Finland; FR, France; GR, Greece; IE, Ireland; IT, Italy; NL, the Netherlands; PT, Portugal.

setting, we test whether yield spreads and first differences are stationary using the augmented Dickey-Fuller test statistic (Dickey and Fuller, 1979). The augmented Dickey-Fuller test shows that yield spreads are non-stationary, while the first differences are stationary. Since stationarity is a condition for VAR models (Sims, 1980), we opt to use the first differences to analyse spillovers. Henceforth, we will use the term 'yield spread' and 'first difference of yield spread' interchangeably.

Table 2: Correlations between 10-year government bond yield spreads

	AT	BE	ES	FI	FR	GR	IE	IT	NL	PT
AT	1.00	0.87	0.64	0.82	0.83	0.62	0.64	0.68	0.89	0.64
BE	0.87	1.00	0.82	0.62	0.89	0.82	0.86	0.80	0.77	0.88
ES	0.64	0.82	1.00	0.40	0.87	0.87	0.78	0.90	0.63	0.91
FI	0.82	0.62	0.40	1.00	0.64	0.30	0.36	0.51	0.82	0.32
FR	0.83	0.89	0.87	0.64	1.00	0.81	0.67	0.91	0.76	0.84
GR	0.62	0.82	0.87	0.30	0.80	1.00	0.77	0.79	0.50	0.95
IE	0.64	0.86	0.78	0.36	0.67	0.77	1.00	0.64	0.58	0.86
IT	0.68	0.80	0.90	0.51	0.91	0.79	0.64	1.00	0.62	0.82
NL	0.89	0.77	0.63	0.82	0.76	0.50	0.58	0.62	1.00	0.57
PT	0.64	0.88	0.91	0.32	0.84	0.95	0.86	0.82	0.57	1.00

Abbreviations: AT, Austria; BE, Belgium; ES, Spain; FI, Finland; FR, France; GR, Greece; IE, Ireland; IT, Italy; NL, the Netherlands; PT, Portugal.

The correlations between the 10-year sovereign yield spreads are displayed in Table 2. Here, we observe that sovereign yield spreads in the Eurozone are highly correlated. High correlation is found among core countries (e.g. Belgium-France, 0.889), among periphery countries (e.g. Spain-Portugal, 0.912), and between core and periphery countries (e.g. France-Italy, 0.914).

4 Methodology

4.1 Dynamic parameter estimates

The framework to measure the strength and direction of spillovers proposed by Diebold and Yilmaz (2009, 2012) is based on the forecast variance decomposition of a VAR(p) model. The vector autoregressive model under consideration for this study is a covariance stationary VAR(p) model

$$y_t = \sum_{i=1}^{p} \Phi_i y_{t-i} + \varepsilon_t, \tag{1}$$

where y_t is a vector with n elements containing all sovereign yield spreads at time t, and $\varepsilon_t \sim (0, \Sigma)$ is a vector of independently and identically distributed disturbances. The estimated parameters $\Phi_1, \ldots, \Phi_p$ can be used to compute the spillover measures using the method described in Sections 4.2 and 4.3. For the VAR-order, we set $p = 2$, following Diebold and Yilmaz (2009, 2012). To check for robustness of the VAR-model we compare estimation results with $p = 1, 2$, and 4 in Appendix B.1, and we find that the results are not sensitive to the choice of VAR-order p.

The full sample estimates summarise the spillovers between sovereign debt markets. However, throughout the sample period January 1999-July 2023, the Eurozone has undergone numerous developments, such as economic and financial integration, the great financial crisis, the Eurozone debt crisis, the COVID-19 pandemic, and the Russian invasion of Ukraine. A wide range of studies, such as Antonakakis and Vergos (2013), Claeys and Vašíček (2014), and Fernández-Rodríguez et al. (2015), show that global and European events have a strong influence on the time-variation of spillovers. To evaluate the time-variation of the linkages among sovereign debt markets in the Eurozone since the adoption of the common currency, we require time-varying VAR parameter estimates. These time-varying parameter estimates can in turn be used to compute the spillover measures from Sections 4.2 and 4.3, which enable us to assess the extent and nature of the temporal variation of the spillover measures.

In our study, we perform a comparison of three different approaches to estimating time-varying parameters. First, we follow Diebold and Yilmaz (2009, 2012), who obtain time-varying parameter estimates using a 200-day rolling-window estimation approach. While this approach generates spillover plots that accurately capture the increase in spillover when a shock occurs, they do not necessarily capture the downward movement in a timely manner. On the contrary,

the spillover indices often exhibit large jumps up and down after a shock occurs or when an observation that pertains to a shock exits the rolling window. Furthermore, in the rolling-window approach observations outside of the rolling-window are discarded while they may contain valuable information. When selecting the rolling window size, the researcher has to make a trade-off between the usage of available data and persistence. In Appendix B.2, we compare estimation results with a 50, 100, 200, and 500-day rolling window, finding that the resulting spillover measures are very sensitive to the choice of the window-length. After careful consideration, we deem a 200-day rolling window to be appropriate for our application.

To avoid large jumps up and down after observations pertaining to shocks exit the rolling window, we assign decreasing weights to older observations, without entirely discarding these potentially informative observations. That is, we estimate the VAR model using weighted least squares, such that the observation at time $\tau - k$ is given weight λ^k, for $k = 0, 1, 2, \ldots$, and weight zero for $k < 0$, with $0 < \lambda < 1$, resulting in VAR estimates for $t = \tau$. Repeating this for $\tau = 1, 2, \ldots, T$ yields a sequence of VARs with smoothly time-varying parameter estimates. The specification of this approach, which we will henceforth refer to as repeated weighted least squares, depends on the choice of λ. From the comparison of estimation results with $\lambda = 0.98, 0.99, 0.995$, and 0.998 in Appendix B.3, we find that the estimates with larger value λ produce smoother spillover measures and tend to underestimate their counterparts estimated with lower values of λ. The resulting spillover measures are relatively sensitive to the specification of λ, however, the results are less sensitive to the selection of λ than the rolling-window approach is sensitive to the choice of the window-length. Based on a comparison of different values of λ, we determine to set $\lambda = 0.995$. Compared to the rolling-window approach, the repeated weighted least squares approach assigns lower weight to observations between 2 and 200 days old and larger weight to observations older than 200 days. For example, a 100-day-old observation has weight 0.61 compared to weight 1, whereas a 300-day-old observation's weight equals 0.22 compared to zero in the rolling-window approach. Although by design, this weighting will not reproduce any abrupt change, this approach utilises all available information, assigning greater weight to more recent data and yielding smooth parameter estimates that gradually capture changes in spillovers.

Although the repeated weighted least squares is able to produce smooth parameter estimates utilising all available observations, historical observations remain very influential as they carry substantial weight, regardless of the value of these particular observations. Antonakakis et al. (2020) propose to obtain parameter estimates using a time-varying parameter (TVP-VAR) model using the Kalman filter with forgetting factors in the spirit of Koop and Korobilis (2014). In this approach, the covariance matrix is allowed to be time-variant, providing an assessment of the accuracy of the estimation. The information contained in the covariance matrix can in turn be used to update the parameter estimates.

Because little is known about the nature of parameter changes, we allow the parameters to follow a random walk, an approach which has been popular for economic time series at least since Cooley and Prescott (1976). The TVP-VAR(p) model can be written in state-space form as follows:

$$y_t = \Phi_t z_{t-1} + \varepsilon_t \qquad \varepsilon_t|\Omega_{t-1} \sim N(0, \Sigma_t) \tag{2}$$

$$vec(\Phi_t) = vec(\Phi_{t-1}) + \xi_t \qquad \xi_t|\Omega_{t-1} \sim N(0, \Xi_t) \tag{3}$$

with

$$z_{t-1} = \begin{pmatrix} y_{t-1}^+ \\ \vdots \\ y_{t-p}^+ \end{pmatrix} \qquad \Phi_t' = \begin{pmatrix} \Phi_{1t} \\ \vdots \\ \Phi_{pt} \end{pmatrix}$$

where Ω_{t-1} represents all available information until $t-1$, y_t, and z_t are $n \times 1$ and $np \times 1$ vectors, respectively, Φ_t and Φ_{it} are $n \times np$ and $n \times n$-dimensional matrices, respectively, ε_t is an $n \times 1$ vector, and ξ_t is an $n^2p \times 1$ vector, whereas the time-varying covariance matrices Σ_t and Ξ_t are $n \times n$ and $n^2p \times n^2p$ dimensional matrices, respectively. Moreover, $vec(\Phi_t)$ is the vectorisation of Φ_t which is an $n^2p \times 1$ vector.

To reduce the computational intensity of estimating the state-space model, we implement forgetting factors in the Kalman filter algorithm (Kalman, 1960), in the spirit of Koop and Korobilis (2013, 2014). The basic idea is to replace Σ_t and Ξ_t by estimates and, once this is done, analytically derive the distribution of Φ_t. To use the Kalman filter, we assume that all disturbances are normally distributed, i.e. $\varepsilon_t|\Omega_{t-1} \sim N(0, \Sigma_t)$ and $\xi_t|\Omega_{t-1} \sim N(0, \Xi_t)$. Under this assumption, we can write

$$vec(\Phi_t)|z_{1:t-1} \sim N(vec(\Phi_{t|t-1}), \Sigma_{t|t-1}^{\Phi}), \tag{4}$$

that is, we know that the vectorisation of parameters Φ_t given all sovereign yield spreads till $t-1$ are normally distributed with mean $vec(\Phi_{t|t-1})$ and variance $\Sigma_{t|t-1}^{\Phi}$. In this notation, $\Phi_{t|t-1}$ and $\Sigma_{t|t-1}^{\Phi}$ are respectively Φ_t and Σ_t^{Φ} given all available information until $t-1$. $\Phi_{t|t-1}$ and $\Sigma_{t|t-1}^{\Phi}$ are obtained from the predication step of the Kalman filter:

$$\Phi_{t|t-1} = \Phi_{t-1|t-1} \tag{5}$$

$$\Sigma_{t|t-1}^{\Phi} = \Sigma_{t-1|t-1}^{\Phi} + \Xi_t \tag{6}$$

This is the only place where Ξ_t enters the Kalman filter, thus, if we replace the preceding equation by

$$\Sigma_{t|t-1}^{\Phi} = \frac{1}{\kappa_1}\Sigma_{t-1|t-1}^{\Phi}, \tag{7}$$

there is no longer a need to estimate or simulate Ξ_t. Note, that equations 6 and 7 imply that

$$\Xi_t = (1 - \kappa_1^{-1})\Sigma_{t-1|t-1}^{\Phi}, \tag{8}$$

The constant κ_1 is referred to as "forgetting factor" because this specification implies that an observation j periods in the past has weight κ_1^j in the filtered estimate of Φ_t, hence partially forgetting historic observations. κ_1 is restricted to the interval $0 < \kappa_1 < 1$. A similar approximation is used to remove the need to estimate Σ_t. We follow Koop and Korobilis (2013) by using an exponentially weighted moving average (EWMA) to model volatility (RiskMetrics, 1996; Brockwell and Davis, 2016), i.e.

$$\Sigma_t = \kappa_2 \Sigma_{t-1|t-1} + (1 - \kappa_2)\varepsilon_t' \varepsilon_t, \tag{9}$$

where $\varepsilon_t = y_t - \Phi_{t|t-1} z_{t-1}$ is produced by the Kalman filter.

The application of forgetting factors requires us to select a value for κ_1 and κ_2. For κ_1, we assume that daily changes are relatively slow and stable under the random walk specification. In order to achieve this slow time variation in the coefficients, we set $\kappa_1 = 0.99$. For the decay factor κ_2 in the EWMA estimator, RiskMetrics (1996) suggests values in the region of $(0.94, 0.98)$. Because we use daily data, we opt for a relatively stable specification by setting $\kappa_2 = 0.98$. In Appendix B.4, we compare estimation results for several alternative values of forgetting factors, finding that the choice of κ_1 and κ_2 has some influence on the magnitude of peaks, but is much less sensitive to the estimation specification than the other estimation methods. Note that the constant parameter specification can be achieved by setting the decay factors $\kappa_1 = 1$ and $\kappa_2 = 1$. Estimation procedures to allow the decay factors to be time-varying exist, however, we decide to keep them constant, as Koop and Korobilis (2013) found that the value-added by time-varying decay factors was questionable while it increased the computational burden of the Kalman filter significantly.

We initialise the Kalman filter using the Primiceri (2005) prior, setting the initial value of Φ_t, Σ_t^Φ, and Σ_t equal to the ordinary least squares estimate using the first 250 days of the sample, i.e.

$$vec(\Phi_0) \sim N(vec(\Phi_{OLS}), \Sigma_{OLS}^\Phi), \tag{10}$$

$$\Sigma_0 = \Sigma_{OLS}, \tag{11}$$

where Φ_{OLS}, Σ_{OLS}^Φ, Σ_{OLS} are the ordinary least squares estimates for the first 250 observations.

Together, equations 4, 5, 6, 8 form the prediction step of the Kalman filter with forgetting factors. Next, we update Φ_t, Σ_t^Φ, and Σ_t given the information at time t. First, we compute the Kalman gain

$$G_t = \Sigma_{t|t-1}^\Phi z_{t-1}' \big(z_{t-1} \Sigma_{t|t-1}^\Phi z_{t-1}' + \Sigma_t\big)^{-1}, \tag{12}$$

which explains how much the parameters Φ_t and the parameter uncertainty Σ_t^Φ should be adjusted in any given state. If the parameter uncertainty $\Sigma_{t|t-1}^\Phi$ is small *(large)*, it means that the parameter Φ_t should be similar *(adjusted to)* their prior states. On the other hand, if the

error variance Σ_t is small *(large)*, meaning that the estimation is very accurate *(inaccurate)*, the parameters Φ_t should be similar to *(adjusted to)* their prior values. In the updating step, we use the Kalman gain to update Φ_t, Σ_t^{Φ} using the information at time t:

$$\Phi_{t|t} = \Phi_{t|t-1} + G_t(y_t - \Phi_{t|t-1} z_{t-1}), \tag{13}$$

$$\Sigma^{\Phi}_{t|t} = (1 - G_t)\Sigma^{\Phi}_{t|t-1}, \tag{14}$$

and we update Σ_t given information at time t using the EWMA specification as follows:

$$\Sigma_t = \kappa_2 \Sigma_{t-1|t-1} + (1 - \kappa_2)\varepsilon'_{t|t}\varepsilon_{t|t}, \tag{15}$$

where $\varepsilon_{t|t} = y_t - \Phi_{t|t} z_{t-1}$ is the measurement error at time t. Equations 12, 13, 13, and 15 form the updating step of the Kalman filter algorithms. Combining the prediction and updating step, the Kalman filter algorithm can be formulated as follows:

Prediction Step:

$$\begin{aligned}
vec(\Phi_t)|z_{1:t-1} &\sim N(vec(\Phi_{t|t-1}), \Sigma^{\Phi}_{t|t-1}) \\
\Phi_{t|t-1} &= \Phi_{t-1|t-1} \\
\varepsilon_t &= y_t - \Phi_{t|t-1} z_{t-1} \\
\Sigma_t &= \kappa_2 \Sigma_{t-1|t-1} + (1 - \kappa_2)\varepsilon'_t \varepsilon_t \\
\Xi_t &= (1 - \kappa_1^{-1})\Sigma^{\Phi}_{t-1|t-1} \\
\Sigma^{\Phi}_{t|t-1} &= \Sigma^{\Phi}_{t-1|t-1} + \Xi_t
\end{aligned}$$

Updating Step:

$$\begin{aligned}
vec(\Phi_t)|z_{1:t} &\sim N(vec(\Phi_{t|t}), \Sigma^{\Phi}_{t|t}) \\
G_t &= \Sigma^{\Phi}_{t|t-1} z'_{t-1} \big(z_{t-1} \Sigma^{\Phi}_{t|t-1} z'_{t-1} + \Sigma_t\big)^{-1} \\
\Phi_{t|t} &= \Phi_{t|t-1} + G_t(y_t - \Phi_{t|t-1} z_{t-1}) \\
\Sigma^{\Phi}_{t|t} &= (1 - G_t)\Sigma^{\Phi}_{t|t-1} \\
\varepsilon_{t|t} &= y_t - \Phi_{t|t} z_{t-1} \\
\Sigma_{t|t} &= \kappa_2 \Sigma_{t-1|t-1} + (1 - \kappa_2)\varepsilon'_{t|t}\varepsilon_{t|t},
\end{aligned}$$

Repeating these computations for every value of $t = 1, \ldots, T$ and saving the value of parameter estimates Φ_t, we obtain a set of time-varying parameter estimates $\{\Phi_1, \ldots, \Phi_T\}$. After we have estimated the time-varying parameters, we need to transform the TVP-VAR model into a moving-average representation and use the parameter estimates to compute the spillover index, as is shown in Section 4.2. To estimate the TVP-VAR model, we make use of the *ConnectednessApproach* package of Gabauer (2022).

4.2 Spillover measures

To compute the spillover measure of Diebold and Yilmaz (2009, 2012), we need to use the parameter estimates from the previous section to rewrite the model in moving average representation, that is,

$$y_t = \sum_{i=0}^{\infty} A_{t,i}\varepsilon_{t-i}, \tag{16}$$

where the coefficient matrices $A_{t,i}$ can be computed recursively using $A_{t,i} = \Phi_{t,1}A_{t,i-1} + \Phi_{t,2}A_{t,i-2} + \cdots + \Phi_{t,p}A_{t,i-p}$, with $A_{t,0}$ being an $n \times n$ identity matrix and $A_{t,i} = 0$ for $i < 0$. The moving average coefficients are crucial for the computation of the general forecast variance decomposition. Following Koop et al. (1996) and Pesaran and Shin (1998), we calculate the H-step-ahead forecast error variance decomposition as

$$\theta_{t,i,j}(H) = \frac{\sigma_{t,j,j}^{-1} \sum\limits_{h=0}^{H-1} (e_i' A_{t,h}\Sigma_t e_j)^2}{\sum\limits_{h=0}^{H-1} e_i' A_{t,h}\Sigma_t A_{t,h}' e_i}, \tag{17}$$

where Σ_t is the estimated covariance matrix of the error vector ε_t, which is available from the Kalman filter in the time-varying parameter approach, $\sigma_{t,j,j}$ the estimated standard deviation of the error term for the jth equation, and e_i a selection vector with one as the ith element and all other elements zero. The diagonal elements of $\theta_t(H)$ contain the contributions of shocks to the yield spread i to its own forecast error variance, the off-diagonal elements show the cross contributions of yield spread j to the forecast error variance of yield spread i. Under the generalised forecast error variance decomposition, the own and cross-variable variance contribution shares do not sum to one, hence, each element of $\theta_t(H)$ is normalised, such that

$$\tilde{\theta}_{t,i,j}(H) = \frac{\theta_{t,i,j}(H)}{\sum\limits_{j=1}^{n} \theta_{t,i,j}(H)}, \tag{18}$$

where $\sum_{j=1}^{n} \tilde{\theta}_{t,i,j}(H) = 1$ and $\sum_{i,j=1}^{n} \tilde{\theta}_{t,i,j}(H) = n$ by construction. Using the volatility contributions from the generalised forecast error variance decomposition, we can compute the total spillover index, as proposed by Diebold and Yilmaz (2012):

$$S_t(H) = \frac{\sum\limits_{i,j=1, i\neq j}^{n} \tilde{\theta}_{t,i,j}(H)}{\sum\limits_{i,j=1}^{n} \tilde{\theta}_{t,i,j}(H)} \cdot 100 = \frac{\sum\limits_{i,j=1, i\neq j}^{n} \tilde{\theta}_{t,i,j}(H)}{n} \cdot 100, \tag{19}$$

which gives the average contribution of spillovers from shocks to all (other) variables to the total forecast error variance. To gain insight into the direction of spillovers, we measure the directional spillovers received by yield i from all other markets j as:

$$S_{i\cdot,t}(H) = \frac{\sum\limits_{j=1, j\neq i}^{n} \tilde{\theta}_{t,i,j}(H)}{\sum\limits_{i,j=1}^{n} \tilde{\theta}_{t,i,j}(H)} = \frac{\sum\limits_{j=1, j\neq i}^{n} \tilde{\theta}_{t,i,j}(H)}{n} \cdot 100. \tag{20}$$

In similar fashion, we measure the directional spillovers transmitted by sovereign bond yield i to all other markets j as:

$$S_{\cdot i,t}(H) = \frac{\sum_{j=1,j\neq i}^{n} \tilde{\theta}_{t,j,i}(H)}{\sum_{i,j=1}^{n} \tilde{\theta}_{t,j,i}(H)} = \frac{\sum_{j=1,j\neq i}^{n} \tilde{\theta}_{t,j,i}(H)}{n} \cdot 100. \tag{21}$$

We obtain the net spillover from market i to all other markets j as:

$$S_{i,t}(H) = S_{\cdot i,t}(H) - S_{i\cdot,t}(H). \tag{22}$$

The net spillover is simply the difference between the transmitted spillovers and those received from other markets. Finally, we can measure how much each market contributes to another market using the net pairwise spillover measure, which is defined as:

$$S_{i,j,t}(H) = \left(\frac{\tilde{\theta}_{t,j,i}(H)}{\sum_{i,q=1}^{n} \tilde{\theta}_{t,i,q}(H)} - \frac{\tilde{\theta}_{t,i,j}(H)}{\sum_{i,q=1}^{n} \tilde{\theta}_{t,j,q}(H)} \right) \cdot 100 \tag{23}$$

$$= \left(\frac{\tilde{\theta}_{t,j,i}(H) - \tilde{\theta}_{t,i,j}(H)}{n} \right) \cdot 100. \tag{24}$$

The net pairwise spillover between sovereign bond yield i and j is simply the difference between shocks transmitted from yield i to market j and those transmitted from j to i.

4.3 Multiple shock spillover measures

The sovereign debt market is a fast-moving market, often responding instantly to global and EMU-wide developments. The spillover index as proposed by Diebold and Yilmaz (2009, 2012) uses a forecast error variance decomposition. However, since we work with daily data, the occurrence of multiple shocks within a single period is quite plausible, potentially triggering other shocks. To account for the possibility of developments occurring in several countries simultaneously, we propose a novel spillover measure that enables us to analyse spillovers from a group of countries to the remaining countries. This new spillover measure uses the concept of multiple shock impulse response functions of van der Zwan (2023). Using the estimated moving average coefficients, we calculate the H-step ahead multiple shock forecast error variance decomposition as

$$\theta^{\mathcal{S}}_{t,i}(H) = \frac{\sum_{h=0}^{H-1} e_i' A_{t,h} \Sigma_t P (P' \Sigma_t P)^{-1} P' \Sigma_t (A_{t,h})' e_i}{\sum_{h=0}^{H-1} e_i' A_{t,h} \Sigma_t A_{t,h}' e_i}, \tag{25}$$

where $\mathcal{S}$ represents a shock to multiple variables in the VAR model, Σ_t is the estimated covariance matrix of the error vector ε_t, $A_{t,h}$ are the moving average coefficients, e_i is a selection vector with one as the ith element and all other elements zero, and P is the permutation matrix, a matrix structured according to the shock $\mathcal{S}$. For example, a shock to first and third variable

corresponds to a permutation matrix $P = [e_1, e_3]$. This multiple shock forecast error variance decomposition can be interpreted as a measure for the fraction of the H-step-ahead forecast error variance explained by the shock $\mathcal{S}$, thus the percentage of unanticipated changes in variable i's forecast due to multiple shocks occurring simultaneously.

In literature, periphery countries are often regarded as the main source of spillovers in the sovereign debt market in the Eurozone (Antonakakis and Vergos, 2013; Claeys and Vašíček, 2014; Fernández-Rodríguez et al., 2015). Hence, in our situation, it is interesting to analyse the spillover dynamics of common shocks to core and periphery countries. We compute the multiple shock forecast error variance decomposition for shocks to core countries and to periphery countries, which we denote as $\mathcal{C}$ and $\mathcal{P}$ respectively. Under the multiple shock forecast error variance decomposition, the own and cross-variable variance contribution shares do not sum to one, hence, each element of $\theta_t^{\mathcal{C}}(H)$ and $\theta_t^{\mathcal{P}}(H)$ is normalised, such that

$$\tilde{\theta}_{t,i}^{\mathcal{C}}(H) = \frac{\theta_{t,i}^{\mathcal{C}}(H)}{\theta_{t,i}^{\mathcal{C}}(H) + \theta_{t,i}^{\mathcal{P}}(H)} \qquad \tilde{\theta}_{t,i}^{\mathcal{P}}(H) = \frac{\theta_{t,i}^{\mathcal{P}}(H)}{\theta_{t,i}^{\mathcal{C}}(H) + \theta_{t,i}^{\mathcal{P}}(H)}, \tag{26}$$

where $\tilde{\theta}_{t,i}^{\mathcal{C}}(H) + \tilde{\theta}_{t,i}^{\mathcal{P}}(H) = 1$ and $\sum_i^n \left(\tilde{\theta}_{t,i}^{\mathcal{C}}(H) + \tilde{\theta}_{t,i}^{\mathcal{P}}(H)\right) = n$ by construction. We use the normalised multiple shock forecast error variance decomposition to calculate the spillover measures of Diebold and Yilmaz (2009, 2012) modified to account for shocks to multiple countries simultaneously. The total spillover index can be calculated as

$$S_t(H) = \frac{\sum\limits_{i\in\mathcal{P}} \tilde{\theta}_{t,i}^{\mathcal{C}}(H) + \sum\limits_{i\in\mathcal{C}} \tilde{\theta}_{t,i}^{\mathcal{P}}(H)}{\sum\limits_{i\in\{\mathcal{C},\mathcal{P}\}} (\tilde{\theta}_{t,i}^{\mathcal{C}}(H) + \tilde{\theta}_{t,i}^{\mathcal{P}}(H))} \cdot 100 = \frac{\sum\limits_{i\in\mathcal{P}} \tilde{\theta}_{t,i}^{\mathcal{C}}(H) + \sum\limits_{i\in\mathcal{C}} \tilde{\theta}_{t,i}^{\mathcal{P}}(H)}{n} \cdot 100, \tag{27}$$

where $\mathcal{C}$ and $\mathcal{P}$ are the set of indices of core and periphery countries respectively. The measure gives the average contribution of spillovers from shocks in core countries to yield spreads in periphery countries, and vice versa. To measure the spillover of core and periphery shocks on yield spreads, we measure the directional spillovers received by yield spread i from shocks to core and periphery as:

$$S_{ti} = \frac{1}{2}\left(I(i \in \mathcal{C})\tilde{\theta}_{t,i}^{\mathcal{P}} + I(i \in \mathcal{P})\tilde{\theta}_{t,i}^{\mathcal{C}}\right) \cdot 100, \tag{28}$$

where $I(\cdot)$ is an indicator which is 1 if the condition is true and 0 otherwise. In words, the directional spillover to yield spread i is the mean of the spillovers from the joint shock not including yield spread i. We measure the directional spillovers transmitted by the joint shocks to core and periphery countries to all sovereign yield spreads as

$$S_{t\cdot}^{\mathcal{C}}(H) = \frac{\sum\limits_{i\in\mathcal{P}} \tilde{\theta}_{t,i}^{\mathcal{C}}(H)}{\sum\limits_{i\in\{\mathcal{C},\mathcal{P}\}} (\tilde{\theta}_{t,i}^{\mathcal{C}}(H) + \tilde{\theta}_{t,i}^{\mathcal{P}}(H))} \cdot 100 = \frac{\sum\limits_{i\in\mathcal{P}} \tilde{\theta}_{t,i}^{\mathcal{C}}(H)}{n} \cdot 100, \tag{29}$$

$$S_{t\cdot}^{\mathcal{P}}(H) = \frac{\sum\limits_{i\in\mathcal{C}} \tilde{\theta}_{t,i}^{\mathcal{P}}(H)}{\sum\limits_{i\in\{\mathcal{C},\mathcal{P}\}} (\tilde{\theta}_{t,i}^{\mathcal{C}}(H) + \tilde{\theta}_{t,i}^{\mathcal{P}}(H))} \cdot 100 = \frac{\sum\limits_{i\in\mathcal{C}} \tilde{\theta}_{t,i}^{\mathcal{P}}(H)}{n} \cdot 100. \tag{30}$$

These spillover measures allow us to assess the strength and direction of spillovers when multiple shocks occur simultaneously in the core and periphery of the Eurozone.

5 Results

5.1 Multiple shock spillover analysis

To measure spillovers from the Eurozone core to the periphery, and the other way around, we use our novel multiple shock spillover measures. Table 3 presents the multiple shock spillover table computed over the full-sample period. The columns under $\mathcal{C}$ and $\mathcal{P}$ depict spillovers from a shock to the core and periphery respectively, to each country in the Eurozone, i.e. the fraction of forecast error variance that can be attributed to a core/periphery shock. The last column contains the received spillover per country, that is, if a country belongs to the core, the fraction of forecast error variance that can be attributed to a periphery shock, and vice versa. The bottom row displays the amount of spillover generated by the core and periphery respectively. The multiple shock spillover index is shown in the bottom-right corner.

Table 3: Multiple shock spillover table, period 04/01/1999 - 01/08/2023

	$\mathcal{C}$	$\mathcal{P}$	Received
AT	84.0	16.0	16.0
BE	70.9	29.1	29.1
FI	96.5	3.5	3.5
FR	76.6	23.4	23.4
NL	85.2	14.8	14.8
ES	28.5	71.5	28.5
GR	4.3	95.7	4.3
IE	13.7	86.3	13.7
IT	27.0	73.0	27.0
PT	11.0	89.0	11.0
Transmitted	84.4	87.0	Spillover index = 17.1%

Note: this table presents the multiple shock spillover measures, based on Equations (26)-(30), calculated from multiple shock forecast error variance decompositions based on 10-step-ahead forecasts. Abbreviations: AT, Austria; BE, Belgium; ES, Spain; FI, Finland; FR, France; GR, Greece; IE, Ireland; IT, Italy; NL, the Netherlands; PT, Portugal.

Table 3 shows that the multiple shock spillover index over the full sample is equal to 17.1%, meaning that 17.1% of forecast error variance can be traced back to spillover from shocks to the core and periphery. Moreover, we find that a shock to the periphery generates slightly more spillover than a shock to the core, although the difference is minor. Spain, Italy, Belgium, and to a lesser extent France, are most sensitive to spillovers from other sovereign debt markets in the Eurozone. For Spain and Italy, respectively 28.5% and 27.0% of the forecast error variance can

be traced back to a simultaneous shock to the core countries. This is unsurprising, as previous studies such as Broto and Pérez-Quirós (2011) find that Spain and Italy are more affected by EMU-wide developments than by internal dynamics. For Belgium and France, spillovers from a shock to the periphery amount to 29.1% and 23.4% respectively. These four countries are characterised by high public debt, with Italy (142.4%), France (111.9%), Spain (111.2%), and Belgium (106.0%) taking the second, third, fourth, and sixth rank in the EU in terms of debt-to-GDP. The high amount of public debt in Spain, Italy, Belgium, and France makes their sovereign bond markets subject to spillovers from other sovereign debt markets. The countries receiving the least amount of spillovers are Greece and Finland. For Finland, this result is unsurprising as Finland has a moderate debt-to-GDP ratio of 74.3% and its economy functions relatively independently of the periphery countries. In contrast, the debt-to-GDP ratio in Greece equals 166.5%, making it the country with the highest public debt in the EU. Furthermore, the fallout of the financial crisis led to financial distress in Greece, setting off a sequence of events that we now know as the sovereign debt crisis. These two phenomena would lead one to believe Greece to be more vulnerable to spillovers from the Eurozone core but results in Table 3 show that this is not the case.

During the sample period from 1999 to 2023, many developments have occurred in the global economy and financial markets. The establishment of the EMU and the continuing economic and financial integration in the EU have structurally affected cross-border dynamics between markets. During this period, several large global events such as the Great Financial Crisis, the Eurozone debt crisis, and the COVID-19 pandemic, have strongly impacted financial markets. To analyse the temporal variation of spillovers in the sovereign debt market during this time period, we compute spillover measures using time-varying parameters. To investigate which estimation method yields the best assessment of spillover dynamics, we estimate time-varying parameters using three different methods: a 200-day rolling-window, repeated weighted least squares, and a TVP-VAR model.

Figure 2 displays the multiple shock spillover index throughout the sample period computed using the time-varying parameter estimates. Since the introduction, several peaks can be clearly identified, most of which can directly be linked to global economic and financial events. Although the euro has been used as accounting currency since 1999, the introduction of physical currency and the adoption of the euro by the general public was not until the beginning of 2002. The introduction of the physical euro was accompanied by a spike in the multiple shock spillover index. The spike following the introduction of the euro was succeeded by an episode of relatively low spillovers that lasted until 2005. In the years leading up to the financial crisis, we observe an increasing trend in the multiple shock spillover index, eventually reaching its peak on January 2, 2008. In 2015 and 2016, two relatively smaller spikes occurred simultaneously with the ECB's introduction of the asset purchase programme (APP). As a result of the global financial crisis in 2008, key interest rates controlled by the ECB came close to their effective lower bound - the

Figure 2: Total multiple shock spillover index, period 08/10/1999 - 01/08/2023

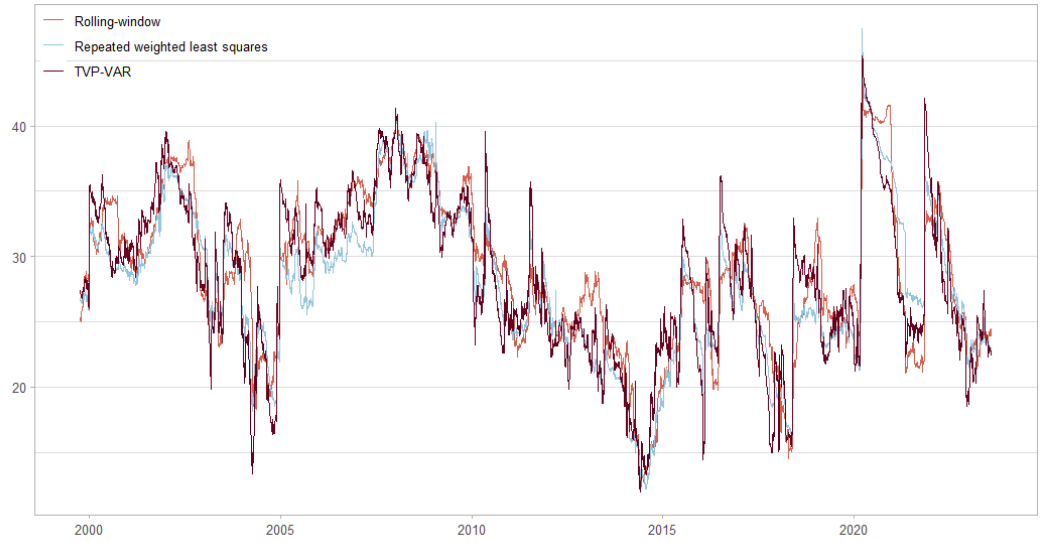

Note: the plot depicts the multiple shock spillover index calculated using Equation (27) with time-varying parameter estimates obtained using 200-day rolling-window estimates, repeated weighted least squares where a k-day-old observation is assigned weight λ^k with $\lambda = 0.995$, and TVP-VAR with decay factors $\kappa_1 = 0.99$ and $\kappa_2 = 0.98$.

point at which lowering them further would have little to no effect. To bring inflation back to the ECB's target of 2% over the medium term, the ECB turned to unconventional monetary policy measures, among which the APP. On January 22, 2015, the ECB announced that it would start purchasing assets amounting to €60 billion per month from March 2015 onwards. The effects of the APP can be observed in the total spillover index, with an observable peak on June 11, 2015. In June 2016, the ECB announced that the monthly purchases under the APP would be expanded to €80 billion which gave rise to another increase in spillovers. More recently, an elevation in the total spillover index occurred right around the start of the COVID-19 pandemic in Europe. This peak was later succeeded by another spike in the total spillover index after a surge in COVID-19 cases and tightening pandemic prevention measures during the start of 2021. The more recent peaks in the total spillover index are of greater magnitude compared to earlier peaks, reflecting an increase in the connectedness of sovereign debt markets in the Eurozone. The size of the spillover increases might also be magnified by the ECB's pandemic emergency purchase programme (PEPP), an unconventional monetary policy measure initiated in March 2020 to counter the economic and financial risk posed to the euro area posed by the COVID-19 outbreak. Remarkably, the multiple shock spillover index experiences a negative trend throughout the sovereign debt crisis. This indicates that spillovers from shocks to the core to periphery countries, and the other way around, decreased after the financial crisis and kept decreasing throughout the sovereign debt crisis. This stands in contrast with the prevalent view that financial distress, accompanied by unprecedented yield spreads, originated in periphery countries such as Greece, Portugal, and Ireland, and later spread across the Eurozone.

In comparison, the rolling-window, repeated weighted least squares, and TVP-VAR approach produce very similar-looking time-varying spillover patterns, simultaneously detecting peaks and troughs in the spillover index. However, upon closer inspection, there are a number of subtle differences between the spillover measures. Most notably, the spillover index for the 200-day rolling window estimates exhibit episodes of increased spillovers that last for exactly 200 days. These increases arise after a shock, after which the index tends to stay high as long as the observation that pertains to the day of the shock is included in the fixed-length rolling window. The repeated weighted least squares approach produces smooth changes in the total spillover index, however, this does not resolve the persistence as old observations still carry significant weight. In Figure 2, we see that in general, the TVP-VAR model tends to overestimate spillovers during peaks compared to the repeated weighted least squares approach, while it underestimates spillovers during periods of low spillovers. This corresponds to our previous comment that the repeated weighted least squares renders smoother (i.e. less variable) estimates. However, it is very important to note that the results are very much subject to the specification of both models as the weights and decay factors have a strong influence on the variability of the spillover index for both models.

Figure 3 presents the directional spillovers to each country's sovereign yield spreads from simultaneous shocks to the core and periphery. The received spillover plots depict a substantial amount of temporal variation. Especially, the increase in spillover during the financial crisis stands out. First, directional spillovers to Spain, France, Greece, Italy, the Netherlands, and Portugal increased around 2005, shortly followed by increases in received spillovers in Ireland, Belgium, and Austria. While these elevated spillover measures returned to normal levels in some countries, the received spillovers remained high throughout the sovereign debt crisis in some countries, such as Austria, Belgium, Spain, and Italy. Overall, received spillovers experienced a negative trend during the sovereign debt crisis, indicating a declining amount of spillover between the core and periphery. After both crises, directional spillover to Greece and the Netherlands never recovered to pre-crisis levels. During the COVID-19 pandemic, directional spillovers to all countries experienced a sudden increase, indicating a surge of spillover between the core and periphery.

In Figure 4, we observe the amount of spillover transmitted by a shock to the core and periphery. To delve deeper into the destinations of the transmitted spillovers, we decompose the transmitted spillover measure into the countries of destination in Figure 5. In the first period, prior to the physical introduction of the euro, we observe high transmitted spillovers from a periphery shock to core countries. Directional spillovers from a periphery shock to core countries' sovereign yield spreads were initially moderate, but increased around the introduction of the physical euro, in particular to Greece, Ireland, and Italy. The largest increase in transmitted spillover occurred in the years leading up to and during the financial crisis. The increase in transmitted spillovers from a core shock increased a few years prior to the financial crisis, around 2005. In this period, spillovers to Greece, Italy, and Greece increased strongly, adding to spillovers from Spain already present pre-crisis. Later, spillover to Ireland also increased,

Figure 3: Directional spillovers *to* each country's sovereign yield spreads from a simultaneous shock to core and periphery in the period 08/10/1999 - 01/08/2023. Estimated using a 200-day rolling-window, repeated weighted least squares, and a TVP-VAR model.

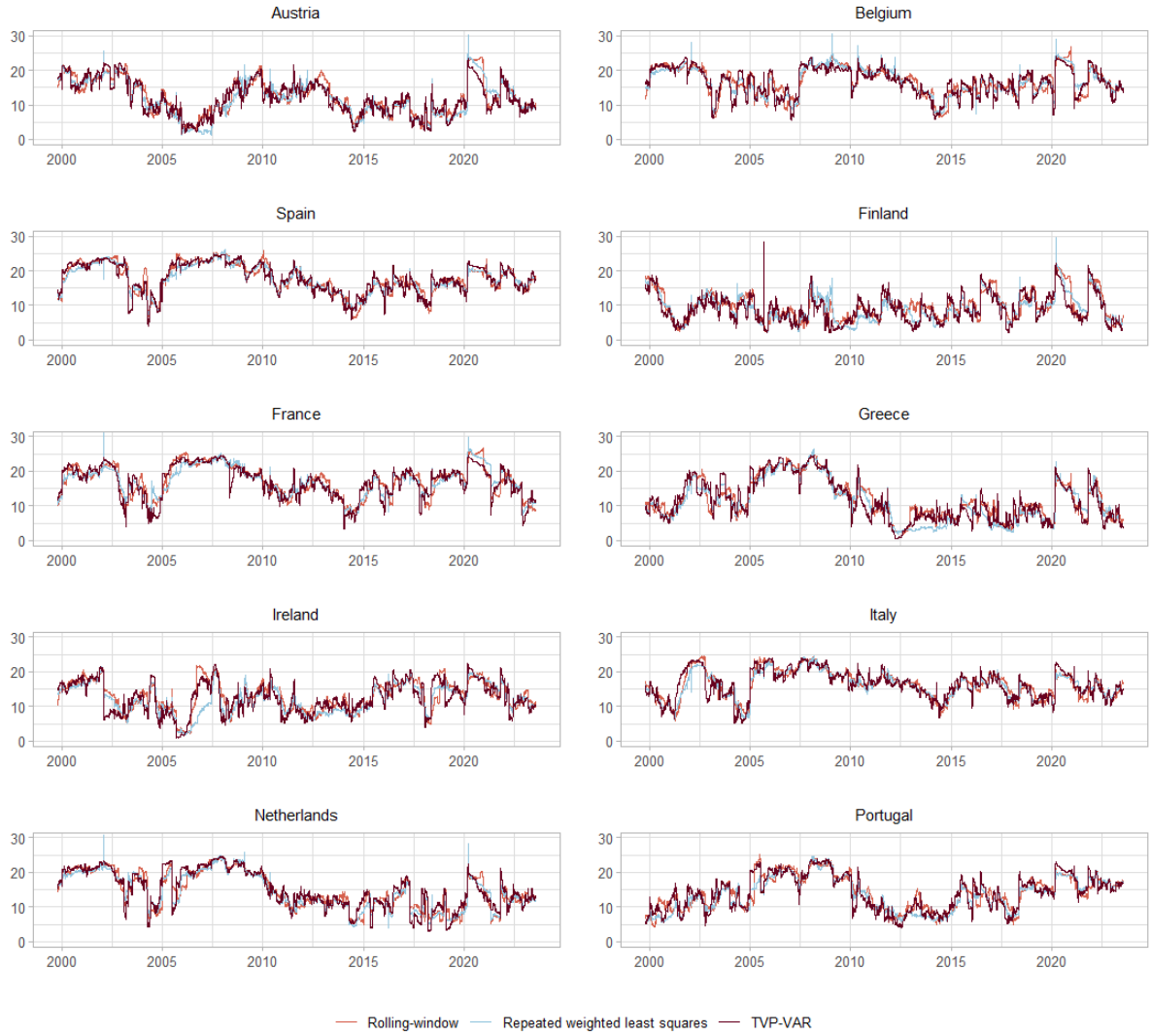

Note: the plot depicts the multiple shock received spillover measure calculated using Equation (28) with time-varying parameter estimates obtained using 200-day rolling-window estimates, repeated weighted least squares where a k-day-old observation is assigned weight λ^k with $\lambda = 0.995$, and TVP-VAR with decay factors $\kappa_1 = 0.99$ and $\kappa_2 = 0.98$.

bringing the transmitted spillover to a new high. The increase of transmitted spillovers from a periphery shock was of a smaller magnitude and increased more steadily. First, in the period between 2004 and 2007, spillovers to France and Portugal increased, followed by substantial increases in spillovers to Belgium in the first half of 2007 pushing the transmitted spillovers to peak levels. The elevated level of transmitted spillovers from a core shock persisted until 2010, whereas the transmitted spillovers of a periphery shock remained at increased levels throughout the sovereign debt crisis, supplying spillover to core countries, especially Belgium and France. This corresponds with studies such as Antonakakis and Vergos (2013) and Claeys and Vašíček

Figure 4: Directional spillovers *from* simultaneous shocks to core and periphery country's sovereign yield spreads, period 08/10/1999 - 01/08/2023. Estimated using a 200-day rolling-window, repeated weighted least squares, and a TVP-VAR model.

Note: the plot depicts the multiple shock transmitted spillover measure calculated using Equation (29) and (30) with time-varying parameter estimates obtained using 200-day rolling-window estimates, repeated weighted least squares where a k-day-old observation is assigned weight λ^k with $\lambda = 0.995$, and TVP-VAR with decay factors $\kappa_1 = 0.99$ and $\kappa_2 = 0.98$.

(2014), who found that sovereign debt markets in the periphery of the Eurozone became dominant transmitters of spillovers to yield spreads in core countries during the sovereign debt crisis. We note that post-crisis, spillovers of simultaneous shocks to the core and periphery to the Netherlands and Greece decrease structurally. Around 2015, the ECB started with the APP, giving rise to a range of smaller peaks occurring between 2015 and 2017. In these peaks, we note that a substantial fraction of the increase in transmitted spillovers is absorbed by Ireland. For the directional spillover from a periphery shock, increases in spillovers to France, Finland, and the Netherlands stand out. Finally, sovereign yield spreads experienced a surge of spillovers from simultaneous shocks during the outbreak COVID-19 pandemic. This surge of spillovers has affected all countries, although the increase of spillovers to Spain is relatively limited compared to other countries in the Eurozone.

The different estimation methods produce almost identical time-varying patterns in the directional multiple shock spillover measures. However, small discrepancies between different measures exist, exhibiting similar patterns as the differences between estimates of the multiple shock spillover index. Although the rolling-window multiple shock spillover index exhibits sev-

Figure 5: Directional spillovers *from* simultaneous shocks to core and periphery country's sovereign yield spreads decomposed into five recipients of spillovers, period 08/10/1999 - 01/08/2023. Estimated using the TVP-VAR model.

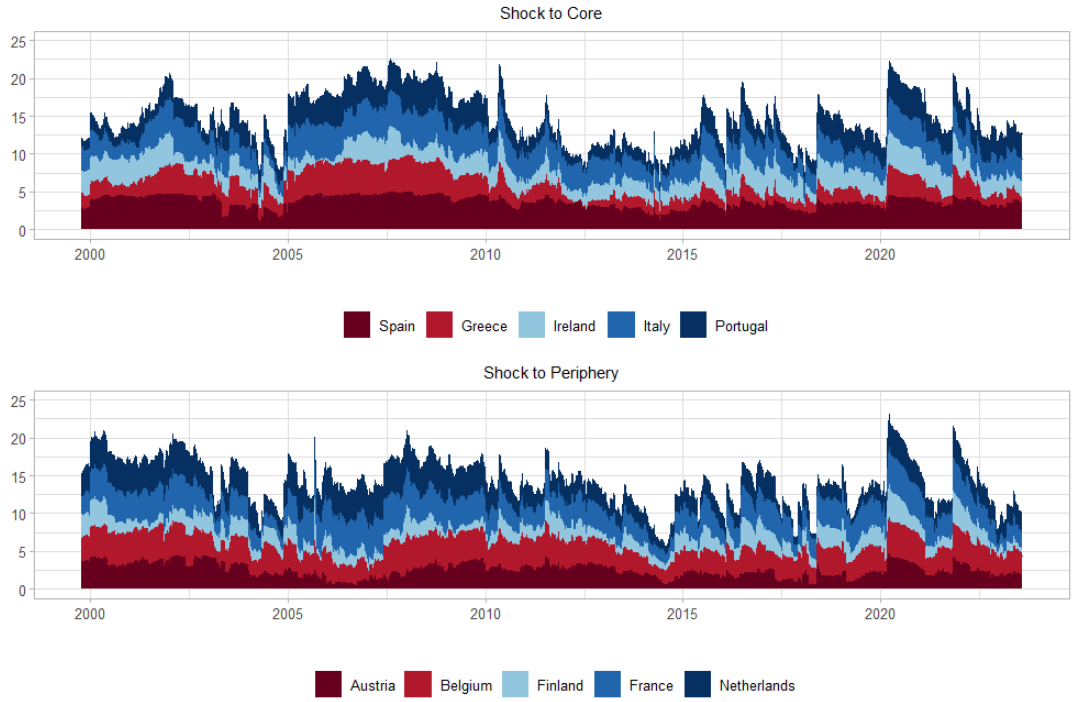

Note: the plot depicts the multiple shock transmitted spillover measure calculated using Equation (29) and (30) with time-varying parameter estimates obtained using TVP-VAR with decay factors $\kappa_1 = 0.99$ and $\kappa_2 = 0.98$, decomposed into the destination countries of the transmitted spillovers.

eral 200-day episodes of elevated spillovers, the directional spillover measures depict fewer of these episodes. Nevertheless, in a small number of cases, the rolling-window estimates of directional spillovers do not adjust quickly to changes, unlike other measures. For example, in 2020, the transmitted spillovers from a simultaneous shock to the periphery increased in response to the outbreak of the COVID-19 pandemic. After the initial panic subsided, the transmitted spillover measures estimates with repeated weighted least squares and TVP-VAR quickly declines, whereas the rolling-window estimate remained high for a 200-day period in which it greatly overestimates the other spillover measures. In several instances, the repeated weighted least squares approach is observed to adjust slowly to change in comparison to other spillover measures. Notably, in Figure 3, the directional spillover to Ireland in 2006 adjust relatively slowly to changes compared to the spillover measures computed using the other approaches. In general, we recognise that the TVP-VAR model adjusts quickest to changes, whereas the rolling-window approach has the tendency to remain at an increased level after shocks, and the repeated weighted least squares approach produces smooth. but slowly changing, estimates.

5.2 Bilateral spillover analysis

Table 4 presents the full-sample estimates of the direction and intensity of spillovers between different sovereign bond markets in the Eurozone. The entries of Table 4 report the own and cross variance shares of a shock to sovereign yield spreads onto other sovereign yield spreads. Here, the ijth entry is the estimated contribution to the forecast error variance of yield spread i coming from shocks to yield spread j. The received and transmitted spillovers per country i can be computed by taking the sum over all entries in row i and column i respectively. The total spillover index is presented in the lower right corner.

Table 4: Spillover table, period 04/01/1999 - 01/08/2023

	AT	**BE**	**FI**	**FR**	**NL**	**ES**	**GR**	**IE**	**IT**	**PT**	**Received**
AT	43.1	13.7	2.6	12.9	8.5	7.6	0.6	2.5	6.7	1.8	56.9
BE	10.7	32.9	1.9	14.5	8.3	11.7	0.9	4.9	11.0	3.2	67.1
FI	3.7	3.7	77.7	3.8	4.5	2.2	0.3	1.2	2.2	0.7	22.3
FR	10.4	15.0	2.1	34.7	14.0	9.3	0.7	2.6	9.1	2.2	65.3
NL	8.3	10.5	3.1	17.1	44.4	7.1	0.3	2.3	5.6	1.2	55.6
ES	5.9	11.5	1.2	8.9	5.7	32.5	1.6	6.8	19.4	6.4	67.5
GR	1.4	2.7	0.3	1.9	0.6	4.7	76.3	3.2	4.9	3.9	23.7
IE	2.9	7.6	0.9	3.9	2.8	11.0	1.9	50.5	8.6	9.9	49.5
IT	5.4	11.3	1.3	9.2	4.8	20.3	1.5	5.5	34.7	5.8	65.3
PT	2.3	5.6	0.7	3.3	1.6	10.4	2.6	10.7	9.2	53.7	46.3
Transmitted	50.9	81.7	14.1	75.5	50.8	84.4	10.5	39.7	76.7	35.1	Total spillover index = 52.0%
Transmitted, including own	94.1	114.6	91.8	110.2	95.3	116.9	86.7	90.2	111.4	88.8	
Net spillovers	-5.9	14.6	-8.2	10.2	-4.7	16.9	-13.3	-9.8	11.4	-11.2	

Note: the table shows spillover measures, based on Equations (18)-(22), calculated from generalised forecast error variance decompositions based on 10-step-ahead forecasts. The received, transmitted, and net spillovers displayed in the table are N times larger than the ones computed using Equations (20)-(22). Abbreviations: AT, Austria; BE, Belgium; ES, Spain; FI, Finland; FR, France; GR, Greece; IE, Ireland; IT, Italy; NL, the Netherlands; PT, Portugal.

The results in Table 4 highlight the influential role of Spain, Italy, France, and Belgium in sovereign debt markets in the Eurozone. These countries represent the four primary recipients and transmitters of spillover effects. Additionally, they are the sole contributors with a positive net spillover, indicating that they transmit more spillover than they receive. In contrast, the remaining countries exhibit negative net spillovers. For the first three countries in this category, their prominent role in the transmission of spillovers can be attributed to the size of their economies. France, Italy, and Spain are the second, third, and fourth-largest economies in the EU. Furthermore, as previously noted, these countries are characterised by high public debt. The size of the economy and the high public debt gives a plausible explanation for the prominent role of these countries in the Eurozone debt market. Belgium, despite having a moderately sized economy, has, with a debt-to-GDP ratio of 106.0%, the second highest debt in the core, making it a prominent importer and exporter of spillovers (Metiu, 2012; Ang and Longstaff, 2011).

Finland and Greece are among the least influential countries in the Eurozone debt market, taking first and second rank in received and transmitted spillovers. The multiple shock spillover index measures identify the same countries as least subject to spillovers. Although Greece was the first country to face financial distress during the sovereign debt crisis, the spillover table exhibits no evidence of spillovers from Greece to other Eurozone countries. The limited influence of Greece is affirmed by other studies, such as Philippas and Siriopoulos (2013), who provide evidence showing that the overall spillover effects of the Greek market on other European bond markets are of minor importance. According to Mink and De Haan (2013) spillovers from Greece to the rest of the EU could arguably be reduced by investors' acknowledgment of the bad state of Greek public finance in early 2010, giving them a wake-up call regarding the domestic fiscal position of other countries.

From Table 4, several interesting bilateral spillover relations stand out. For example, France is strongly connected to both Belgium and the Netherlands. Respectively, 15.0% and 14.0% of France's forecast error variance come from innovations in Belgium and the Netherlands. Correspondingly, France's sovereign yield spread spills over into the yield spread in Belgium and the Netherlands with 14.5% and 17.1% of forecast error variance coming from shocks in France. As noted, France and Belgium are dominant players in spillover dynamics in the core, which is also reflected in the bilateral linkages. Similarly, a strong bilateral relation between Spain and Italy can be found in the periphery, where Spain transmits 20.3% and receives 19.4% to and from Italy. These bilateral linkages further affirm the prominent role of Spain, Italy, France, and Belgium in sovereign debt markets in the Eurozone.

Figure 6 presents the temporal variation of the ordinary spillover index throughout the sample period. The total spillover index depicts several distinct periods in which the index reaches record levels. These instances mostly occur simultaneously with the peak levels in the multiple shock spillover index, with a few notable exceptions. During this period, yield spreads reached unprecedented levels, in particular in countries such as Greece, Portugal, and Ireland. Although this period is also noticeable in the total spillover index, the increase is relatively moderate compared to the magnitude of the sovereign debt crisis. The peaks in spillovers during the Eurozone crisis perfectly coincide with important events, for example, the spillover index achieved a record level of 80.1 in response to the first bailout package for Greece on May 5th, 2010. In contrast to the ordinary total spillover index, the multiple shock spillover index exhibits a negative trend throughout the sovereign debt crisis. This implies that during the sovereign debt crisis, a large share of spillovers between sovereign yield spreads occurred within the core and the periphery. This is in line with Antonakakis and Vergos (2013), who find that the within-effect of spillovers is substantial during the sovereign debt crisis. A second difference can be observed around the introduction of the APP, where the amount of spillover is much higher compared to the multiple shock spillover index, again indicating the importance of the within-effect.

Figure 6: Total spillover index, period 08/10/1999 - 01/08/2023

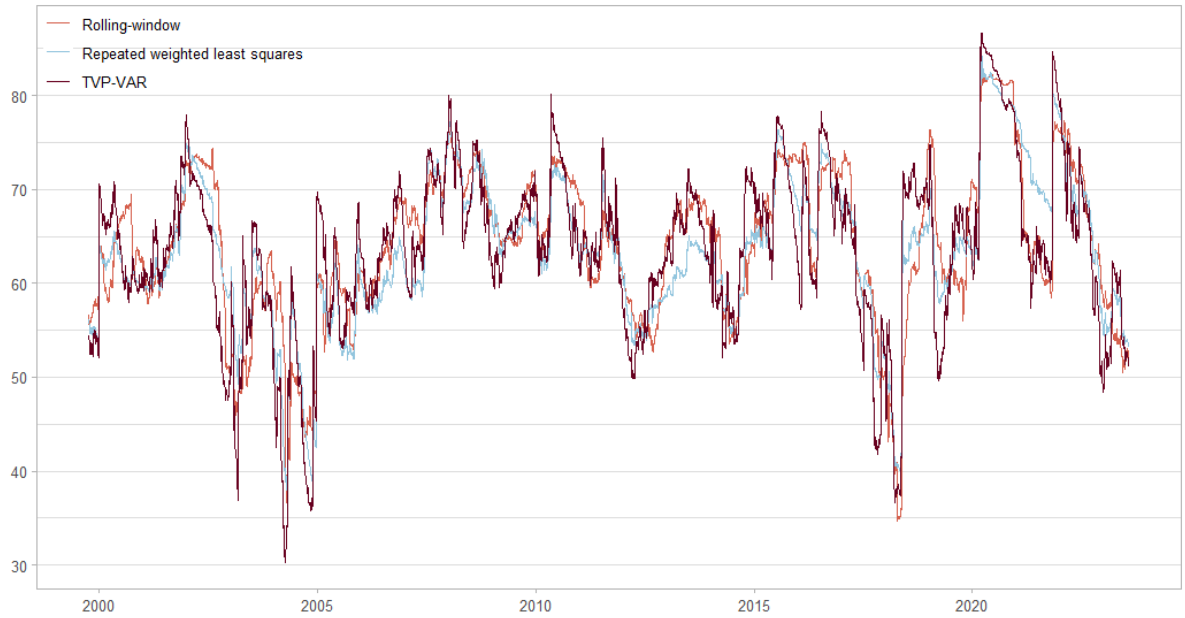

Note: the plot depicts the total spillover index calculated using Equation (19) with time-varying parameter estimates obtained using 200-day rolling-window estimates, repeated weighted least squares where a k-day-old observation is assigned weight λ^k with $\lambda = 0.995$, and TVP-VAR with decay factors $\kappa_1 = 0.99$ and $\kappa_2 = 0.98$.

The comparison of the estimation methods for the ordinary spillover index yields similar results as discussed in previous sections. The TVP-VAR model adjusts quickest to changes, whereas the rolling-window approach has the tendency to remain at an increased level after shocks, such as can be seen in the pandemic period between 2020 and 2021. The repeated weighted least squares approach produces smooth, but slowly changing, estimates.

Figures 7 and 8 illustrate the bidirectional spillover to and from individual sovereign yield spreads over the period since the introduction of the euro. Examining whether countries function as net importers or net exporters of spillovers within the Eurozone, Figure 9 presents the time-varying net spillover measure, indicating the difference between transmitted and received spillovers. In general, transmitted spillovers exhibit greater temporal variation than received spillovers. We also note that most countries are not consistently net recipients nor net transmitters, but they rather switch back and forth between being a net recipient and net transmitter throughout the sample period. Additionally, we observe that substantial increases and decreases in received spillovers are frequently accompanied by corresponding movements in transmitted spillovers, and vice versa. The different estimation methods produce almost identical time-varying patterns in the directional and net spillover measures. However, small discrepancies between the different measures exist, exhibiting similar patterns as the differences between estimates of the total spillover index. Although the rolling-window total spillover index exhibits several 200-day episodes of elevated spillovers, the directional and net spillover measures depict fewer of

Figure 7: Directional spillovers *to* each country's sovereign yield spreads in the period 08/10/1999 - 01/08/2023. Estimated using a 200-day rolling-window, repeated weighted least squares, and a TVP-VAR model.

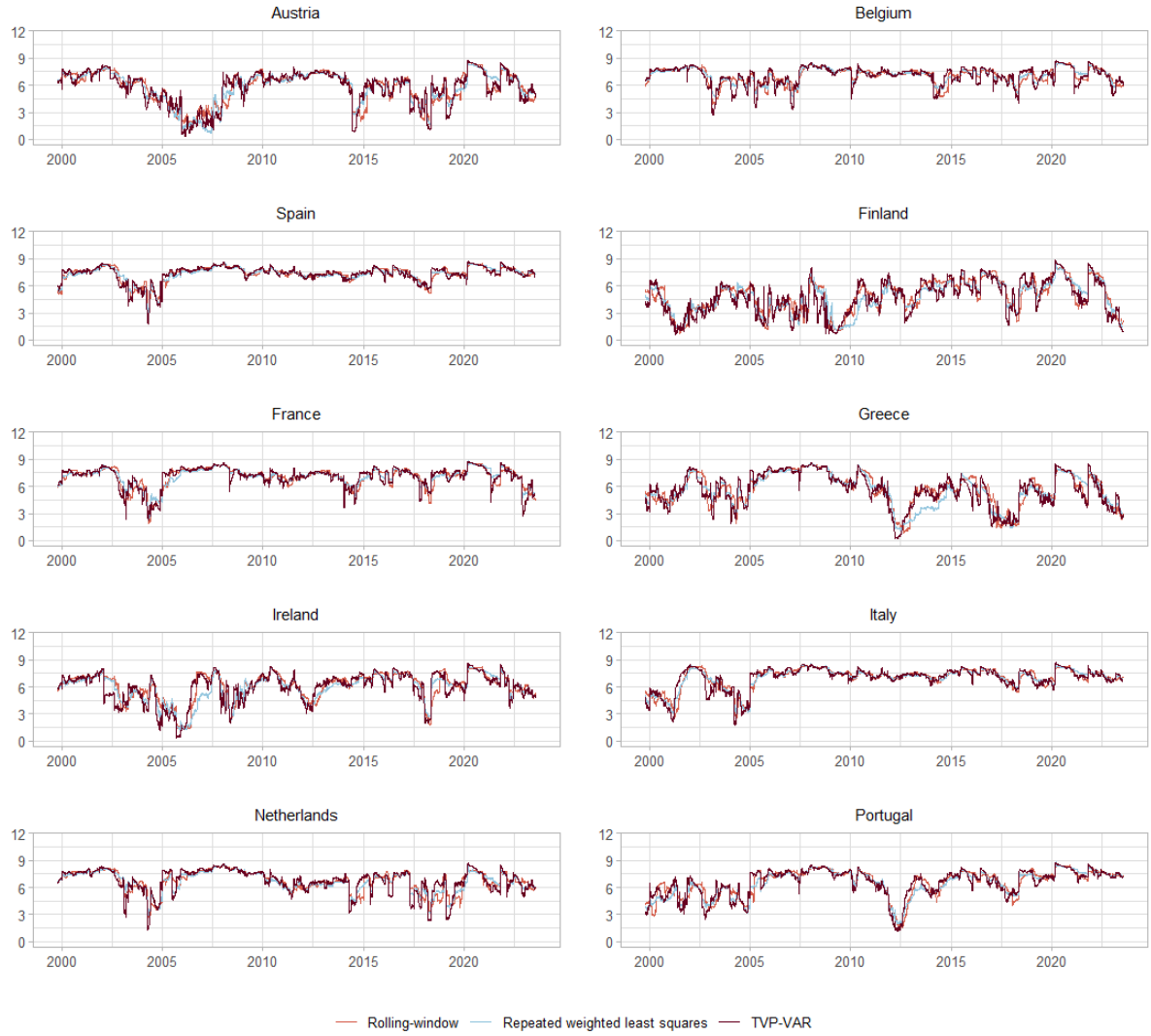

Note: the plot depicts the received spillover calculated using Equation (20) with time-varying parameter estimates obtained using 200-day rolling-window estimates, repeated weighted least squares where a k-day-old observation is assigned weight λ^k with $\lambda = 0.995$, and TVP-VAR with decay factors $\kappa_1 = 0.99$ and $\kappa_2 = 0.98$.

these episodes. However, in a small number of cases, the rolling-window estimate of directional spillovers does not adjust quickly to changes, unlike other measures. For example, in 2006 the rolling-window estimate of the transmitted spillovers of Ireland exhibits a 200-day period during which it greatly overestimates spillovers, compared to the other approaches. In several instances, the repeated weighted least squares approach is observed to adjust slowly to change in comparison to other spillover measures. Notably, in Figure 7, the directional spillover to Greece displays an upward trend between 2012 and 2015. However, whereas the rolling-window and TVP-VAR approaches experience swift increases during this period, the spillover measure estimated using

Figure 8: Directional spillovers *from* each country's sovereign yield spreads in the period 08/10/1999 - 01/08/2023. Estimated using a 200-day rolling-window, repeated weighted least squares, and a TVP-VAR model.

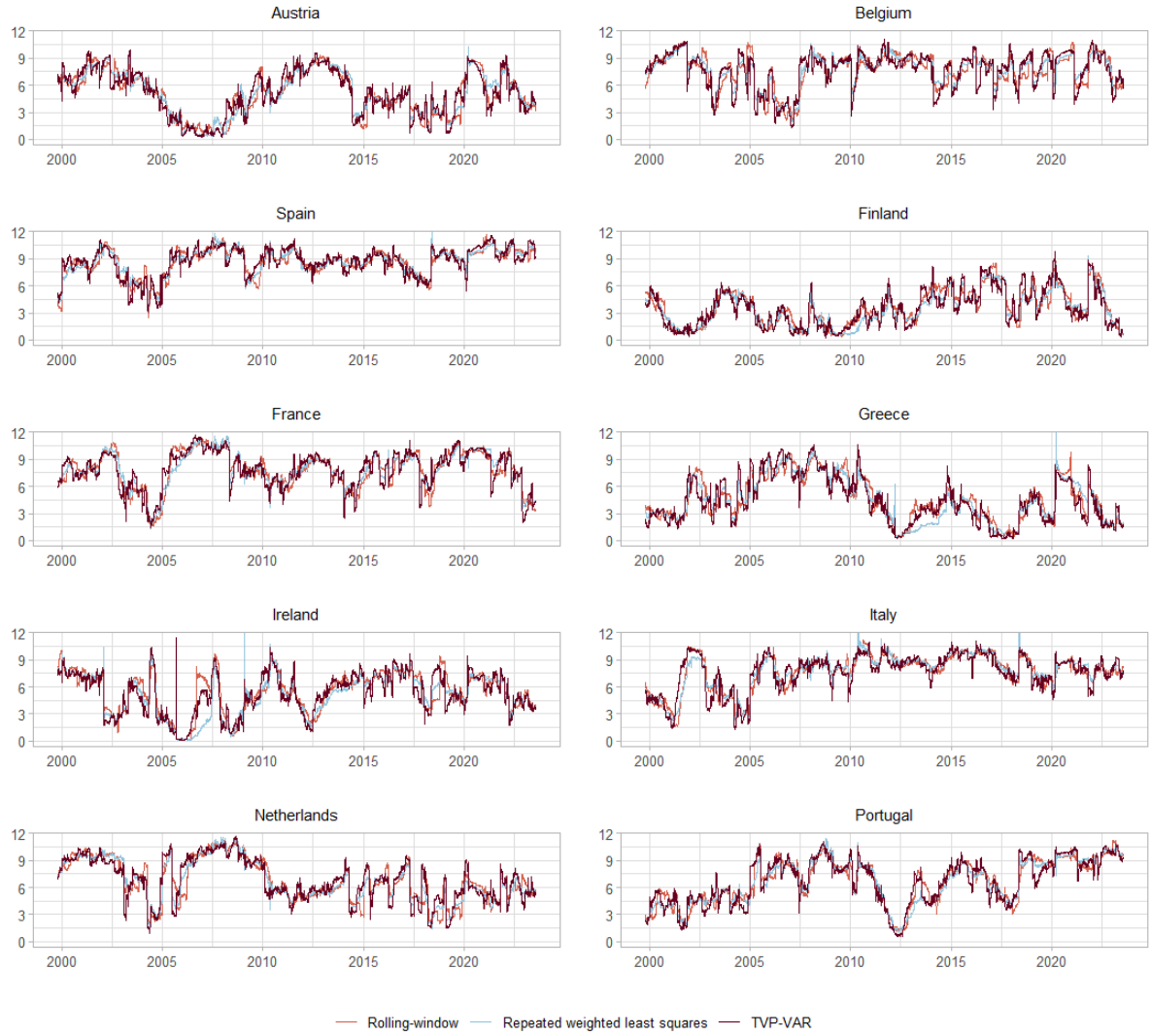

Note: the plot depicts the transmitted spillover calculated using Equation (21) with time-varying parameter estimates obtained using 200-day rolling-window estimates, repeated weighted least squares where a k-day-old observation is assigned weight λ^k with $\lambda = 0.995$, and TVP-VAR with decay factors $\kappa_1 = 0.99$ and $\kappa_2 = 0.98$.

the repeated weighted least squares approach increases at a more gradual pace. Another instance of this phenomenon is observed in the received spillovers in Finland between 2009 and 2011. In general, we recognise that the TVP-VAR model adjusts quickest to changes, whereas the rolling-window approach has the tendency to remain at an increased level after shocks, and the repeated weighted least squares approach produces smooth, but slowly changing, estimates. Based on both directional and net spillover measures, Spain appears to be a consistent net transmitter, only rarely receiving more spillovers than it transmits. Italy is also a major net transmitter of spillovers, although it had gone back and forth between being a net recipient

Figure 9: Net spillovers of each country's sovereign yield spreads in the period 08/10/1999 - 01/08/2023. Estimated using a 200-day rolling-window, repeated weighted least squares, and a TVP-VAR model.

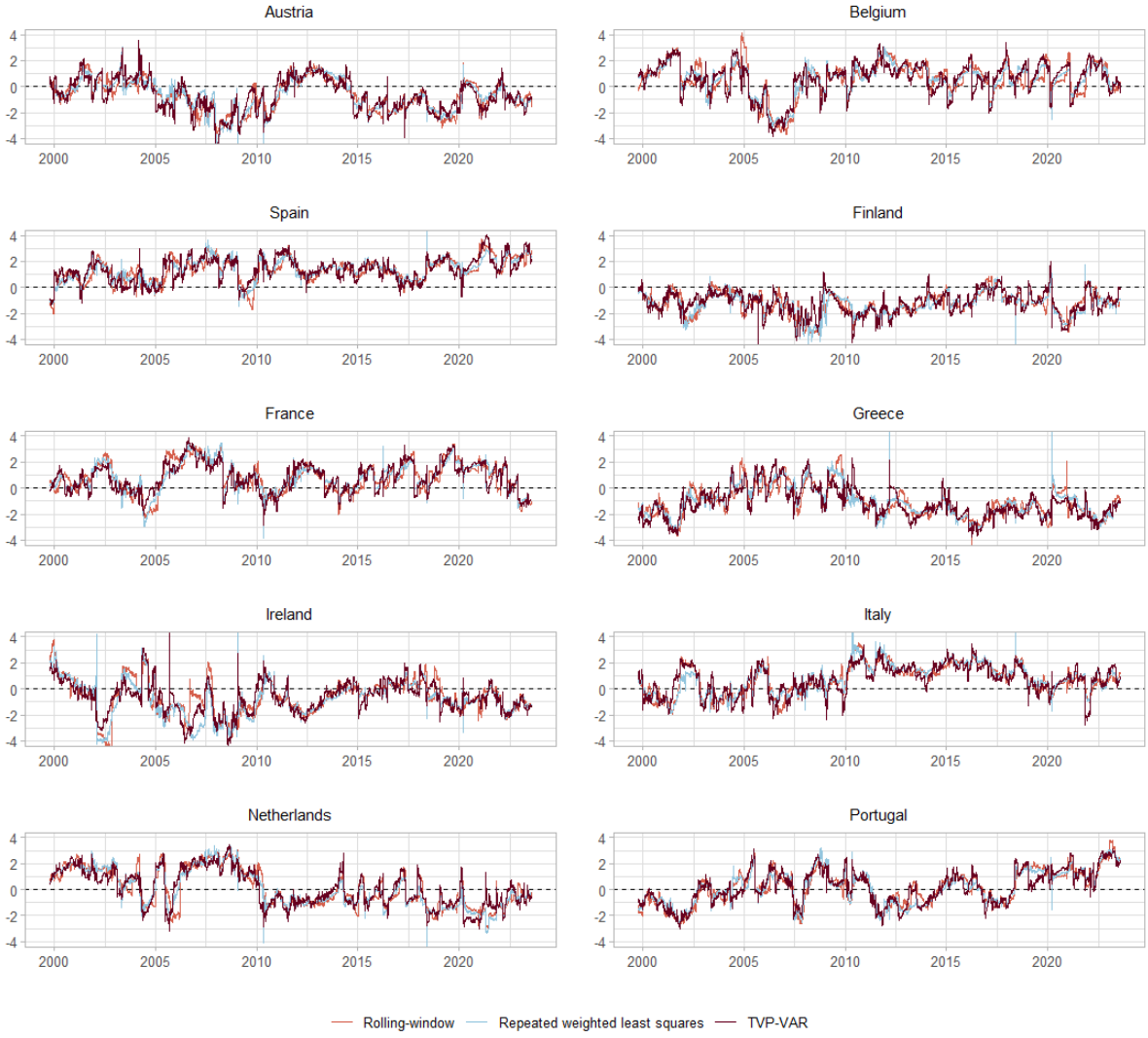

Note: the plot depicts the net spillover index calculated using Equation (22) with time-varying parameter estimates obtained using 200-day rolling-window estimates, repeated weighted least squares where a k-day-old observation is assigned weight λ^k with $\lambda = 0.995$, and TVP-VAR with decay factors $\kappa_1 = 0.99$ and $\kappa_2 = 0.98$.

and net transmitter before the financial crisis, it has solidified its position as one of the most consistent net transmitters since 2010. The importance of Spain and Italy in the transmission of spillovers in the Eurozone is in line with previous studies, such as Galariotis et al. (2016), who find that spillovers run from larger peripheral economies such as Spain and Italy to core countries, and Broto and Pérez-Quirós (2011) who finds both countries to be more affected by events on other EMU markets than by domestic events. Furthermore, France has played a significant role as a spillover supplier, albeit having had more short-lived episodes as a net recipient. Finally, Belgium has predominantly acted as a net transmitter, except for a period between 2005 and 2008. Moreover, the magnitude of net spillovers has been inconsistent dur-

ing the last decade. The role of France and Belgium as a channel to and from the Eurozone core has been documented extensively (De Santis, 2012; Metiu, 2012). Throughout the whole period, only Finland has experienced consistently negative net spillovers, indicating its role as a net recipient. Directional spillovers to Finland have been inconsistent, and Finland transmitted minimal spillovers, resulting in net negative spillovers. Most countries are neither net recipients nor net recipients throughout the sample, but they rather switch back and forth, experiencing episodes as net recipients and net transmitters. For example, Austria has been a large transmitter of spillovers in two multi-year periods: 2000-2004 and 2009-2014. During these episodes, Austria has been a net transmitter, while functioning as a net recipient throughout the rest of the sample period. Portugal has exhibited a positive trend in transmitted spillovers since the sovereign debt crisis, turning it into a net transmitter in 2019. Before the sovereign debt crisis, Portugal had already experienced several episodes with positive net spillovers. During the initial decade of the euro, Ireland has been going back and forth between being a net recipient and net transmitter of spillovers due to unstable transmitted spillovers. In the subsequent decade, the directional spillovers from Ireland stabilised, resulting in a minor net transmitter status between 2014 and 2017, followed by a shift towards negative net spillovers. In certain countries, we observe a structural break somewhere in the sample period. For example, Greece has been a net transmitter until 2010. In the period leading up to the sovereign debt crisis, directional spillovers from Greece dropped substantially, leading to Greece becoming a net recipient of spillovers. Mink and De Haan (2013) argue that this reduction of directional spillovers from Greece to the rest of the Eurozone could arguably be attributed to investors' acknowledgment of the bad state of Greek public finance in early 2010, giving them a wake-up call regarding the domestic fiscal position of other countries. After the sovereign debt crisis, Greece continued to exhibit low levels of transmitted spillovers. Similarly, the Netherlands acts as a net transmitter before the sovereign debt crisis, then shifts to being a net recipient of spillovers.

5.3 Comparison

The full-sample multiple shock spillover index equals 17.1%, which is substantially lower than the ordinary spillover index which amounts to 52.0%. The primary reason why the multiple shock spillover index is lower than the ordinary spillover index, is the fact that the multiple shock spillover measures neglect spillovers within the core and periphery. For example, as previously discussed, a large fraction of directional spillovers to France originate from Belgium and the Netherlands. As the multiple shock spillover measures only measure spillovers from a shock to the periphery to France, the received spillovers from Belgium and the Netherlands are not included in the multiple shock spillover measures resulting in a lower received spillover measure and total spillover index. This difference explains the vast majority of the discrepancy between both indices.

Figure 10: Comparison of the multiple shock index and the ordinary spillover index corrected for the within-effect.

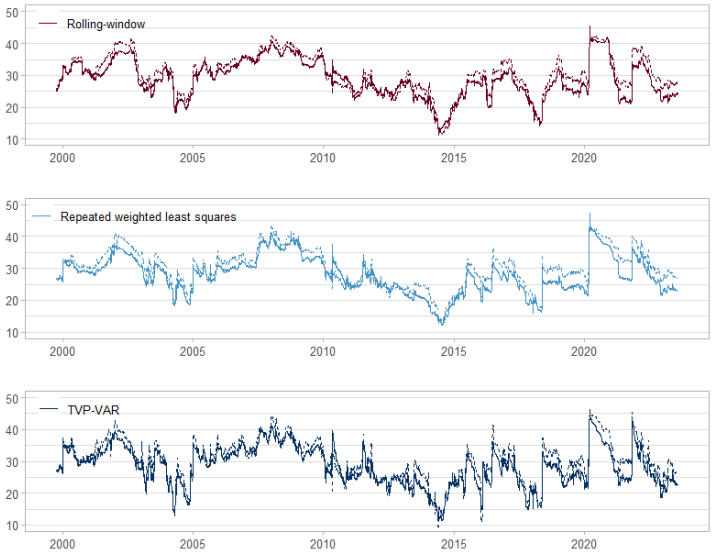

Note: the plot compares the multiple shock spillover index and a benchmark index based on the ordinary spillover index adjusted to ignore the within-effect calculated with time-varying parameter estimates obtained using 200-day rolling-window estimates, repeated weighted least squares where a k-day-old observation is assigned weight λ^k with $\lambda = 0.995$, and TVP-VAR with decay factors $\kappa_1 = 0.99$ and $\kappa_2 = 0.98$. The benchmark index is constructed by taking the sum of all spillovers from core countries to periphery countries, and the other way around, disregarding spillovers from core*(periphery)* countries to other core*(periphery)* countries.

To perform a fair comparison between the multiple shock spillover index and the ordinary spillover index, we create a benchmark index by adjusting the ordinary spillover index to exclude spillovers within the core and periphery. In the full sample, this benchmark index equals 20.2%, compared to the multiple shock spillover index being 17.0%. We assess differences over time by evaluating the comparison of dynamic estimates of the multiple shock index and the benchmark for the rolling-window, repeated least squares, and TVP-VAR approach, displayed in Figure 10. The indices slightly deviate, but in general, we find that both indices depict a very similar time-varying pattern. In general, the benchmark overestimates the multiple shock spillover index by a few percentage points. In Figure 11 we zoom in on the difference between the multiple shock spillover index and the benchmark index during four key moments in the existence of the Eurozone: (i) the introduction of physical currency, (ii) the financial crisis, (iii) the sovereign debt crisis, and (iv) the COVID-19 pandemic. These four graphs show that most often both indices produce quite similar results and the benchmark tends to overestimate the multiple shock spillover index. A notable exception to this generalisation occurred during the sovereign debt crisis, immediately after the agreement on the first bail-out package for Greece. The agreement instantaneously gave confidence to investors in sovereign bonds across the Eurozone and the effects of this event were absorbed by all sovereign debt markets simultaneously, causing the multiple shock spillover index to exceed the benchmark index by more than 5%. For the

Figure 11: Comparison of the multiple shock index and the ordinary spillover index corrected for the within-effect during key moments in the existence of the Eurozone.

Note: the plot compares the multiple shock spillover index and a benchmark index based on the ordinary spillover index adjusted to ignore the within-effect calculated with time-varying parameter estimates obtained using a TVP-VAR model with decay factors $\kappa_1 = 0.99$ and $\kappa_2 = 0.98$ during the four key moments in the existence of the Eurozone: (i) the introduction of physical currency, (ii) the financial crisis, (iii) the sovereign debt crisis, and (iv) the COVID-19 pandemic. The benchmark index is constructed by taking the sum of all spillovers from core countries to periphery countries, and the other way around, disregarding spillovers from core*(periphery)* countries to other core*(periphery)* countries.

multiple shock spillover measures to achieve full potential as a spillover measure, the frequent occurrence of simultaneous shock is paramount. In our application, we work with daily data, limiting the added value of our novel spillover measure. However, the multiple shock spillover measure has great potential as a spillover measure for lower-frequency financial markets data.

5.4 Decomposition

To investigate the origins and destinations of spillovers for each country, we break down the spillover measures. In Figure 12, the directional spillovers to each country's sovereign yield spreads are decomposed into the nine countries from which the received spillovers originate. Figure 13 depicts the directional spillovers from each country's sovereign yield spreads decomposed into the destination of the transmitted spillovers. Moreover, we study the net contribution of different countries on the net spillovers from each country using the decomposed net spillovers presented in Figure 14.

In previous sections, we have highlighted the role of Belgium and France in the core of the Eurozone. The decomposed spillover measures in Figures 12, 13, and 14 confirm that Belgium and France receive and transmit substantial spillover from and to periphery countries. Generally, spillovers to and from the periphery contribute positively to Belgium and France's net spillovers.

Figure 12: Directional spillovers *to* each country's sovereign yield spreads in the period 08/10/1999 - 01/08/2023, decomposed into the sources of spillovers. Estimated using the TVP-VAR model.

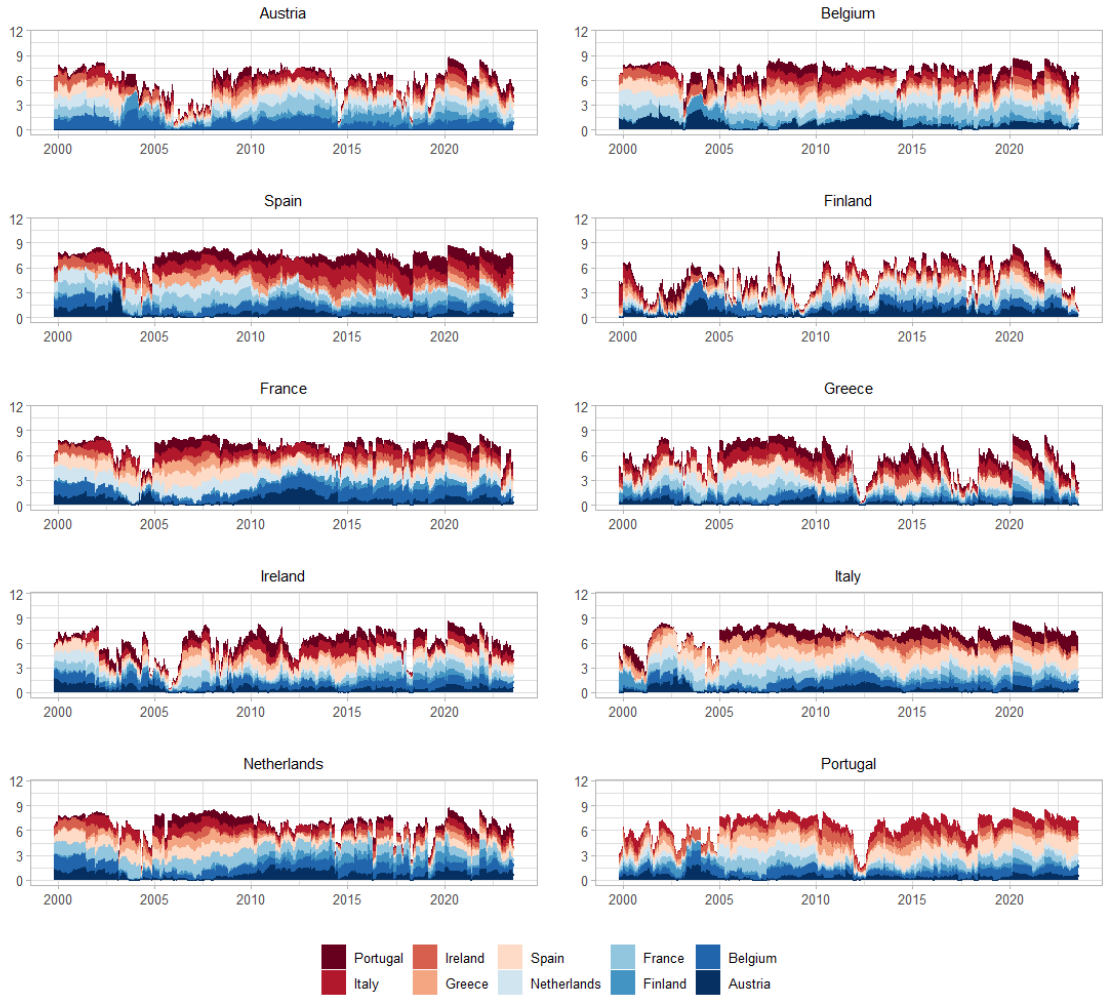

Note: the plot depicts the received spillover calculated using Equation (20) with time-varying parameter estimates obtained using TVP-VAR with decay factors $\kappa_1 = 0.99$ and $\kappa_2 = 0.98$, decomposed into the countries from which the spillovers originate.

However, during the the financial crisis, the contribution of periphery countries to Belgium's net spillover was negative. In the meanwhile, periphery countries' contribution to the net spillover of France was extra positive during the financial crisis. Amidst the sovereign debt crisis, the contribution of the periphery to the net spillovers of both countries was negative. Austria experiences significant spillovers from the periphery. However, the directional spillover from Austria to the periphery is comparatively moderate, resulting in a negative contribution of spillovers to/from the periphery on net spillovers. For the yield spread in Finland, spillovers from the periphery play an important role, but in recent years directional spillovers from Finland to the periphery have caught up. Overall, the contribution of periphery countries on the net spillovers has been negative. Up until the sovereign debt crisis, The Netherlands acted as a net transmitter to periphery countries. However, following the financial crisis, directional spillovers from The

Figure 13: Directional spillovers *from* each country's sovereign yield spreads in the period 08/10/1999 - 01/08/2023, decomposed into the recipients of spillovers. Estimated using the TVP-VAR model.

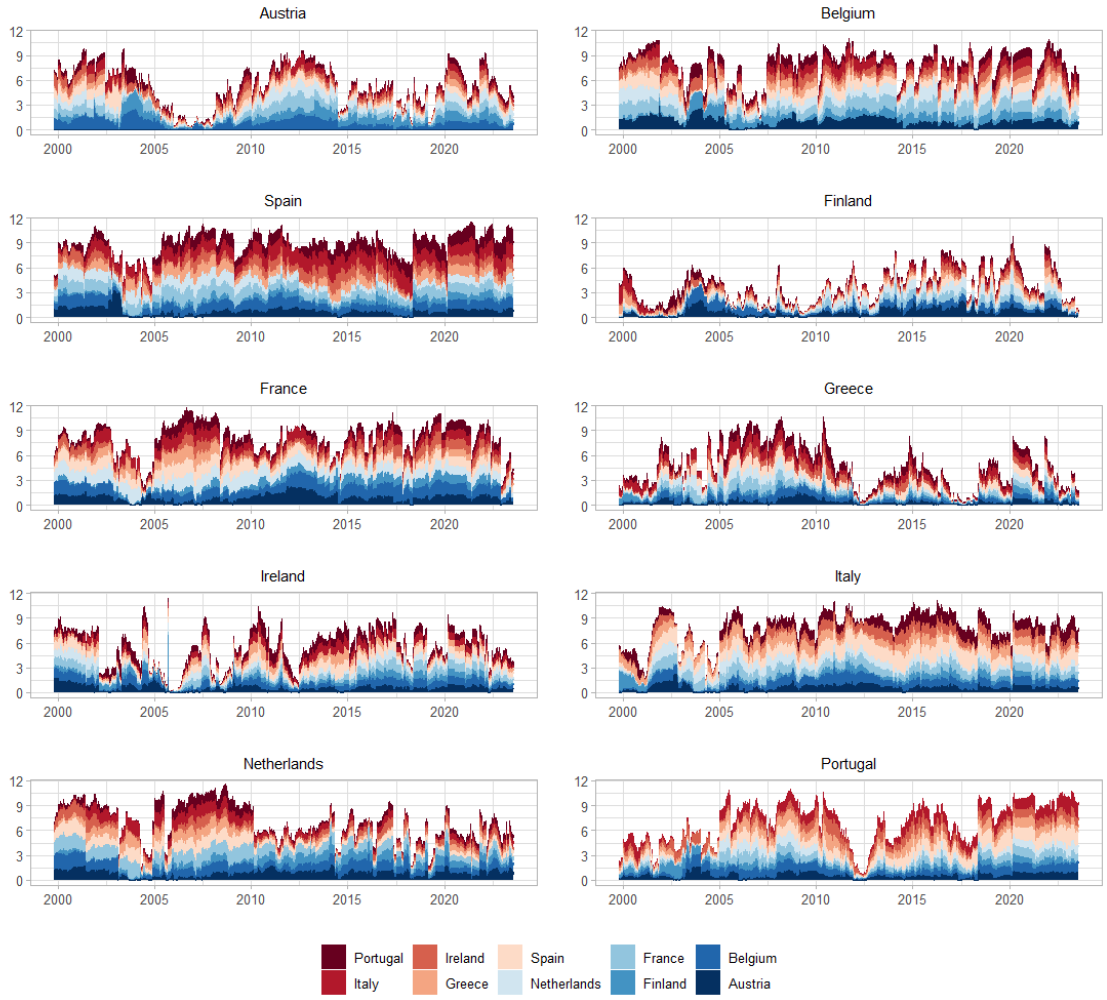

Note: the plot depicts the transmitted spillover calculated using Equation (21) with time-varying parameter estimates obtained using TVP-VAR with decay factors $\kappa_1 = 0.99$ and $\kappa_2 = 0.98$, decomposed into the destination countries of the transmitted spillovers.

Netherlands to periphery countries plummeted, while spillovers from core countries remained approximately constant. Received spillovers remained low post-crisis, leading The Netherlands to become a net recipient of spillovers from the periphery.

The decomposition of spillover measures uncovers that the greatest net transmitters of the Euro-zone periphery, Spain and Italy, transmit the majority of spillovers to other periphery countries. Spillovers to core countries are also considerable, especially during the financial crisis, sovereign debt crisis, and during the pandemic period. Moreover, the bilateral relation between Italy and Spain stands out, as a substantial share of the spillovers to and from Italy originate from Spain, and vice versa. Another noteworthy bilateral relationship exists between Spain and Portugal, with Spain primarily influencing directional spillovers to Portugal. Overall, the net spillovers of

Figure 14: Net spillovers of each country's sovereign yield spreads in the period 08/10/1999 - 01/08/2023, decomposed into the origin of the net spillovers. Estimated using the TVP-VAR model.

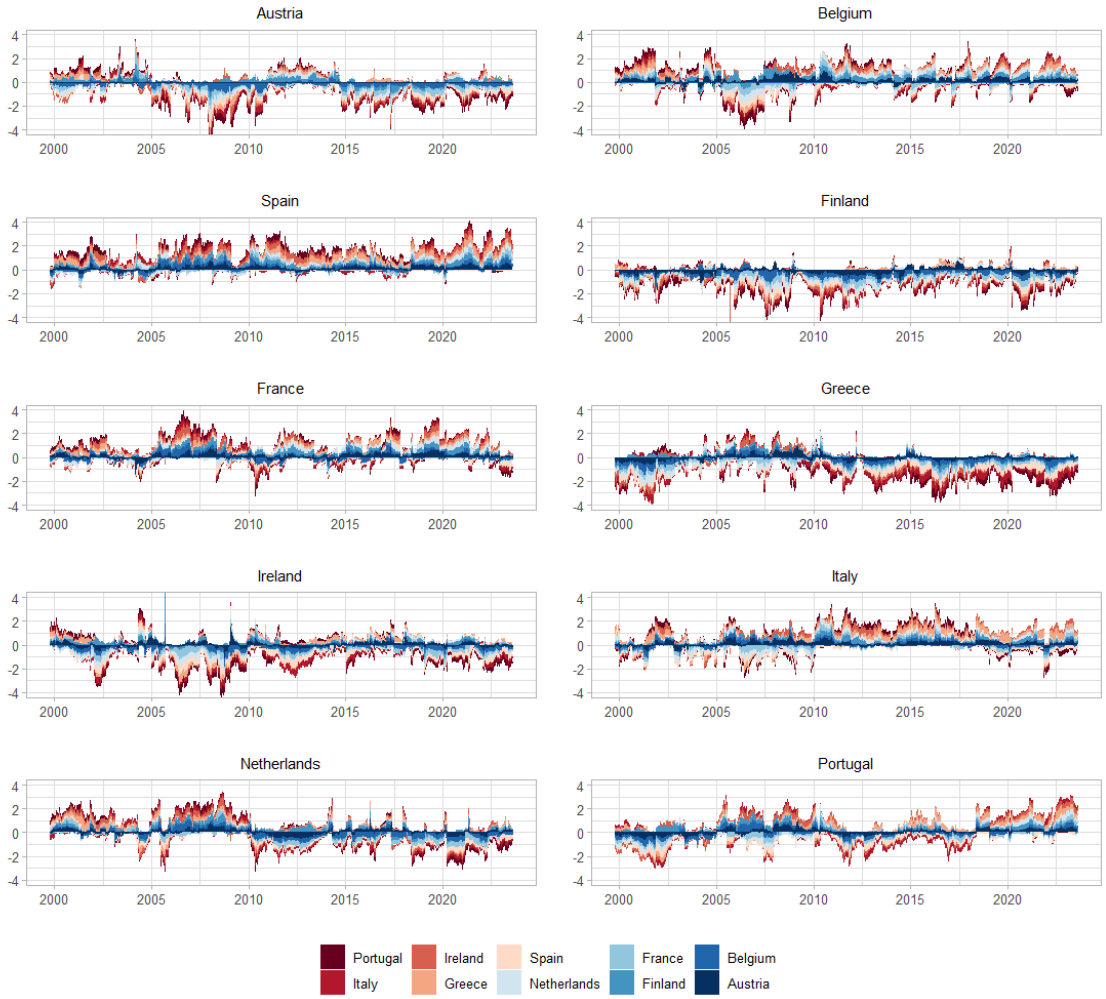

Note: the plot depicts the received spillover calculated using Equation (22) with time-varying parameter estimates obtained using TVP-VAR with decay factors $\kappa_1 = 0.99$ and $\kappa_2 = 0.98$, decomposed into the origin of the net spillovers.

Portugal are comprised of spillovers to/from both core and periphery countries. The influence of Spain and Italy can be observed in Ireland, where the received spillovers are disproportionately influenced by Spain and Italy, especially during the sovereign debt crisis. In the period until 2013, net spillovers of Ireland were negatively influenced by periphery countries, however, this negative influence substantially declined after the sovereign debt crisis. Finally, before the sovereign debt crisis, Greece received spillovers from both core and periphery countries, however, after the crisis spillovers from core countries diminished, while spillovers from periphery countries remained strong. Although Greece transmitted substantial spillovers to other core and periphery countries, the influence of Greece plummeted after the sovereign debt crisis. Overall, Greece has had negative net spillovers which can mostly be attributed to other periphery countries, although the influence of core countries cannot be neglected.

6 Conclusion

To investigate spillover dynamics among sovereign debt markets in the Eurozone since the adoption of the common currency, we measure spillovers using the measures of Diebold and Yilmaz (2009, 2012). We expend their spillover measurement framework by introducing a novel spillover measure that enables us to measure spillovers from a group of countries to the remaining countries. We apply this novel spillover measure to evaluate spillover dynamics between the Eurozone core and periphery countries, and the other way around. As an accurate and timely measurement of spillovers can be of great importance to banks, investors, and policy-makers, we compare three distinct methods of estimating dynamic spillovers: the rolling-window approach (Diebold and Yilmaz, 2009, 2012), the repeated weighted least squares approach (Bataa et al., 2013), and the TVP-VAR approach (Antonakakis et al., 2020). Moreover, we decompose the directional spillovers to gain additional insight into the spillover relations in the Eurozone.

Applying our novel multiple shock spillover index, we find that over the full sample, the multiple shock spillover equals 17.1%. That is, 17.1% of forecast error variance can be traced back to spillovers from simultaneous shocks to sovereign debt markets in the core and periphery of the Eurozone. Spain and Italy are found to be the most susceptible countries to spillovers from the core, whereas Belgium and to a lesser extent France are most receptive to spillovers from the periphery. Moreover, the magnitude of transmitted spillover from a simultaneous shock to the periphery is only slightly larger than from a shock to the core, showing the lack of an unambiguous conclusion regarding the direction of spillovers from the core to the periphery, or the other way around. From our bilateral spillover analysis, we obtain a substantially higher spillover index, amounting to 52.0%. The ordinary and multiple spillover shock differ in the fact that the multiple shock spillover index does not measure spillovers within the core and periphery, resulting in a much lower spillover measure compared to the ordinary spillover index. This indicates that, although a substantial amount of spillovers is transmitted between the core and periphery, the lion's share of spillover occurs within the core and periphery. In both analyses, Belgium, France, Spain, and Italy are the key players when it comes to spillovers in the Eurozone. These four countries, characterised by their large economies and their high public debt, are the main recipients and transmitters of spillovers. The importance of these countries in spillover dynamics in the Eurozone has previously been documented by studies such as Broto and Pérez-Quirós (2011) and Galariotis et al. (2016) for Spain and Italy, and De Santis (2012) and Metiu (2012) for Belgium and France. Two of the main suppliers of spillovers belong to the Eurozone core (Belgium and France), while the other two (Spain and Italy) are part of the periphery, again reflecting the lack of clear direction of spillovers from the periphery to the core, or the other way around. The importance of countries in spillover dynamics can mostly be attributed to the size of the economy and the level of public debt, with large economies with high public debt having a more prominent role.

The spillover indices are not constant over time, as we observe several trends and peaks throughout the sample period, most of which can directly be linked to global events. For example, peaks around the financial crisis, sovereign debt crisis, and the COVID-19 pandemic can be clearly observed. Most of the time increases and decreases in the multiple shock spillover index and the ordinary spillover index take place simultaneously. The only remarkable difference occurred in the sovereign debt, where the multiple shock spillover index experienced a negative trend, which stands in contrast to the ordinary spillover index. This shows that during the sovereign debt crisis, a larger than normal share of spillover occurred within the core and periphery, rather than between the core and periphery, hence studying the within-effect and bilateral relations is crucial to understanding the full extent of spillover dynamics of sovereign debt markets in the Eurozone.

These global events are also visible in the directional spillover measurements, especially during the sovereign debt crisis, with substantial increases in transmitted spillovers from Austria, Spain, France, Ireland, and Portugal. During this time period, Italy was also an important source of spillovers, as it has been consistently since 2005. We observe that spillovers from Greece and the Netherlands structurally decrease after the sovereign debt crisis, for Greece, this is due to a strong decrease of spillovers to the core, while for the Netherlands, a strong decrease of spillovers to the periphery is the cause. In the full sample, we find that Austria, Finland, Greece, Ireland, the Netherlands, and Portugal are net recipients, whereas Belgium, Spain, France, and Italy are net transmitters of spillovers. However, we note that most countries are not consistently net recipients nor net transmitters, but they rather switch back and forth between being a net recipient and net transmitter throughout the sample period. In general, countries tend to switch back and forth between being net recipients and net transmitters during periods of crisis. For example, the Netherlands has been a net transmitter throughout the majority of the period prior the the sovereign debt crisis (1999-2010), but after the sovereign debt crisis, the Netherlands has mostly been a net recipient of spillovers. Unlike studies such as Antonakakis and Vergos (2013) and Claeys and Vašíček (2014) that find that periphery countries transmit to core countries, or studies such as Chatziantoniou and Gabauer (2021) and Umar et al. (2021) that find core countries to be the main transmitters of shocks, we do not find an unambiguous conclusion on the direction of spillovers from the periphery to core, or the other way around.

We compare three different estimation methods to measure the spillover dynamics: the rolling-window approach, the repeated weighted least squares approach, and the TVP-VAR approach. Generally, we find that all methods display very similar time-varying spillover patterns, simultaneously detecting peaks and troughs in the spillover indices. However, upon closer inspection, we see that the spillover index for rolling-window estimates exhibits episodes of increased spillovers that last for exactly 200 days. These increases arise after a shock, after which the index tends to remain high as long as the observation that pertains to the day of the shock is included in the fixed-length rolling window. These 200-day periods of elevated spillovers can be avoided by using the repeated weighted least squares or TVP-VAR approach. The former produces smooth

parameter estimates, however, it does not resolve the persistence as old observations still carry significant weight. The TVP-VAR model on the other hand, albeit being more computationally intensive, produces smooth parameter estimates while swiftly adjusting to new information. For the purpose of timely detection of spillovers, the TVP-VAR model appears to be more suitable than the rolling-window and repeated weighted least squares approach, however, it is difficult to draw a definite conclusion as the underlying spillovers remain unobserved.

Our research contributes to the understanding of spillover dynamics in sovereign debt markets in the Eurozone in a number of ways. First, we introduce a novel multiple shock spillover index that enables us to analyse spillover dynamics between groups of countries. In our case, we use the multiple shock spillover measures to analyse spillovers from a simultaneous shock to the Eurozone core to periphery countries, and the other way around. Furthermore, we analyse dynamic spillovers in the sovereign debt market in the Eurozone using rolling-window, repeated weighted least squares, and TVP-VAR approach and we compare the estimates, finding that for the purpose of timely detection of spillovers, the TVP-VAR is most suitable. Finally, we deconstruct received, transmitted, and net spillover into the origin/destination of spillovers, providing further insight into bilateral spillover dynamics in the Eurozone. For future research, the multiple shock spillover measures could be used to improve understanding of spillovers between the banking system and sovereign yield spreads (Tamakoshi and Hamori, 2013; Alter and Beyer, 2014; Kallestrup et al., 2016), or between international financial markets and sovereign bond markets in the Eurozone Codogno et al. (2003); Bernoth et al. (2012). Furthermore, the multiple shock spillover measures could be used to study spillovers between any set of variables in a time series analysis context.

References

Afonso, A., Arghyrou, M. G., and Kontonikas, A. (2015). The determinants of sovereign bond yield spreads in the EMU. *ECB Working Paper No. 1781*.

Alter, A. and Beyer, A. (2014). The dynamics of spillover effects during the European sovereign debt turmoil. *Journal of Banking & Finance*, 42:134–153.

Ang, A. and Longstaff, F. (2011). Systemic Sovereign Credit Risk: Lessons from the U.S. and Europe. Technical Report w16982, National Bureau of Economic Research, Cambridge, MA.

Antonakakis, N., Chatziantoniou, I., and Gabauer, D. (2020). Refined Measures of Dynamic Connectedness based on Time-Varying Parameter Vector Autoregressions. *Journal of Risk and Financial Management*, 13(4):84.

Antonakakis, N. and Vergos, K. (2013). Sovereign bond yield spillovers in the Euro zone during the financial and debt crisis. *Journal of International Financial Markets, Institutions and Money*, 26:258–272.

Attinasi, M. G., Checherita-Westphal, C. D., and Nickel, C. (2009). What Explains the Surge in Euro Area Sovereign Spreads During the Financial Crisis of 2007-09? *ECB Working Paper No. 1131*.

Balli, F. (2009). Spillover effects on government bond yields in euro zone. Does full financial integration exist in European government bond markets? *Journal of Economics and Finance*, 33(4):331–363.

Bank for International Settlements (2011). The impact of sovereign credit risk on bank funding conditions. *CGFS Papers No. 43*.

Bataa, E., Osborn, D. R., Sensier, M., and Van Dijk, D. (2013). Structural Breaks in the International Dynamics of Inflation. *Review of Economics and Statistics*, 95(2):646–659.

Bekaert, G., Ehrmann, M., Fratzscher, M., and Mehl, A. (2014). The Global Crisis and Equity Market Contagion: The Global Crisis and Equity Market Contagion. *The Journal of Finance*, 69(6):2597–2649.

BenSaïda, A. (2018). The contagion effect in European sovereign debt markets: A regime-switching vine copula approach. *International Review of Financial Analysis*, 58:153–165.

Bernoth, K., Von Hagen, J., and Schuknecht, L. (2012). Sovereign risk premiums in the European government bond market. *Journal of International Money and Finance*, 31(5):975–995.

Brockwell, P. J. and Davis, R. A. (2016). *Introduction to Time Series and Forecasting*. Springer Texts in Statistics. Springer International Publishing, Cham.

Broto, C. and Pérez-Quirós, G. (2011). Sovereign CDS premia during the crisis and their interpretation as a measure of risk. *Economic Bulletin, Banco de España*, pages 133–142.

Bølstad, J. and Elhardt, C. (2018). Capacity, Willingness, and Sovereign Default Risk: Reassuring the Market in Times of Crisis. *Journal of Common Market Studies*, 56(4):802–817.

Caporale, G. M. and Girardi, A. (2011). Fiscal Spillovers in the Euro Area. *DIW Berlin Discussion Paper No. 1164*.

Cappiello, L., Hoerdahl, P., Kadareja, A., and Manganelli, S. (2006). The Impact of the Euro on Financial Markets. *ECB Working Paper No. 598*.

Chatziantoniou, I. and Gabauer, D. (2021). EMU risk-synchronisation and financial fragility through the prism of dynamic connectedness. *The Quarterly Review of Economics and Finance*, 79:1–14.

Christiansen, C. (2007). Volatility-Spillover Effects in European Bond Markets. *European Financial Management*, 13(5):923–948.

Claeys, P. and Vašíček, B. (2014). Measuring bilateral spillover and testing contagion on sovereign bond markets in Europe. *Journal of Banking & Finance*, 46:151–165.

Codogno, L., Favero, C., and Missale, A. (2003). Yield spreads on EMU government bonds. *Economic Policy*, 18(37):503–532.

Cooley, T. F. and Prescott, E. C. (1976). Estimation in the Presence of Stochastic Parameter Variation. *Econometrica*, 44(1):167.

De Grauwe, P. and Ji, Y. (2013). Self-fulfilling crises in the Eurozone: An empirical test. *Journal of International Money and Finance*, 34:15–36.

De Santis, R. A. (2012). The Euro Area Sovereign Debt Crisis: Safe Haven, Credit Rating Agencies and the Spread of the Fever from Greece, Ireland and Portugal. *ECB Working Paper No. 1419*.

Dickey, D. A. and Fuller, W. A. (1979). Distribution of the Estimators for Autoregressive Time Series With a Unit Root. *Journal of the American Statistical Association*, 74(366):427.

Diebold, F. X. and Yilmaz, K. (2009). Measuring Financial Asset Return and Volatility Spillovers, with Application to Global Equity Markets. *The Economic Journal*, 119(534):158–171.

Diebold, F. X. and Yilmaz, K. (2012). Better to give than to receive: Predictive directional measurement of volatility spillovers. *International Journal of Forecasting*, 28(1):57–66.

Ehrmann, M., Fratzscher, M., Gürkaynak, R. S., and Swanson, E. T. (2011). Convergence and Anchoring of Yield Curves in the Euro Area. *Review of Economics and Statistics*, 93(1):350–364.

Favero, C., Pagano, M., and Von Thadden, E.-L. (2010). How Does Liquidity Affect Government Bond Yields? *Journal of Financial and Quantitative Analysis*, 45(1):107–134.

Fernández-Rodríguez, F., Gómez-Puig, M., and Sosvilla-Rivero, S. (2015). Volatility spillovers in EMU sovereign bond markets. *International Review of Economics & Finance*, 39:337–352.

Gabauer, D. (2022). Package 'connectednessapproach'.

Galariotis, E. C., Makrichoriti, P., and Spyrou, S. (2016). Sovereign CDS spread determinants and spill-over effects during financial crisis: A panel VAR approach. *Journal of Financial Stability*, 26:62–77.

Giordano, R., Pericoli, M., and Tommasino, P. (2013). Pure or Wake-up-Call Contagion? Another Look at the EMU Sovereign Debt Crisis. *International Finance*, 16(2):131–160.

González-Sánchez, M. (2018). Causality in the EMU sovereign bond markets. *Finance Research Letters*, 26:281–290.

Gunnella, V., Lebastard, L., Lopez-Garcia, P., Serafini, R., and Zona Mattioli, A. (2021). The impact of the euro on trade: two decades into monetary union. *ECB Occasional Paper No. 283*.

Kallestrup, R., Lando, D., and Murgoci, A. (2016). Financial sector linkages and the dynamics of bank and sovereign credit spreads. *Journal of Empirical Finance*, 38:374–393.

Kalman, R. E. (1960). A New Approach to Linear Filtering and Prediction Problems. *Journal of Basic Engineering*, 82(1):35–45.

Koop, G. and Korobilis, D. (2013). Large time-varying parameter VARs. *Journal of Econometrics*, 177(2):185–198.

Koop, G. and Korobilis, D. (2014). A new index of financial conditions. *European Economic Review*, 71:101–116.

Koop, G., Pesaran, M., and Potter, S. M. (1996). Impulse response analysis in nonlinear multivariate models. *Journal of Econometrics*, 74(1):119–147.

Ludwig, A. (2014). A unified approach to investigate pure and wake-up-call contagion: Evidence from the Eurozone's first financial crisis. *Journal of International Money and Finance*, 48:125–146.

Metiu, N. (2012). Sovereign risk contagion in the Eurozone. *Economics Letters*, 117(1):35–38.

Mink, M. and De Haan, J. (2013). Contagion during the Greek sovereign debt crisis. *Journal of International Money and Finance*, 34:102–113.

Pesaran, H. and Shin, Y. (1998). Generalized impulse response analysis in linear multivariate models. *Economics Letters*, 58(1):17–29.

Philippas, D. and Siriopoulos, C. (2013). Putting the "C" into crisis: Contagion, correlations and copulas on EMU bond markets. *Journal of International Financial Markets, Institutions and Money*, 27:161–176.

Primiceri, G. E. (2005). Time Varying Structural Vector Autoregressions and Monetary Policy. *The Review of Economic Studies*, 72(3):821–852.

RiskMetrics (1996). Technical Document.

Sims, C. A. (1980). Macroeconomics and Reality. *Econometrica*, 48(1):1.

Sosvilla-Rivero, S. and Morales-Zumaquero, A. (2012). Volatility in EMU sovereign bond yields: permanent and transitory components. *Applied Financial Economics*, 22(17):1453–1464.

Tamakoshi, G. and Hamori, S. (2013). Volatility and mean spillovers between sovereign and banking sector CDS markets: a note on the European sovereign debt crisis. *Applied Economics Letters*, 20(3):262–266.

Umar, Z., Riaz, Y., and Zaremba, A. (2021). Spillover and risk transmission in the components of the term structure of eurozone yield curve. *Applied Economics*, 53(18):2141–2157.

van der Zwan, T. (2023). Multiple Shock Impulse Response Functions. *Working Paper*.

A Data

Table 5: List of 10-year benchmark government yields used for the spillover analysis

Country	Mnemonic	Name	Frequency	Source
Austria	TROE10T	RF AUSTRIA GVT BMK BID YLD 10Y - RED. YIELD	Daily	Datastream
Belgium	TRBG10T	RF BELGIUM GVT BMK BID YLD 10Y - RED. YIELD	Daily	Datastream
Spain	TRES10T	RF SPAIN GVT BMK BID YLD 10Y - RED. YIELD	Daily	Datastream
Finland	TRFN10T	RF FINLAND GVT BMK BID YLD 10Y - RED. YIELD	Daily	Datastream
France	TRFR10T	RF FRANCE GVT BMK BID YLD 10Y - RED. YIELD	Daily	Datastream
Germany	TRBD10T	RF GERMANY GVT BMK BID YLD 10Y - RED. YIELD	Daily	Datastream
Greece	TRGR10T	RF GREECE GVT BMK BID YLD 10Y - RED. YIELD	Daily	Datastream
Ireland	TRIE10T	RF IRELAND GVT BMK BID YLD 10Y - RED. YIELD	Daily	Datastream
Italy	TRIT10T	RF ITALY GVT BMK BID YLD 10Y - RED. YIELD	Daily	Datastream
Netherlands	TRNL10T	RF NETHERLANDS GVT BMK BID YLD 10Y - RED. YIELD	Daily	Datastream
Portugal	TRPT10T	RF PORTUGAL GVT BMK BID YLD 10Y - RED. YIELD	Daily	Datastream

B Sensitivity Analysis

B.1 VAR order

To assess the sensitivity of the spillover measurements to the selection of VAR order p, we compare the estimates of the total spillover index and the multiple shock spillover index estimated with VAR orders $p = 1, 2$, and 4 for the rolling-window, repeated weighted least squares, and TVP-VAR approach. In our analysis, we opt for VAR order $p = 2$, following studies such as Claeys and Vašíček (2014). However, the analysis can be conducted using any VAR order, e.g. in the original paper of Diebold and Yilmaz (2009, 2012) the VAR order of choice is $p = 4$.

Figure 15: Sensitivity of the total spillover index to the VAR order in the rolling-window approach.

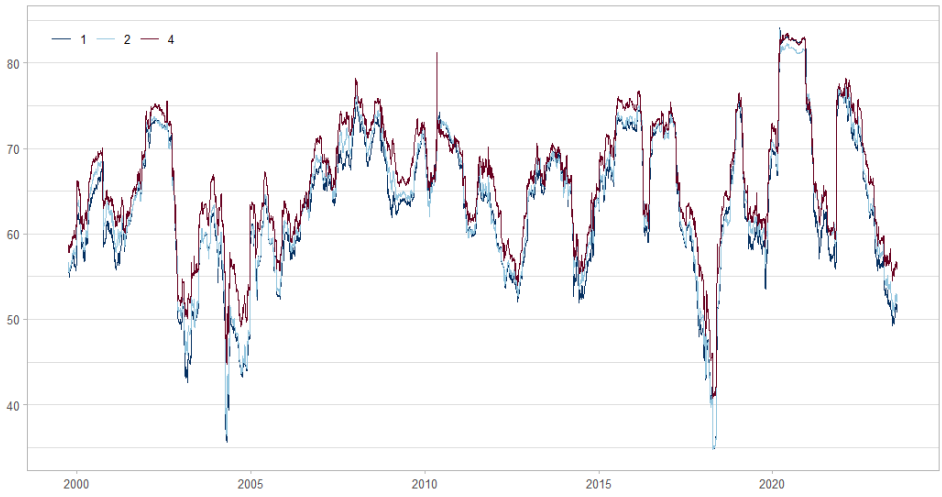

Note: the plot depicts the total spillover index calculated using Equation (19) with time-varying parameter estimates obtained using 200-day rolling-window estimated with VAR orders $p = 1, 2$, and 4.

Figure 16: Sensitivity of the multiple shock spillover index to the VAR order in the rolling-window approach.

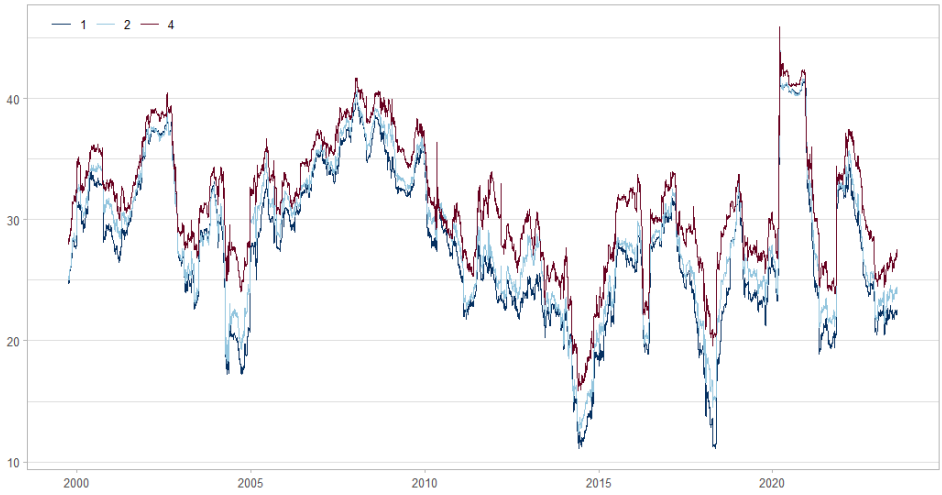

Note: the plot depicts the multiple shock spillover index calculated using Equation (27) with time-varying parameter estimates obtained using 200-day rolling-window estimated with VAR orders $p = 1, 2$, and 4.

Figure 17: Sensitivity of the total spillover index to the VAR order in the repeated weighted least squares approach.

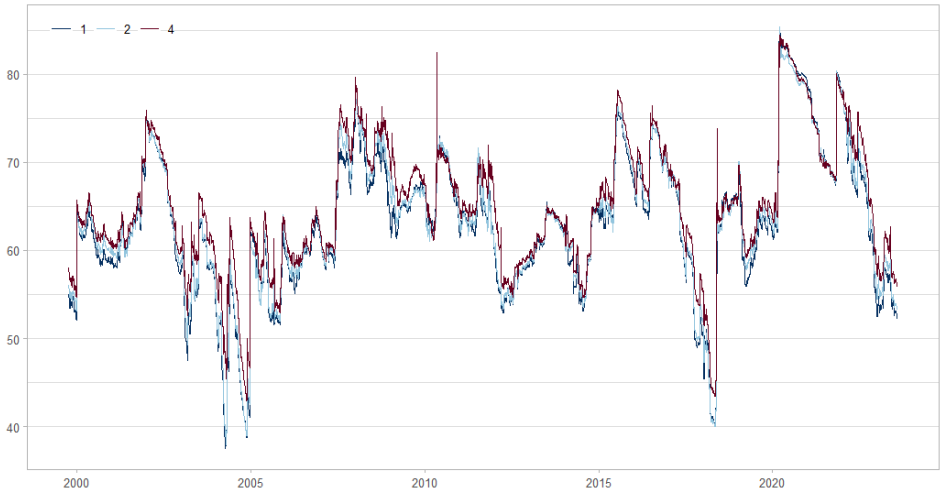

Note: the plot depicts the total spillover index calculated using Equation (19) with time-varying parameter estimates obtained using repeated weighted least squares where a k-day-old observation is assigned weight λ^k where $\lambda = 0.995$ estimated with VAR orders $p = 1, 2$, and 4.

The total spillover indices and multiple shock spillover indices computed using $p = 1, 2$, and 4 are exhibited in Figures 15 and 16 for the rolling-window approach, 17 and 18 for the repeated weighted least squares approach, and 19 and 20 for the TVP-VAR approach. In general, we note that the total spillover indices and multiple shock spillover indices are not very sensitive to the choice of VAR order p. The differences between the multiple shock spillover indices for

Figure 18: Sensitivity of the multiple shock spillover index to the VAR order in the repeated weighted least squares approach.

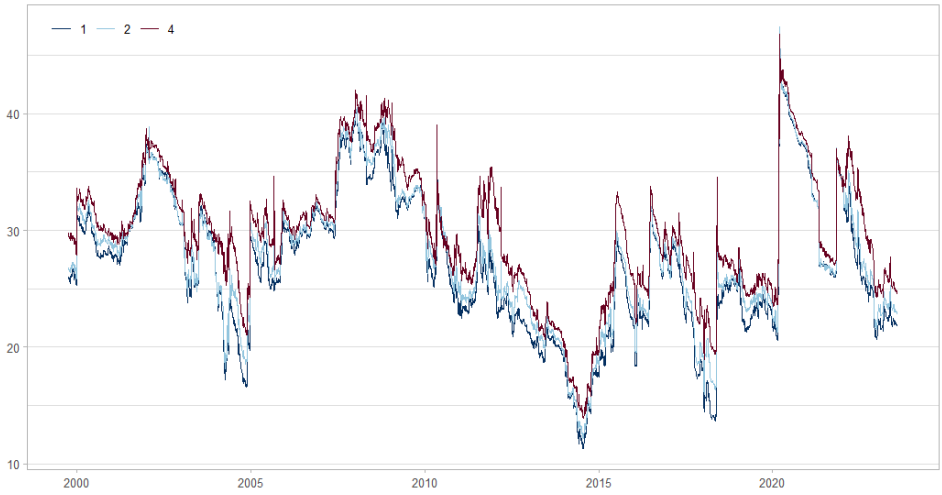

Note: the plot depicts the multiple shock spillover index calculated using Equation (27) with time-varying parameter estimates obtained using repeated weighted least squares where a k-day-old observation is assigned weight λ^k where $\lambda = 0.995$ estimated with VAR orders $p = 1, 2$, and 4.

Figure 19: Sensitivity of the total spillover index to the VAR order in the TVP-VAR approach.

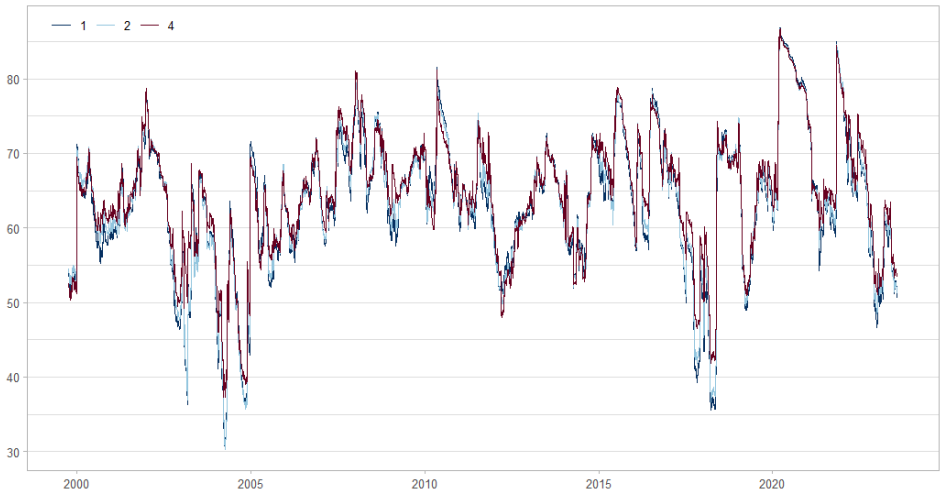

Note: the plot depicts the total spillover index calculated using Equation (19) with time-varying parameter estimates obtained using TVP-VAR model with decay factors $\kappa_1 = 0.99$ and $\kappa_2 = 0.98$ estimated with VAR orders $p = 1, 2$, and 4.

different VAR orders p are larger than the differences between the ordinary spillover indices, showing that the multiple shock spillover index is relatively more sensitive to the choice of VAR order p, albeit sensitivity still being low. For both indices, the rolling-window approach appears to be more sensitive to the choice of VAR order p than the repeated weighted least squares and TVP-VAR approach.

Figure 20: Sensitivity of the multiple shock spillover index to the VAR order in the TVP-VAR approach.

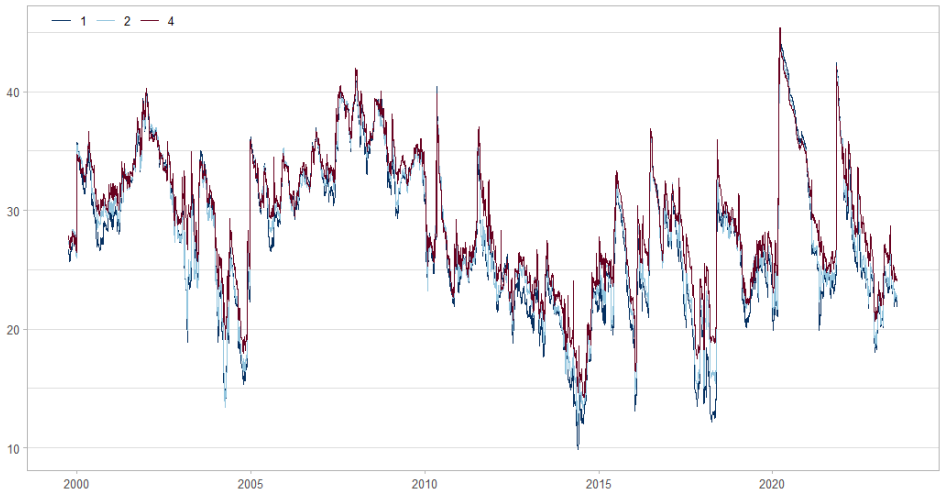

Note: the plot depicts the multiple shock spillover index calculated using Equation (27) with time-varying parameter estimates obtained using TVP-VAR model with decay factors $\kappa_1 = 0.99$ and $\kappa_2 = 0.98$ estimated with VAR orders $p = 1, 2$, and 4.

B.2 Fixed-length window size

The rolling-window estimation approach is subject to the choice of window size. Diebold and Yilmaz (2009, 2012) propose a 200-day rolling window, which is followed by other studies such as Claeys and Vašíček (2014) and Fernández-Rodríguez et al. (2015). Other studies, such as Antonakakis and Vergos (2013) deviate from this standard, opting for a 120-day rolling window. In this section, we compare spillover measures computed using 50, 100, 200, and 500-day rolling windows estimates.

Figure 21: Sensitivity of the total spillover index to the window length.

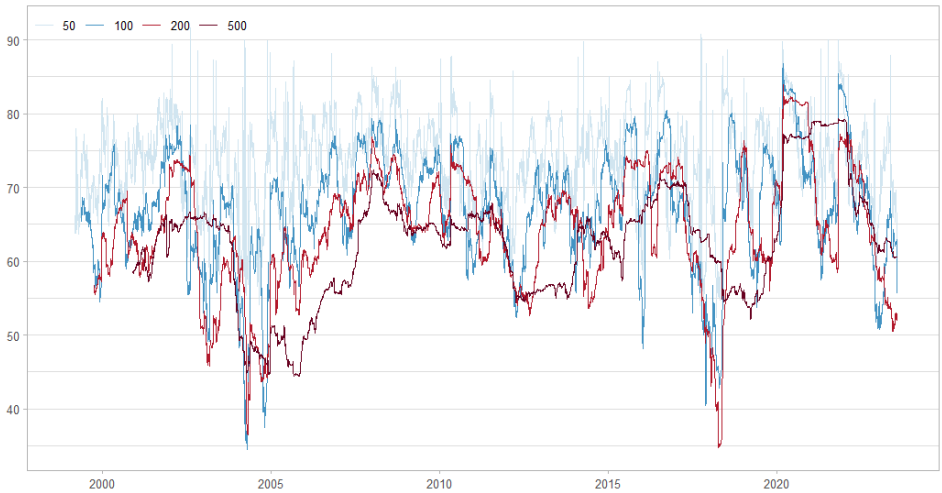

Note: the plot depicts the total spillover index calculated using Equation (19) with time-varying parameter estimates obtained using 50, 100, 200, and 500-day rolling-window estimates.

Figure 22: Sensitivity of received spillovers to the window length.

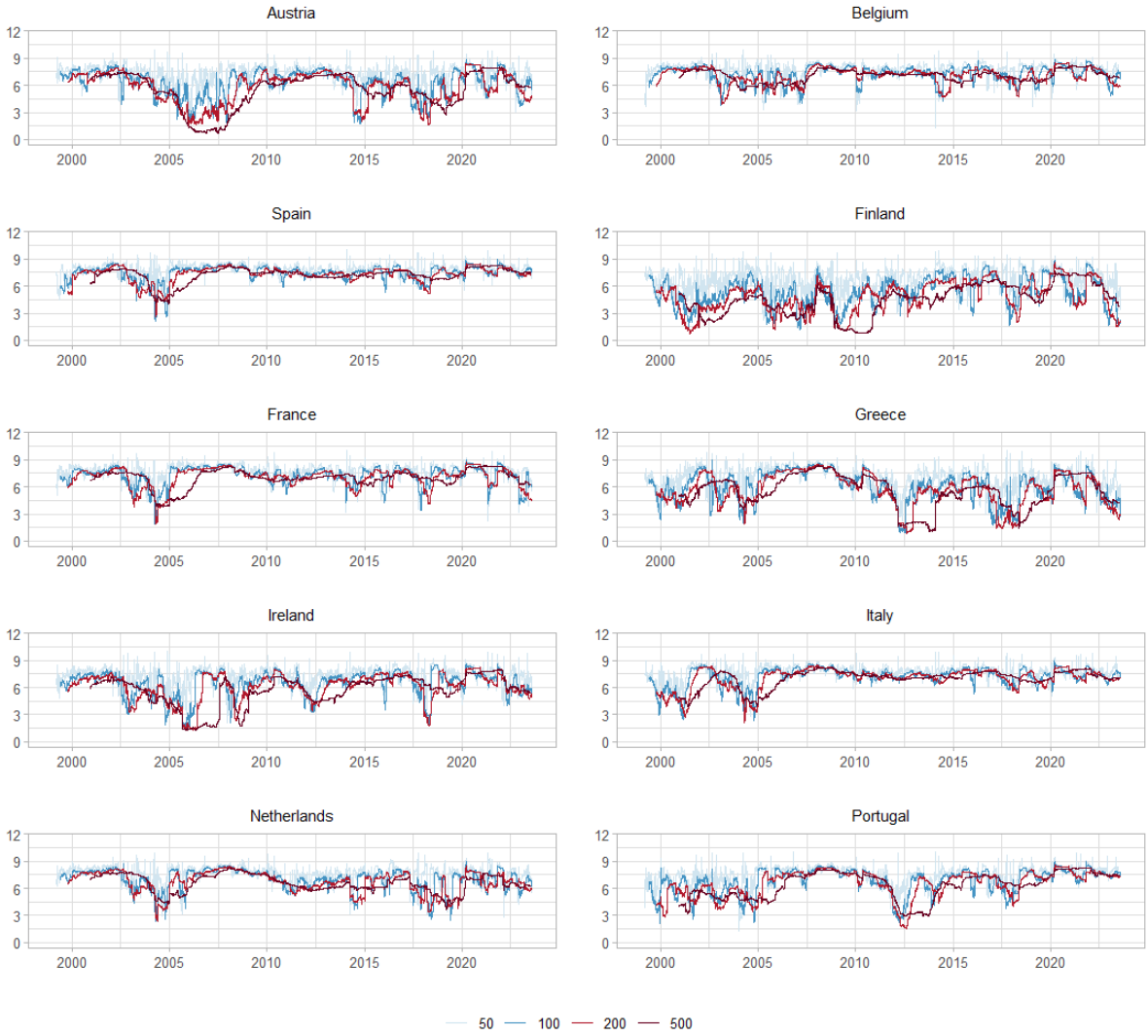

Note: the plot depicts the received spillover calculated using Equation (20) with time-varying parameter estimates obtained using 50, 100, 200, and 500-day rolling-window estimates.

Figure 21 presents the total spillover index estimates using 50, 100, 200, and 500-day rolling-window. The choice of window-length is an important matter, as the resulting total spillover index is very sensitive to the chosen window-length. A short rolling-window results in unstable measurements, resulting in frequent short-lived spikes, impeding one from the ability to see the 'big picture'. However, if the window-size is too large the spillover index becomes very time-invariant and slow-responding to new developments, resulting in a spillover index that only captures big developments such as the financial crisis and the COVID-19 pandemic. Additionally, the choice for a large rolling window leads to a spillover index that depicts longer episodes of elevated spillovers as the observation that pertains to a shock remains in the fixed-length rolling window longer. In general, spillover indices estimated with short window-length tend to overestimate their counterparts estimated with larger rolling windows.

Figure 23: Sensitivity of transmitted spillovers to the window length.

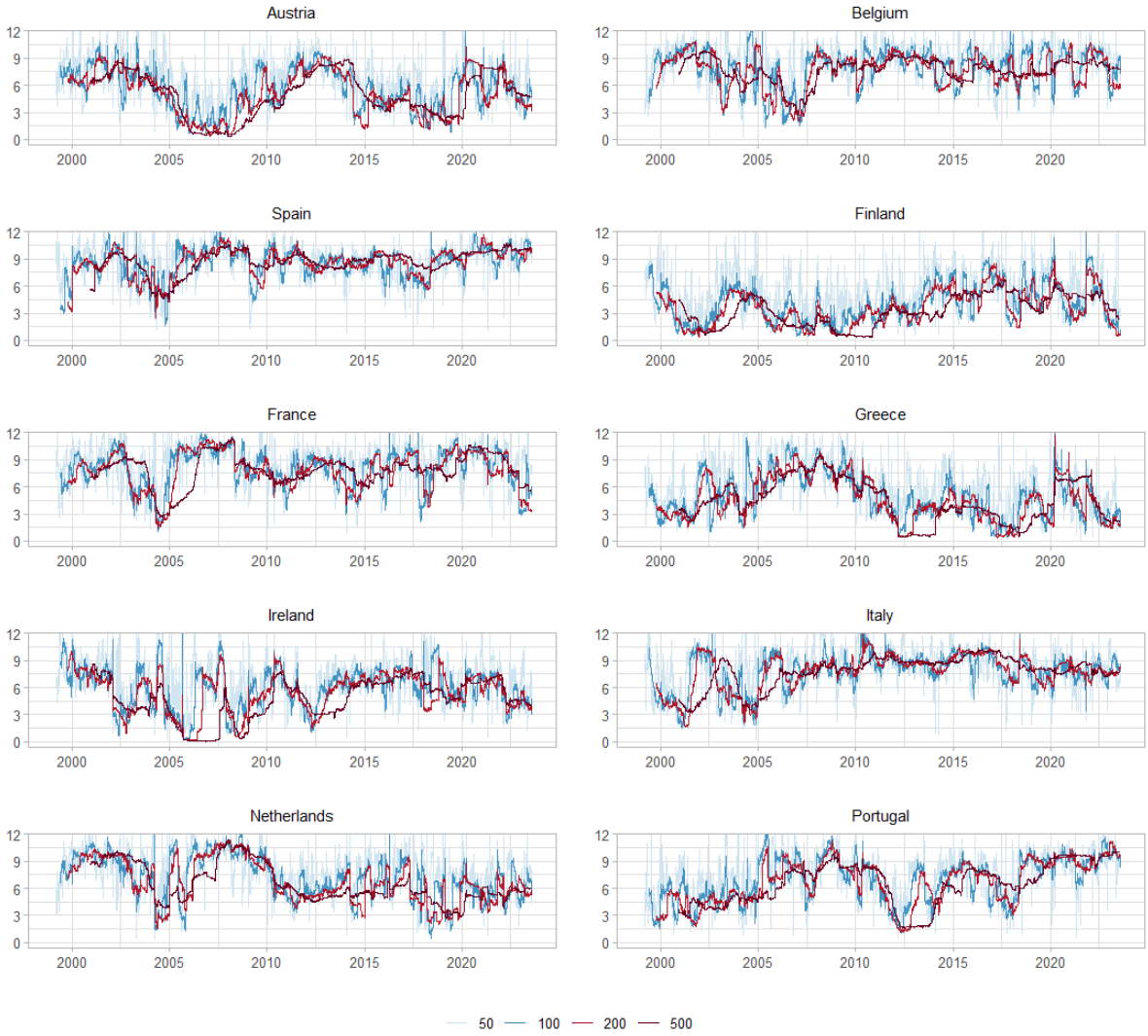

Note: the plot depicts the transmitted spillover calculated using Equation (21) with time-varying parameter estimates obtained using 50, 100, 200, and 500-day rolling-window estimates.

The received, transmitted, and net spillovers are exhibited in Figures 22, 23, and 24 respectively. Similarly to the total spillover index, we find that the received, transmitted, and net spillovers to/from each country are very volatile when estimated with small window-length, making it difficult to draw conclusions on the overall trend in spillovers. However, longer rolling windows result in indices that only capture the main trend and hardly reflect any short-term developments that occur throughout the sample period. The observation that spillover measures with longer rolling windows underestimate their counterparts with short rolling windows is less pronounced in the received, transmitted, and net spillover measures compared to the total spillover index.

Figure 24: Sensitivity of the net spillovers to the window length.

Note: the plot depicts the net spillover calculated using Equation (22) with time-varying parameter estimates obtained using 50, 100, 200, and 500-day rolling-window estimates.

.

Figure 25: Sensitivity of the multiple shock spillover index to the window length.

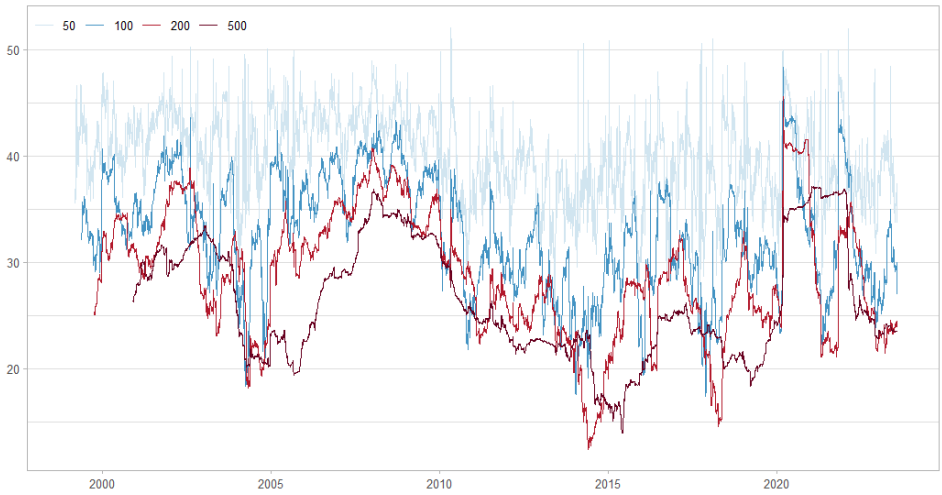

Note: the plot depicts the multiple shock spillover index calculated using Equation (27) with time-varying parameter estimates obtained using 50, 100, 200, and 500-day rolling-window estimates.

Figure 25 displays the multiple shock spillover index computed using parameter estimates obtained using a 50, 100, 200, and 500-day rolling-window approach. Compared to the ordinary spillover index, the multiple shock spillover index is even more sensitive to the choice of window-length. In the multiple shock spillover index estimated with a 50-day rolling window, we can hardly distinguish medium- and long-term trends and the index achieves magnitudes sometimes twice as high as the multiple shock spillover indices estimates with 100- and 200-day rolling windows. On the other hand, the multiple shock spillover index estimated with a 500-day rolling window is only able to medium- and long-term developments, neglecting short-term changes. Moreover, the index depicts episodes of elevated spillovers lasting for 500 days. Similarly to the ordinary spillover index, the multiple shock spillover indices estimated with short window-length tend to overestimate their counterparts estimated with larger rolling windows.

A similar pattern can be found in the received and transmitted spillovers from a simultaneous shock to the core and periphery in Figures 26 and 27. In these figures, measures computed with short window-length produce volatile spillover measures from which hardly any information can be obtained, and which overestimate their counterparts that are estimated with larger rolling windows. The episodes in which the spillover measure remains high for 500 days are less pronounced than in the multiple shock spillover indices, but they remain visible in the spillover measures.

Figure 26: Sensitivity of received spillovers from a simultaneous shock to core and periphery to the window length.

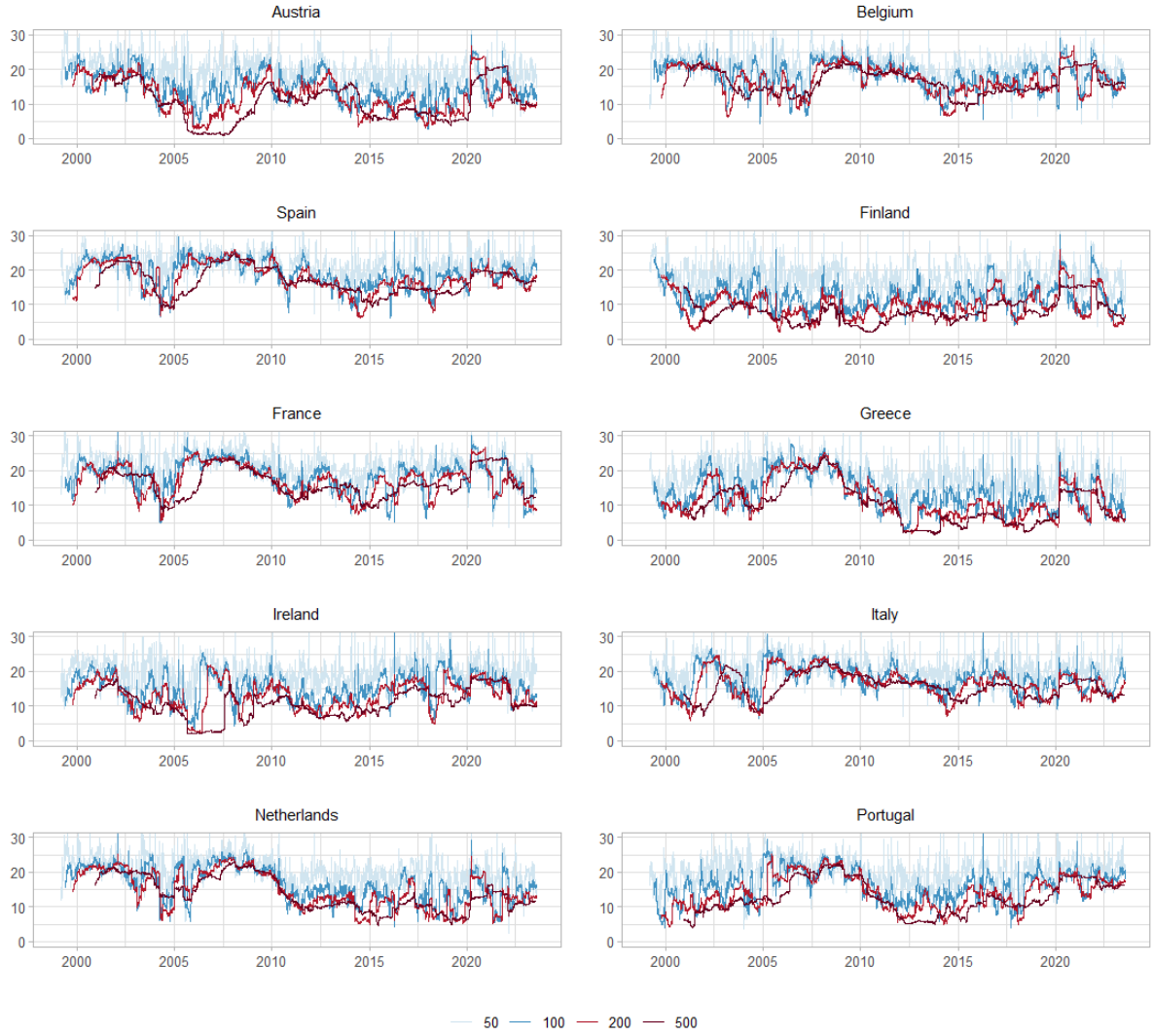

Note: the plot depicts the multiple shock received spillover measure calculated using Equation (28) with time-varying parameter estimates obtained using 50, 100, 200, and 500-day rolling-window estimates.

In conclusion, short rolling windows produce very volatile spillover measures from which hardly any information regarding the 'big picture' can be obtained. On the other hand, if the window-length is too high, the spillover measures only capture long-term trends and react very slowly to changes making it impossible to detect spillovers in a timely manner. Generally, measures estimated with short rolling windows tend to overestimate their counterparts estimated with larger window-lengths.

Figure 27: Sensitivity of transmitted spillovers from a simultaneous shock to core and periphery to the window length.

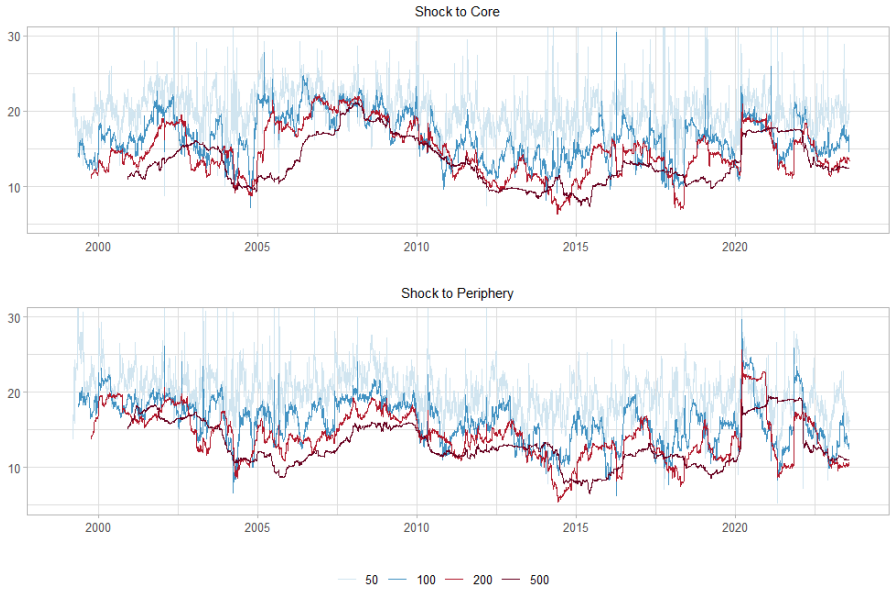

Note: the plot depicts the multiple shock transmitted spillover measure calculated using Equation (29) and (30) with time-varying parameter estimates obtained using 50, 100, 200, and 500-day rolling-window estimates.

B.3 Weighting

In the repeated weighted least squares approach, each observation is assigned a weight based on how old an observation is. By doing so, we give less weight to older observations, without entirely discarding these potentially informative observations. That is, we estimate the VAR

Figure 28: Sensitivity of the total spillover index to the weighting of observations.

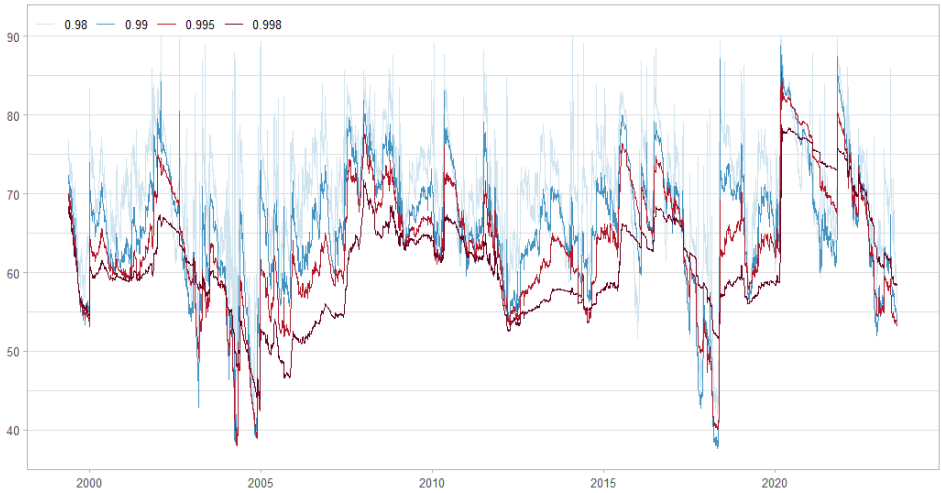

Note: the plot depicts the total spillover index calculated using Equation (19) with time-varying parameter estimates obtained using repeated weighted least squares where a k-day-old observation is assigned weight λ^k with $\lambda = 0.98, 0.99, 0.995$, and 0.998.

Figure 29: Sensitivity of received spillovers to the weighting of observations.

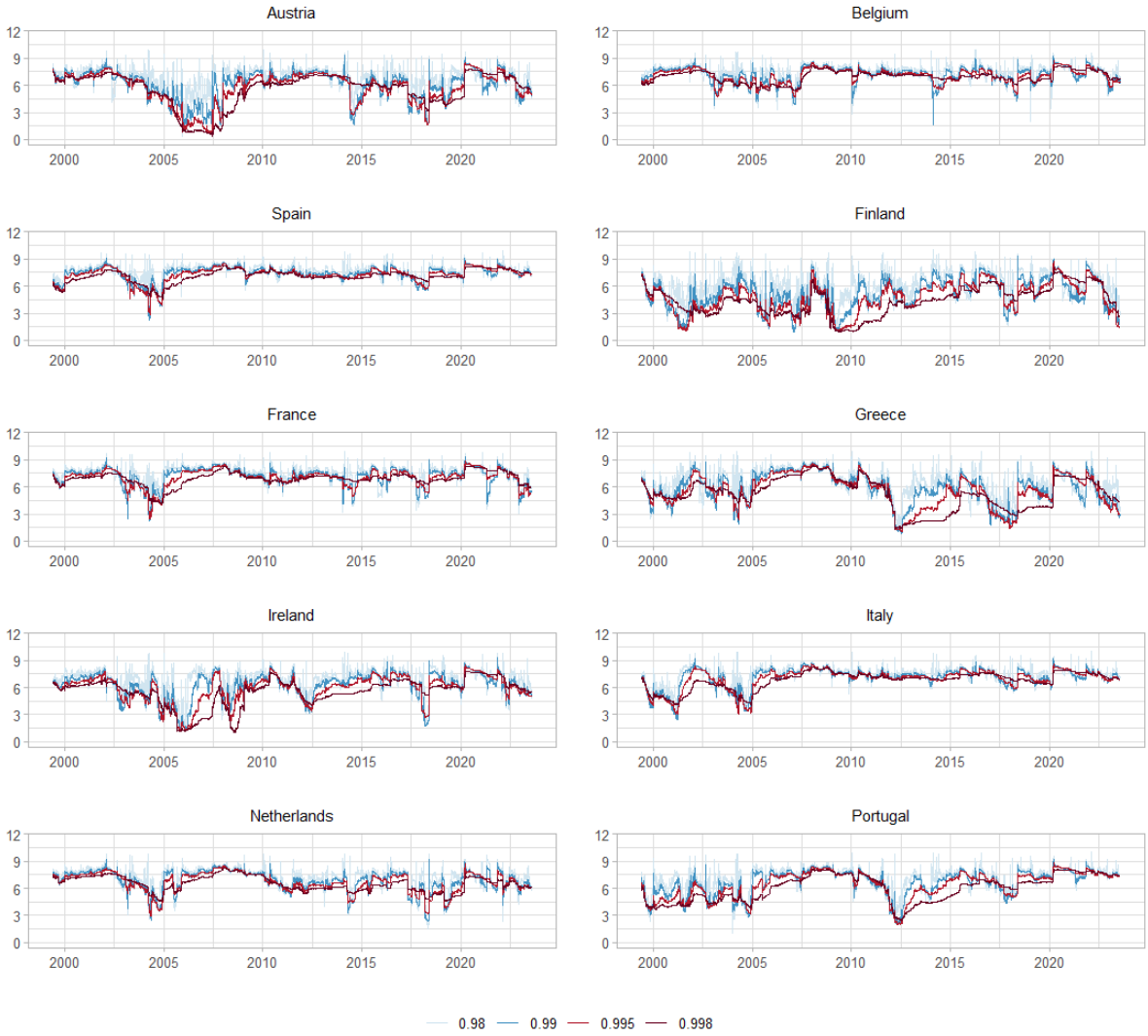

Note: the plot depicts received spillovers calculated using Equation (20) with time-varying parameter estimates obtained using repeated weighted least squares where a k-day-old observation is assigned weight λ^k with $\lambda = 0.98, 0.99, 0.995$, and 0.998.

model using weighted least squares, such that the observation at time $\tau - k$ is given weight λ^k for $k = 0, 1, 2, \ldots$, and weight zero for $k < 0$, with $0 < \lambda < 1$, resulting in VAR estimates for $t = \tau$. Repeating this for $\tau = 1, 2, \ldots, T$ yields a sequence of VARs with smoothly time-varying parameter estimates. In this section, we evaluate the sensitivity of the resulting spillover measures to the choice of λ, hence we compare spillover measures estimated using $\lambda = 0.98, 0.99, 0.995$, and 0.998.

Figure 30: Sensitivity of transmitted spillovers to the weighting of observations.

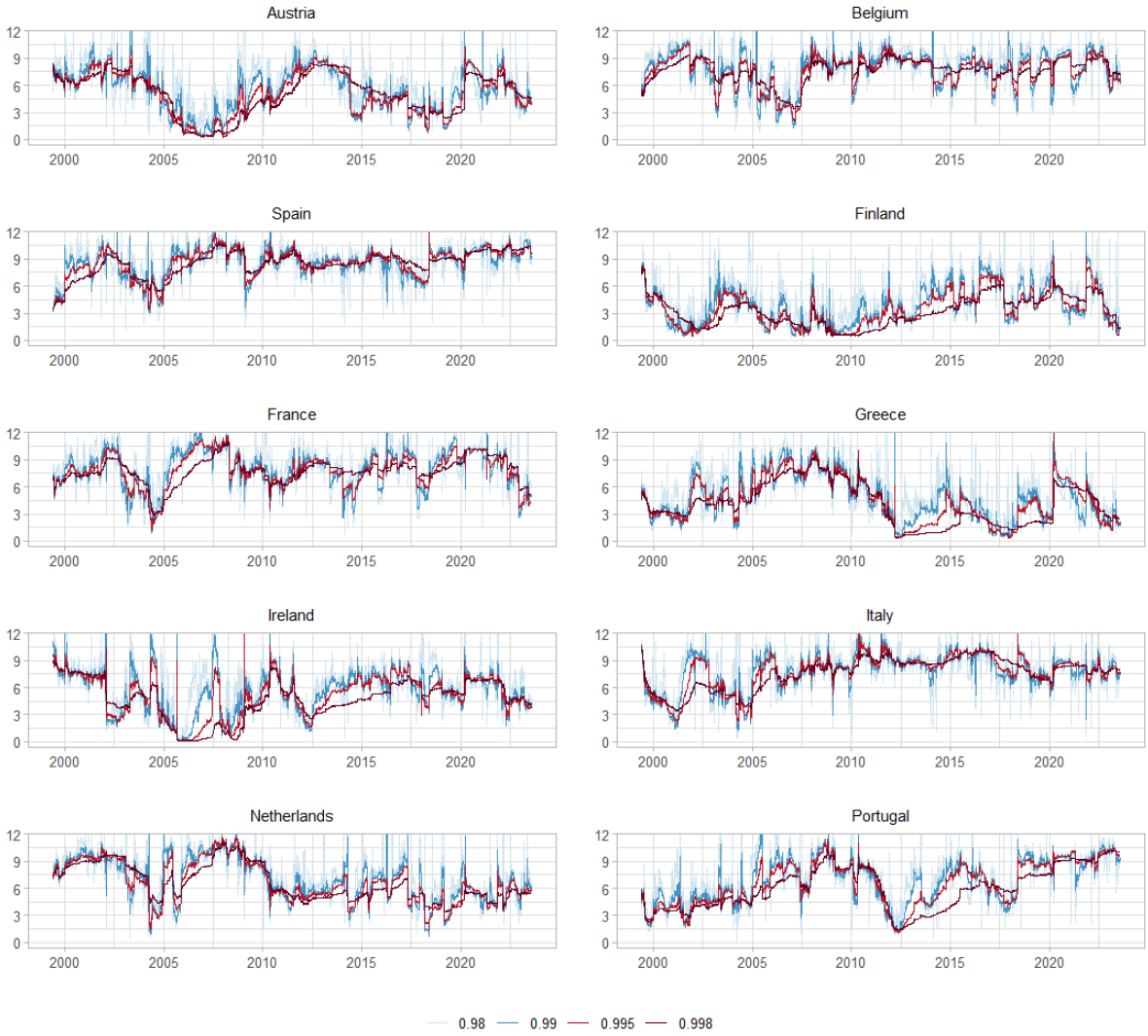

Note: the plot depicts transmitted spillovers calculated using Equation (21) with time-varying parameter estimates obtained using repeated weighted least squares where a k-day-old observation is assigned weight λ^k with $\lambda = 0.98, 0.99, 0.995$, and 0.998.

Figure 28 presents the total spillover index computed using parameter estimates obtained from the repeated weighted least squares approach with $\lambda = 0.98, 0.99, 0.995$, and 0.998. In all indices, changes appear to occur simultaneously, but a lower value of λ results in greater increases compared to the indices based on higher values of λ, which only experience small increases. Due to these frequent peaks, it is difficult to measure medium- and long-term trends in the total spillover indices computed with smaller values of λ. The index with $\lambda = 0.998$ on the other hand captures medium- and long-term trends very well, but hardly measures short-term increases in spillovers. In general, spillover indices estimated with smaller values of λ tend to overestimate their counterparts computed with λ closer to 1.

Figure 31: Sensitivity of net spillovers to the weighting of observations.

Note: the plot depicts net spillovers calculated using Equation (22) with time-varying parameter estimates obtained using repeated weighted least squares where a k-day-old observation is assigned weight λ^k with $\lambda = 0.98, 0.99, 0.995$, and 0.998.

Figures 29, 30, and 31 present the received, transmitted, and net spillover measures calculated with $\lambda = 0.98, 0.99, 0.995$, and 0.998. Although the received spillovers computed with $\lambda = 0.98$ appear to produce stable estimates capturing received spillovers for each country, the transmitted and net spillover measures are very volatile, capturing short-term changes very well, but making it difficult to distinguish real shifts in spillover dynamics from noise. The spillover measures computed with $\lambda = 0.998$ depict only the long-term trends in bilateral spillover dynamics, without any regard for short-term developments.

Figure 32: Sensitivity of the multiple shock spillover index to the weighting of observations.

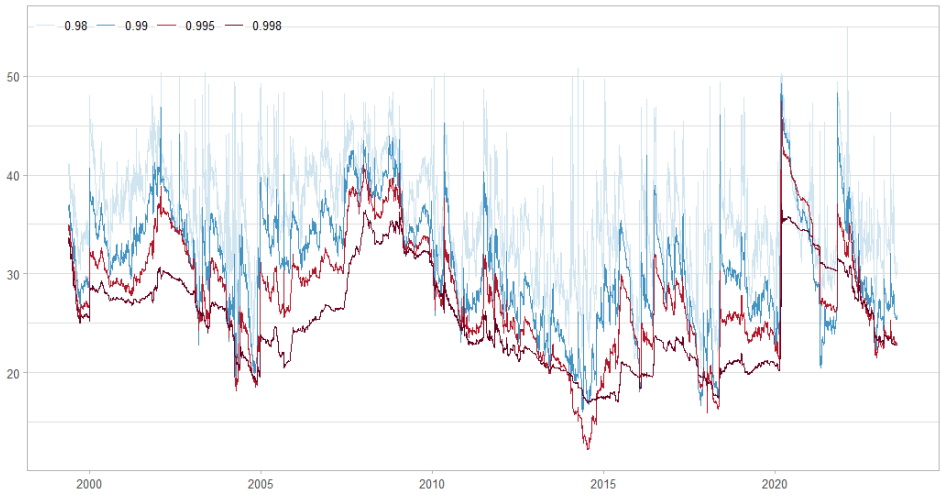

Note: the plot depicts the multiple shock spillover index calculated using Equation (27) with time-varying parameter estimates obtained using repeated weighted least squares where a k-day-old observation is assigned weight λ^k with $\lambda = 0.98, 0.99, 0.995$, and 0.998.

Figure 32 exhibits the multiple shock spillover index estimated with repeated weighted least squares approach with $\lambda = 0.98, 0.99, 0.995$, and 0.998. The multiple shock index computed with $\lambda = 0.98$ is very volatile and strongly overestimates spillovers compared to the indices computed with values of λ closer to 1. Additionally, responses to changes occur with peaks of much greater magnitude than the other indices. Furthermore, the measured magnitude of the indices can tell opposing stories, for example, in 2014 the index computed with $\lambda = 0.98$ reaches a peak, while the index computed with $\lambda = 0.995$ reaches an all-time low.

The received and transmitted spillovers from a simultaneous shock to the core and periphery are displayed in Figures 33 and 34. These measures paint a picture similar, showing the index with $\lambda = 0.98$ to be very volatile and overestimating the other indices. On the other hand, the index with $\lambda = 0.998$ is very time-invariant hence resulting in short-term developments being difficult to detect.

In conclusion, the spillover measures calculated using the parameter estimates obtained using the repeated weighted least squares approach with $\lambda = 0.98$ are very volatile making it difficult to detect medium- and long-term trends. Furthermore, the lower values of λ result in overestimation of spillovers compared to values of λ closer to 1. The closer the value of λ is to 1, the more time-invariant the resulting spillover measure will be, hence creating a trade-off between measuring every short-term development and being able to distinguish medium- and long-term trends.

Figure 33: Sensitivity of received spillovers from a simultaneous shock to core and periphery to the weighting of observations.

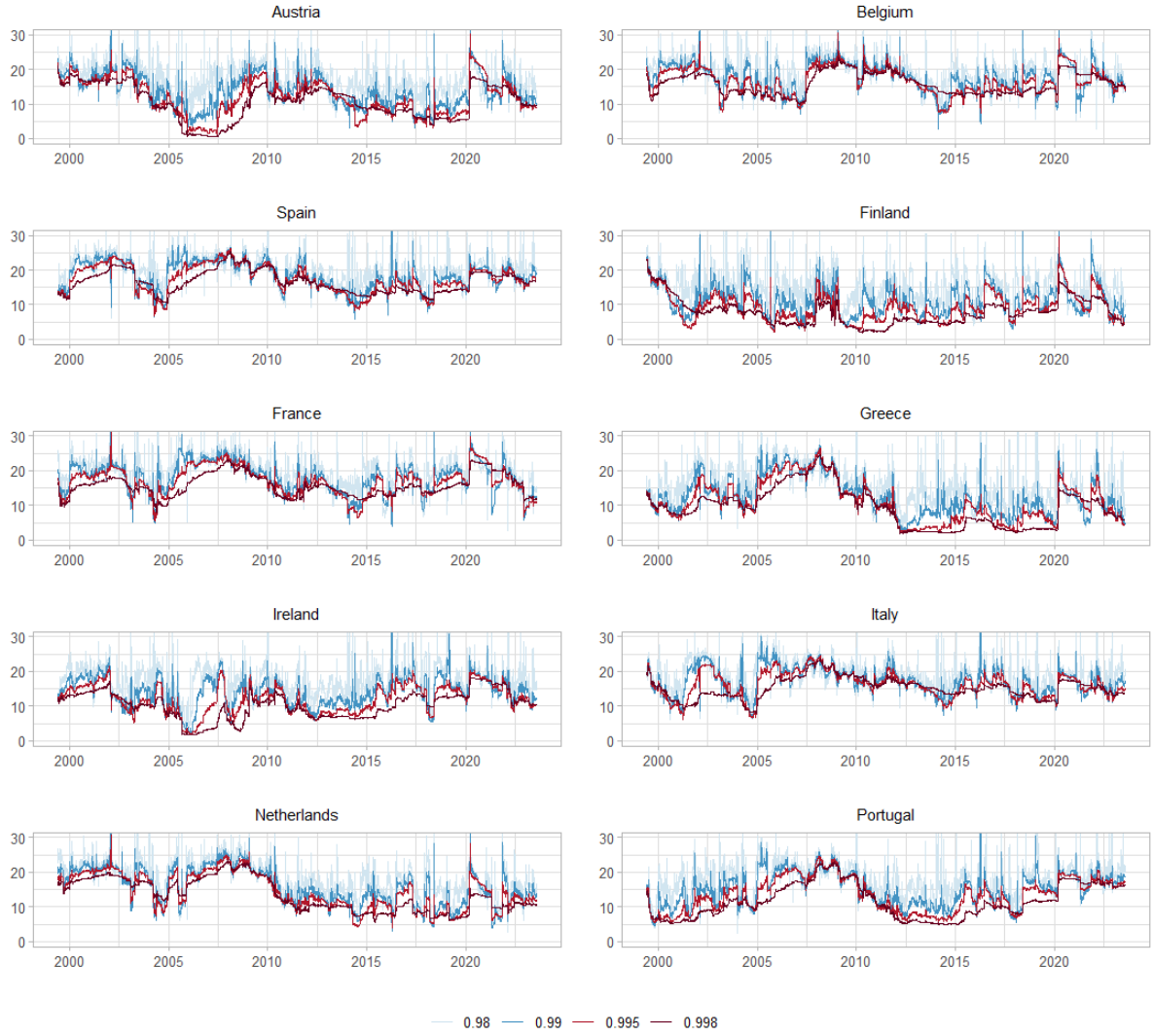

Note: the plot depicts the multiple shock received spillover measure calculated using Equation (28) with time-varying parameter estimates obtained using repeated weighted least squares where a k-day-old observation is assigned weight λ^k with $\lambda = 0.98, 0.99, 0.995$, and 0.998.

.

Figure 34: Sensitivity of transmitted spillovers from a simultaneous shock to core and periphery to the weighting of observations.

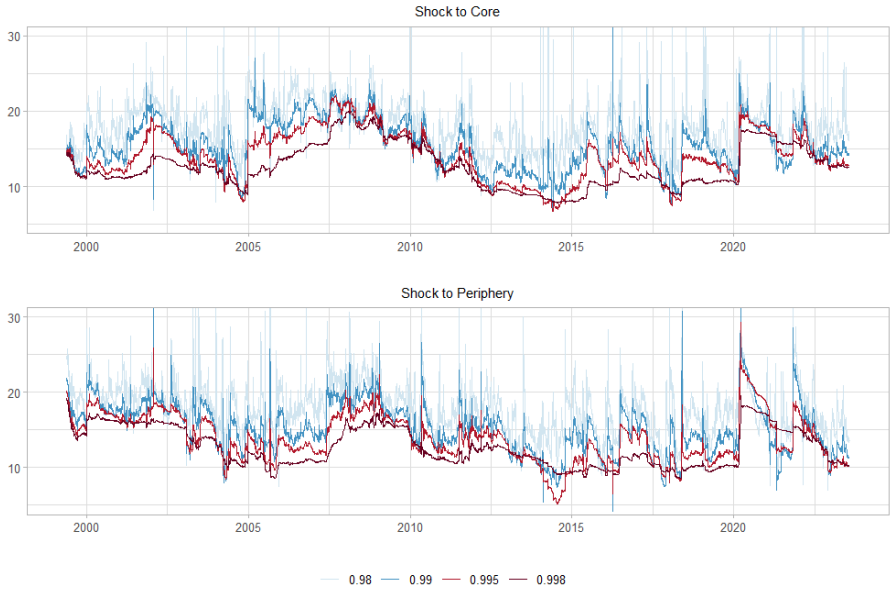

Note: the plot depicts he multiple shock transmitted spillover measure calculated using Equation (29) and (30) with time-varying parameter estimates obtained using repeated weighted least squares where a k-day-old observation is assigned weight λ^k with $\lambda = 0.98, 0.99, 0.995$, and 0.998.

B.4 Forgetting factors

To estimate the TVP-VAR model, we use the Kalman filter with forgetting factors, in the spirit of Koop and Korobilis (2013, 2014). In this section, we assess the sensitivity of spillover

Figure 35: Sensitivity of the total spillover index to the choice of forgetting factors.

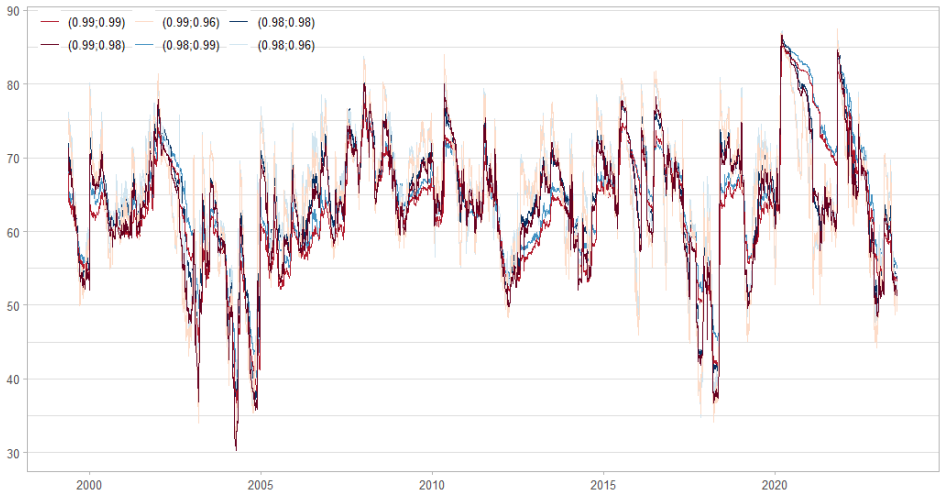

Note: the plot depicts the total spillover index calculated using Equation (19) with time-varying parameter estimates obtained from a TVP-VAR with decay factors $(\kappa_1, \kappa_2) = (0.99, 0.99)$, $(0.99, 0.98)$, $(0.99, 0.96)$, $(0.98, 0.99)$, $(0.98, 0.98)$, and $(0.98, 0.96)$.

Figure 36: Sensitivity of received spillovers to the choice of forgetting factors.

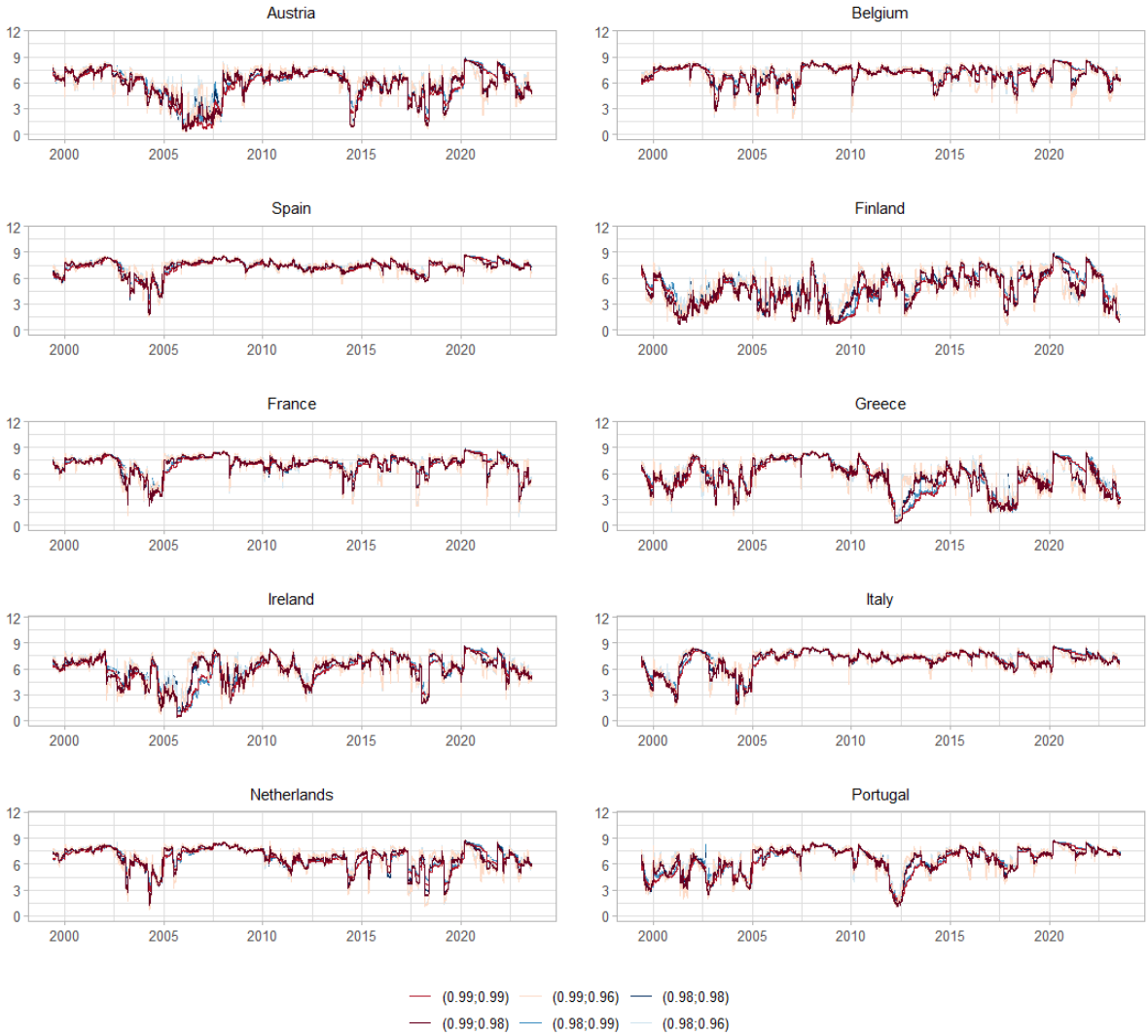

Note: the plot depicts the received spillovers calculated using Equation (20) with time-varying parameter estimates obtained from a TVP-VAR with decay factors $(\kappa_1, \kappa_2) = (0.99, 0.99)$, $(0.99, 0.98)$, $(0.99, 0.96)$, $(0.98, 0.99)$, $(0.98, 0.98)$, and $(0.98, 0.96)$.

measurements to the choice of forgetting factors. To do so, we compute the spillover measures using parameter estimates obtained from a TVP-VAR model estimated with forgetting factors $(\kappa_1, \kappa_2) = (0.99, 0.99)$, $(0.99, 0.98)$, $(0.99, 0.96)$, $(0.98, 0.99)$, $(0.98, 0.98)$, and $(0.98, 0.96)$.

Figure 35 presents the total spillover index estimated using the TVP-VAR approach with forgetting factors $(\kappa_1, \kappa_2) = (0.99, 0.99)$, $(0.99, 0.98)$, $(0.99, 0.96)$, $(0.98, 0.99)$, $(0.98, 0.98)$, and $(0.98, 0.96)$. In this figure, we note that the total spillover indices are very similar, and hence relatively insensitive to the choice of the specification. Especially the choice of κ_1 seems to have relatively little impact on the total spillover index. For κ_2, we see that indices with $\kappa_2 = 0.96$ have peaks of greater magnitude than the other indices.

Figure 37: Sensitivity of transmitted spillovers to the choice of forgetting factors.

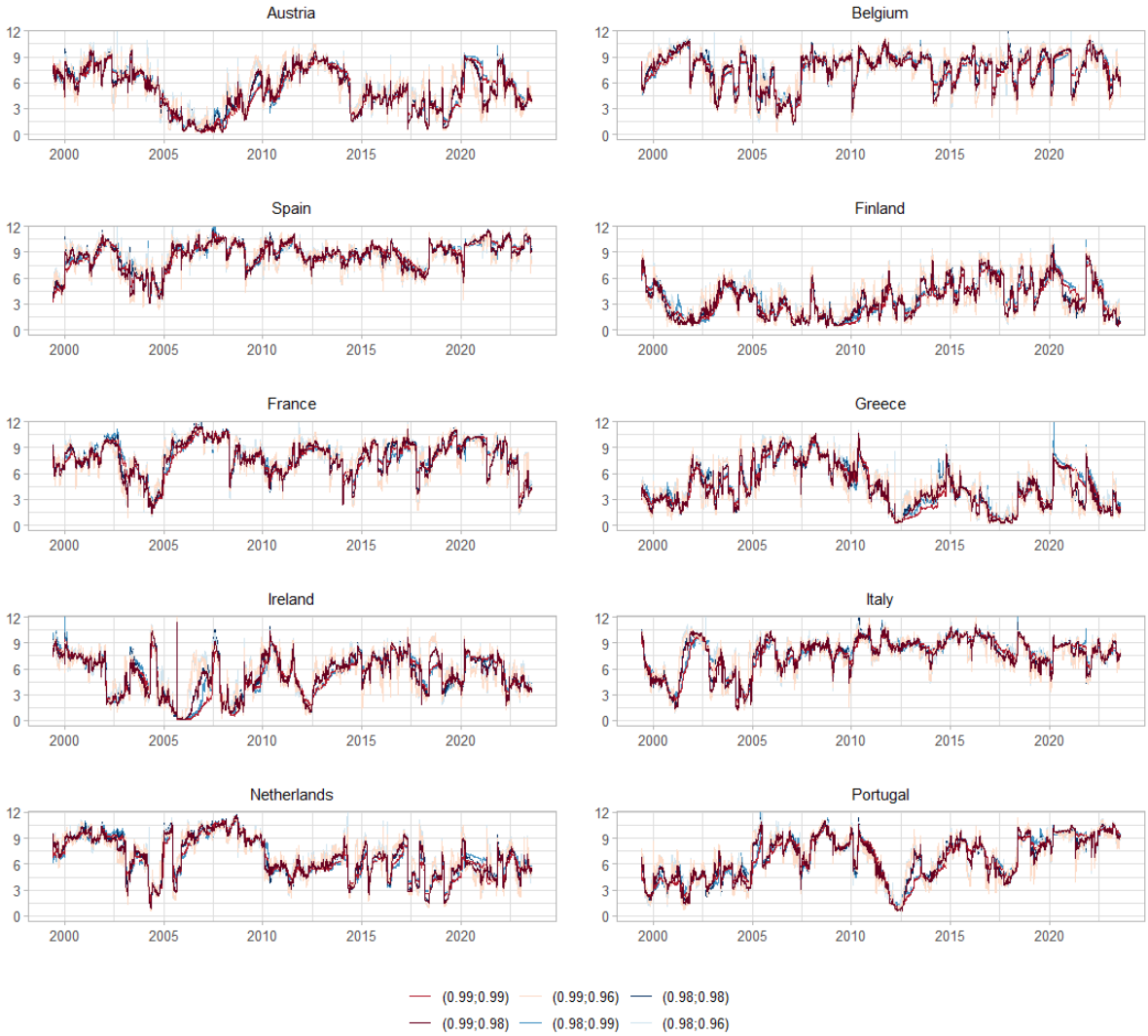

Note: the plot depicts transmitted spillovers calculated using Equation (21) with time-varying parameter estimates obtained from a TVP-VAR with decay factors $(\kappa_1, \kappa_2) = (0.99, 0.99)$, $(0.99, 0.98)$, $(0.99, 0.96)$, $(0.98, 0.99)$, $(0.98, 0.98)$, and $(0.98, 0.96)$.

The received, transmitted, and net spillovers estimated using parameter estimates from the TVP-VAR models with different specifications are depicted in Figures 36, 37, and 38. Again, we find that the differences between the spillover measures obtained from different specifications are subtle.

Figure 38: Sensitivity of net spillovers to the choice of forgetting factors.

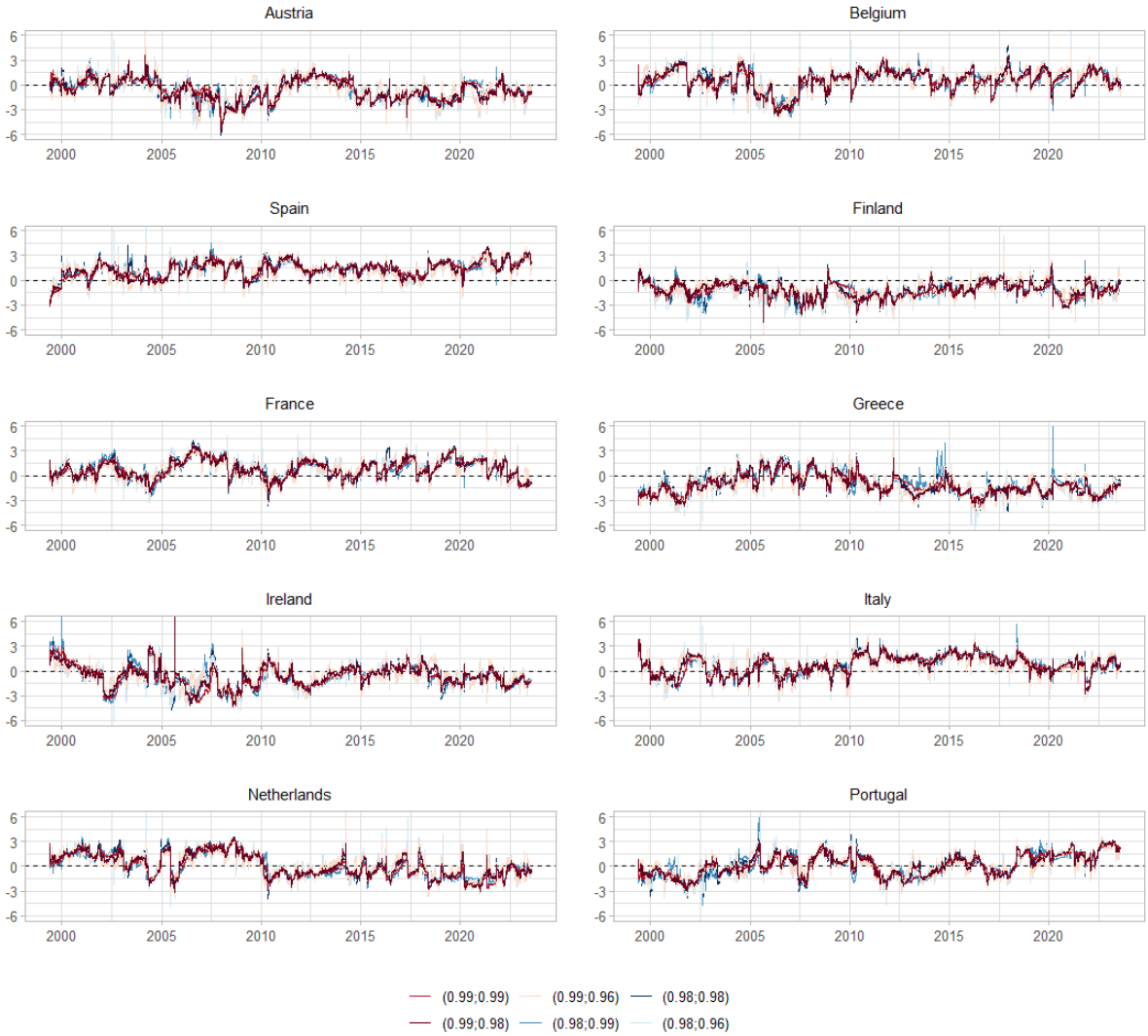

Note: the plot depicts net spillovers calculated using Equation (22) with time-varying parameter estimates obtained from a TVP-VAR with decay factors $(\kappa_1, \kappa_2) = (0.99, 0.99)$, $(0.99, 0.98)$, $(0.99, 0.96)$, $(0.98, 0.99)$, $(0.98, 0.98)$, and $(0.98, 0.96)$.

The multiple shock spillover index calculated with parameter estimates from TVP-VAR models with forgetting factors $(\kappa_1, \kappa_2) = (0.99, 0.99)$, $(0.99, 0.98)$, $(0.99, 0.96)$, $(0.98, 0.99)$, $(0.98, 0.98)$, and $(0.98, 0.96)$ is depicted in Figure 39. We observe that the multiple shock spillover index is more sensitive to the choice of forgetting factors than the ordinary spillover index. Especially the indices computed with $\kappa_2 = 0.96$ can be seen to be more volatile, and in general, overestimating the other indices. However, compared to the rolling-window and repeated weighted least squares approaches, the choice of specifications is much less influential on the resulting spillover measures.

Figure 39: Sensitivity of the multiple shock spillover index to the choice of forgetting factors.

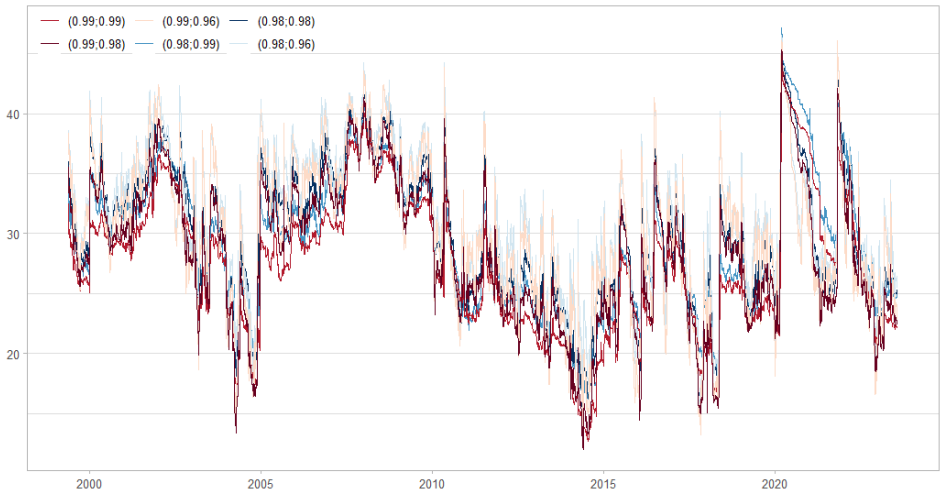

Note: the plot depicts the multiple shock spillover index calculated using Equation (27) with time-varying parameter estimates obtained from a TVP-VAR with decay factors $(\kappa_1, \kappa_2) = (0.99, 0.99)$, $(0.99, 0.98)$, $(0.99, 0.96)$, $(0.98, 0.99)$, $(0.98, 0.98)$, and $(0.98, 0.96)$.

Figure 40: Sensitivity of transmitted spillovers from a simultaneous shock to the core and periphery to the choice of forgetting factors.

Note: the plot depicts the multiple shock transmitted spillover measure calculated using Equation (29) and (30) with time-varying parameter estimates obtained from a TVP-VAR with decay factors $(\kappa_1, \kappa_2) = (0.99, 0.99)$, $(0.99, 0.98)$, $(0.99, 0.96)$, $(0.98, 0.99)$, $(0.98, 0.98)$, and $(0.98, 0.96)$.

The transmitted and received spillovers from a simultaneous shock to the core and periphery are exhibited in Figures 40 and 41. Again, the differences between indices are subtle and insensitive to the choice of forgetting factors κ_1 and κ_2.

Figure 41: Sensitivity of received spillovers from a simultaneous shock to the core and periphery to the choice of forgetting factors.

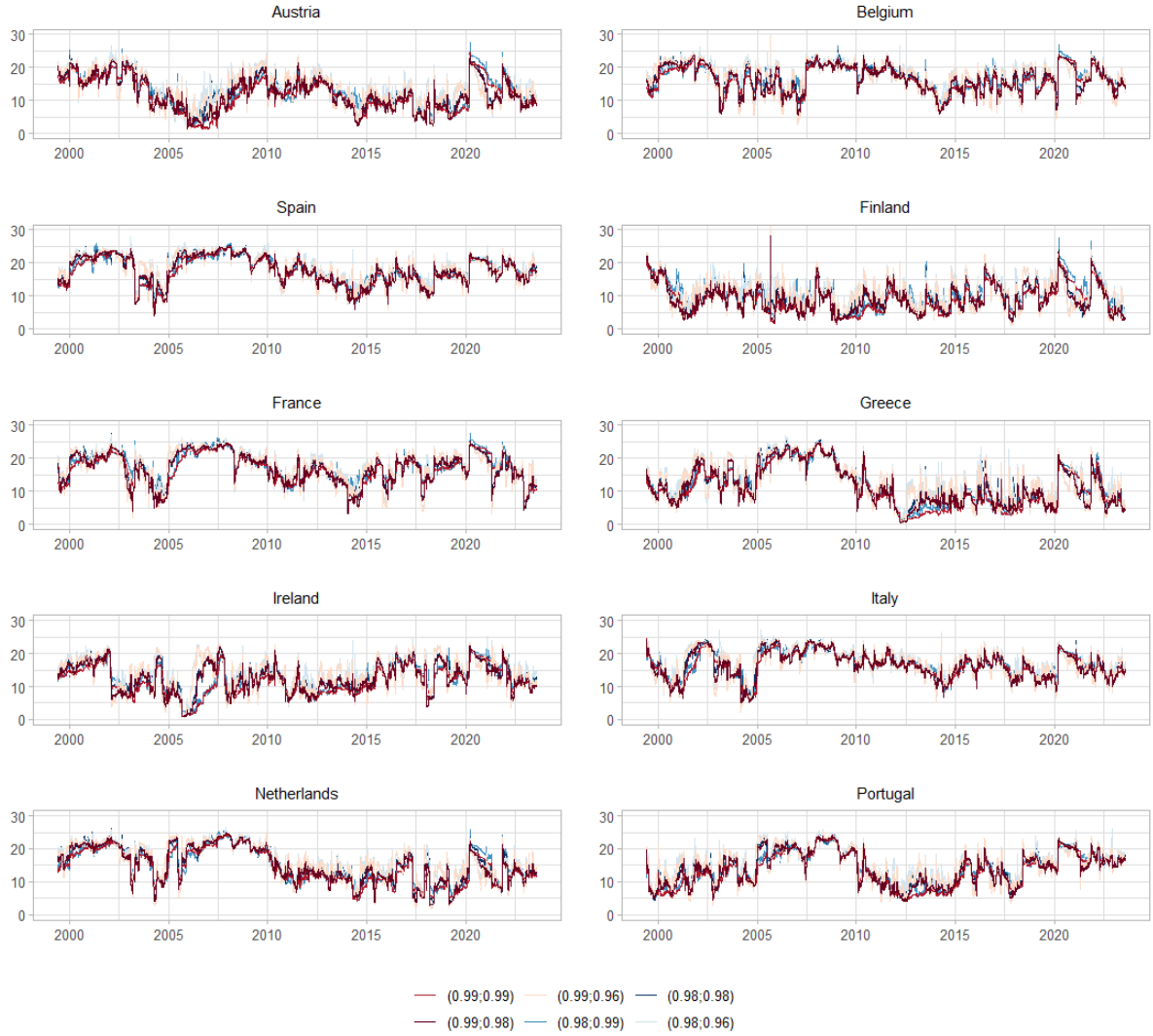

Note: the plot depicts the multiple shock received spillover measure calculated using Equation (28) with time-varying parameter estimates obtained from a TVP-VAR with decay factors $(\kappa_1, \kappa_2) = (0.99, 0.99)$, $(0.99, 0.98)$, $(0.99, 0.96)$, $(0.98, 0.99)$, $(0.98, 0.98)$, and $(0.98, 0.96)$.

.

C Robustness Check

In the period during and after the sovereign debt crisis, the Greek sovereign yield spread experienced a turbulent episode. In this section, we check whether the spillover measures are robust to the influence of Greece's turbulence by comparing estimation results including and

Table 6: Spillover table, excluding Greece

	AT	BE	FI	FR	NL	ES	IE	IT	PT	Received
AT	43.4	13.8	2.6	13.0	8.6	7.7	2.5	6.7	1.9	56.6
BE	10.8	33.2	1.9	14.6	8.4	11.8	4.9	11.1	3.3	66.8
FI	3.7	3.7	77.9	3.8	4.5	2.2	1.2	2.2	0.7	22.1
FR	10.5	15.1	2.1	34.9	14.1	9.4	2.6	9.1	2.2	65.1
NL	8.4	10.5	3.1	17.2	44.6	7.2	2.3	5.7	1.2	55.4
ES	5.9	11.7	1.3	9.1	5.8	33.1	6.9	19.7	6.6	66.9
IE	2.9	7.7	1.0	4.0	2.8	11.2	51.4	8.8	10.1	48.6
IT	5.5	11.5	1.3	9.4	4.9	20.6	5.6	35.2	5.9	64.8
PT	2.4	5.8	0.7	3.4	1.6	10.7	11.1	9.5	55.0	45.0
Transmitted	50.1	79.8	13.9	74.4	50.7	80.7	37.1	72.8	31.8	Total spillover index = 54.6%
Transmitted, including own	93.4	113.0	91.8	109.3	95.3	113.8	88.6	108.0	86.9	
Net	-6.6	13.0	-8.2	9.3	-4.7	13.8	-11.4	8.0	-13.1	

Note: Spillover measures, based on Equations (18)-(22), calculated from generalised forecast error variance decompositions based on 10-step-ahead forecasts. The received, transmitted, and net spillovers displayed in the table are N times larger than the ones computed using Equations (20)-(22). Abbreviations: AT, Austria; BE, Belgium; ES, Spain; FI, Finland; FR, France; IE, Ireland; IT, Italy; NL, the Netherlands; PT, Portugal.

Figure 42: Comparison of the total spillover index computed including and excluding Greece

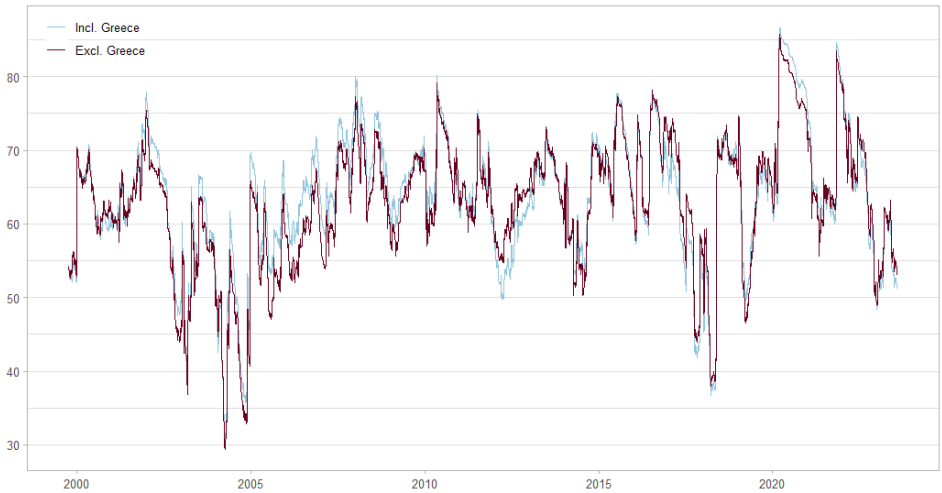

Note: the plot depicts the total spillover index calculated using Equation (19) with parameter estimates obtained from a TVP-VAR model with decay factors $\kappa_1 = 0.99$ and $\kappa_2 = 0.98$, estimated including and excluding Greece.

Figure 43: Comparison of received spillovers computed including and excluding Greece

Note: the plot depicts received spillovers calculated using Equation (20) with parameter estimates obtained from a TVP-VAR model with decay factors $\kappa_1 = 0.99$ and $\kappa_2 = 0.98$, estimated including and excluding Greece.

Figure 44: Comparison of transmitted spillovers computed including and excluding Greece

Note: the plot depicts transmitted spillovers calculated using Equation (21) with parameter estimates obtained from a TVP-VAR model with decay factors $\kappa_1 = 0.99$ and $\kappa_2 = 0.98$, estimated including and excluding Greece.

Figure 45: Comparison of net spillovers computed including and excluding Greece

Note: the plot depicts net spillovers calculated using Equation (22) with parameter estimates obtained from a TVP-VAR model with decay factors $\kappa_1 = 0.99$ and $\kappa_2 = 0.98$, estimated including and excluding Greece.

excluding Greece. The full-sample spillover table is exhibited in Table 6. The spillover measures look very similar to the spillover table including Greece, identifying the same net recipients and net transmitters, and the total spillover index being 54.6% compared to 52.0%.

Figure 42 presents the total spillover index computed including and excluding Greece. In this figure, we can see that the difference between including and excluding is minimal, with both indices only deviating slightly during the financial and sovereign debt crisis. The received, transmitted, and net spillovers, depicted in Figures 43, 44, and 45 also show minimal difference between the spillover measures including and excluding Greece.

Table 7 presents the multiple shock spillover index, again, very similar to the multiple shock spillover table including Greece. The multiple shock spillover index equals 17.1%, compared to 17.0% including Greece. The received and transmitted spillovers in Figures 47 and 48 also look very similar. One interesting difference to note is in the upper graph of Figure 48, where we see that the transmitted spillover from a shock to the core is slightly higher during the financial crisis in the index in which Greece is included.

From the comparison of spillover measures including and excluding Greece, we conclude that Greece does not have a disproportionate influence on the spillover measures.

Table 7: Multiple shock spillover table, excluding Greece

	C	P	Received
AT	84.0	16.0	16.0
BE	70.9	29.1	29.1
FI	96.5	3.5	3.5
FR	76.6	23.4	23.4
NL	85.2	14.8	14.8
ES	28.5	71.5	28.5
IE	13.7	86.3	13.7
IT	27.0	73.0	27.0
PT	11.0	89.0	11.0
Transmitted	80.2	86.9	Spillover index =17.1%

Note: Multiple shock spillover measures, based on Equations (26)-(30), calculated from multiple shock forecast error variance decompositions based on 10-step-ahead forecasts. Abbreviations: AT, Austria; BE, Belgium; ES, Spain; FI, Finland; FR, France; IE, Ireland; IT, Italy; NL, the Netherlands; PT, Portugal.

Figure 46: Comparison of the multiple shock spillover index computed including and excluding Greece

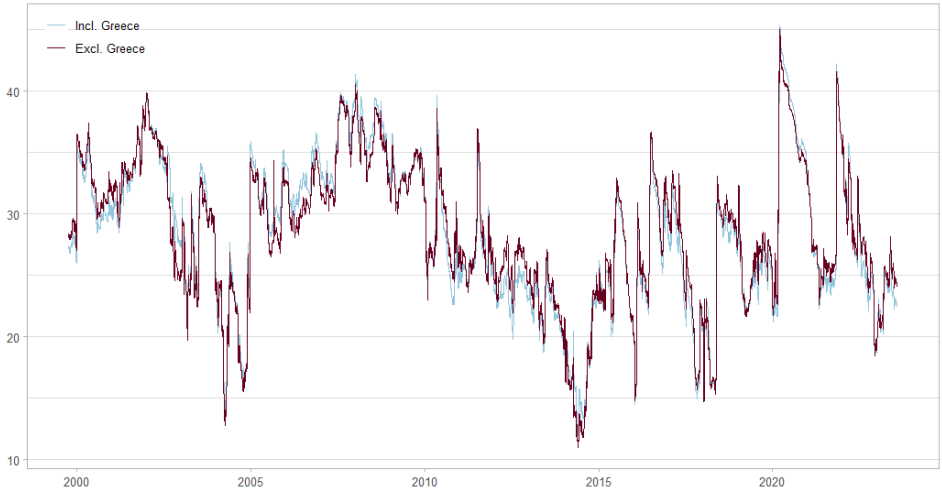

Note: the plot depicts the multiple shock spillover index calculated using Equation (19) with parameter estimates obtained from a TVP-VAR model with decay factors $\kappa_1 = 0.99$ and $\kappa_2 = 0.98$, estimated including and excluding Greece.

Figure 47: Comparison of received spillovers from a simultaneous shock to core and periphery computed including and excluding Greece

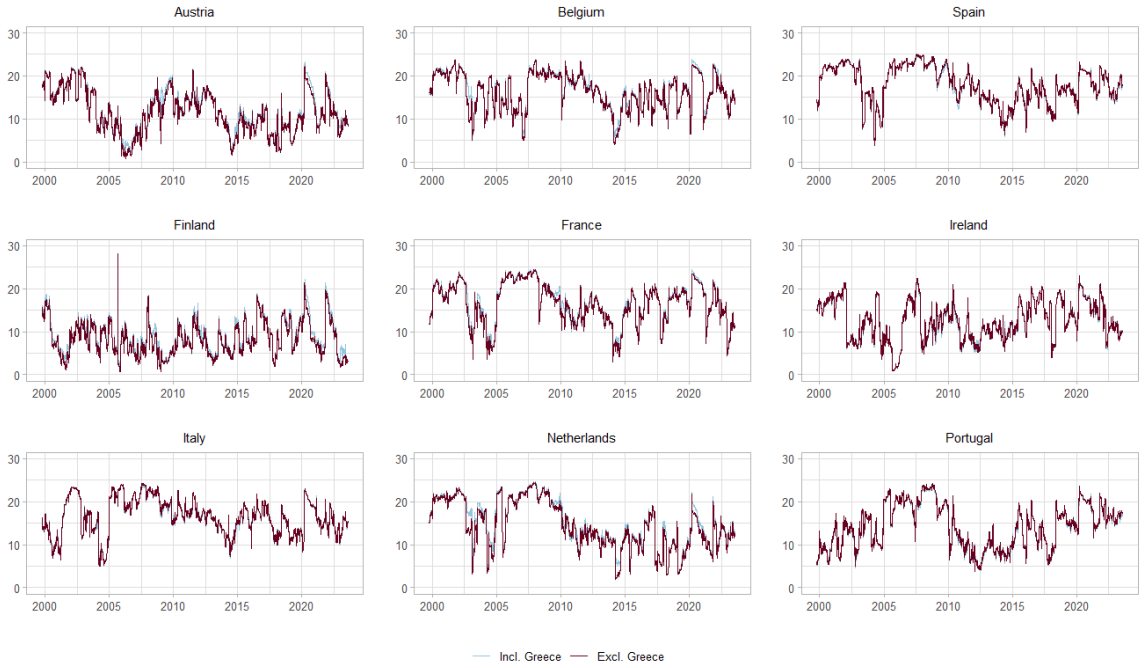

Note: the plot depicts multiple shock received spillover measure calculated using Equation (28) with parameter estimates obtained from a TVP-VAR model with decay factors $\kappa_1 = 0.99$ and $\kappa_2 = 0.98$, estimated including and excluding Greece.

Figure 48: Comparison of transmitted spillovers from a simultaneous shock to core and periphery computed including and excluding Greece

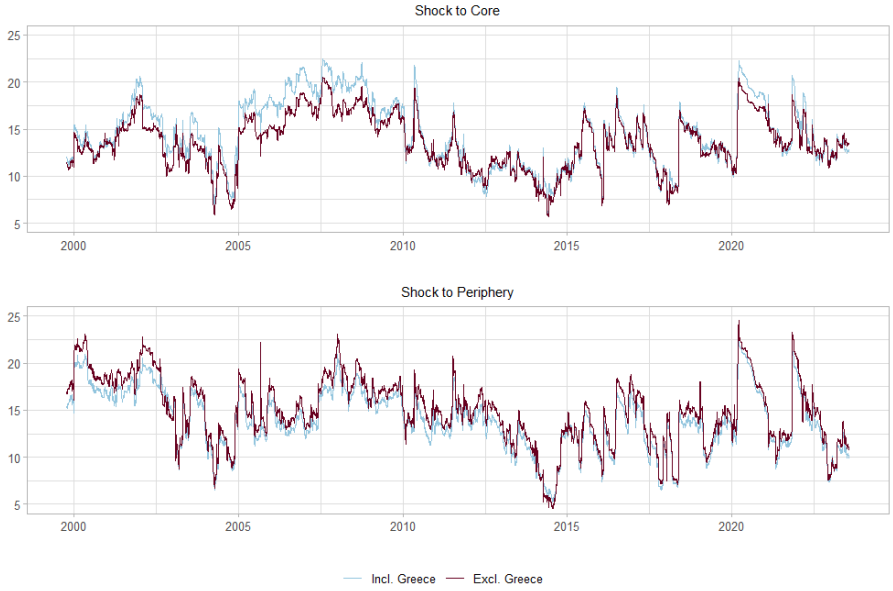

Note: the plot depicts multiple shock transmitted spillover measure calculated using Equation (29) and (30) with parameter estimates obtained from a TVP-VAR model with decay factors $\kappa_1 = 0.99$ and $\kappa_2 = 0.98$, estimated including and excluding Greece.